WOOD AND FIBER SCIENCE

The Sustainable Natural Materials Journal

Volume 56, Number 3_2024 *(ISSN 0735-6161)*

Open Access

JOURNAL OF THE

SWST – International Society of Wood Science and Technology

SOCIETY OF WOOD SCIENCE AND TECHNOLOGY

2023–2024 Officers of the Society

WOOD AND FIBER SCIENCE

Wood and Fiber Science is published quarterly in January, April, July, and October by the Society of Wood Science and Technology, P.O. Box 6155, Monona, WI 53716-6155

There are three classes of membership (electronic only) in the Society: Members – dues $150; Retired Members – dues $75; Student Members – dues $25. We also have membership category for individuals from Emerging Countries where individual members pay $30, individual students pay $10; Emerging Group of 10 pay $290, and Student Groups of 10 pay $90. Institutions and individuals who are not members pay $300 per volume (electronic only). Applications for membership and information about the Society may be obtained from the Executive Director, Society of Wood Science and Technology, P.O. Box 6155, Monona, WI 53716-6155 or found at the website http://www.swst.org.

Site licenses are also available with a charge of:
- $300/yr for single online membership, access by password and email
- $500/yr for institutional subscribers with 2–10 IP addresses
- $750/yr for institutional subscribers with 11–50 IP addresses
- $1000/yr for institutional subscribers with 51–100 IP addresses
- $1500/yr for institution subscribers with 101–200 IP addresses
- $2000/yr for institutions subscribers with over 200 IP addresses.

New subscriptions begin with the first issue of a new volume. All subscriptions are to be ordered through the Executive Director, Society of Wood Science and Technology.

The Executive Director, at the Business Office shown below, should be notified 30 days in advance of a change of email address.

Business Office: Society of Wood Science and Technology, P.O. Box 6155, Monona, WI 53716-6155.
Editorial Office: Jeff Morrell, jmorrell@usc.edu.au

EDITORIAL AND PUBLICATION POLICY

Wood and Fiber Science as the official publication of the Society of Wood Science and Technology publishes papers with both professional and technical content. Original papers of professional concern, or based on research of international interest dealing with the science, processing, and manufacture of wood and composite products of wood or wood fiber origin will be considered.

All manuscripts are to be written in US English, the text should be proofread by a native speaker of English prior to submission. Any manuscript submitted must be unpublished work not being offered for publication elsewhere.

Papers will be reviewed by referees selected by the editor and will be published in approximately the order in which the final version is received. Research papers will be judged on the basis of their contribution of original data, rigor of analysis, and interpretations of results; in the case of reviews, on their relevancy and completeness.

As of January 1, 2022, Wood and Fiber Science will be an online only, Open Access journal. There will be no print copies. Color photos/graphics will be offered at no additional cost to authors. The Open Access fee will be $1800/article for SWST members and $2000/article for nonmembers. The previous five years of articles are still copyright protected (accept those that are identified as Open Access) and can be accessed through member subscriptions. Once a previous article has reached its 5th anniversary date since publication, it becomes Open Access.

Technical Notes

Authors are invited to submit Technical Notes to the Journal. A Technical Note is a concise description of a new research finding, development, procedure, or device. The length should be **no more than two printed pages** in WFS, which would be five pages or less of double-spaced text (TNR12) with normal margins on 8.5 x 11 paper, including space for figures and tables. In order to meet the limitation on space, figures and tables should be minimized, as should be the introduction, literature review and references. The Journal will attempt to expedite the review and publication process. As with research papers, Technical Notes must be original and go through a similar double-blind, peer review process.

On-line Access to *Wood and Fiber Science* Back Issues

SWST is providing readers with a means of searching all articles in *Wood and Fiber Science* from 1968 to present Articles from 1968 to 2017 are available to anyone, but in order to see 2017 to 2021 articles you must have an SWST membership or subscription. SWST members and subscribers have full search capability and can download PDF versions of the papers If you do not have a membership or subscription, you will not be able to view the full-text pdf.

Visit the SWST website at http://www.swst.org and go to Wood & Fiber Science Online. Click on either SWST Member Publication access (SWST members) or Subscriber Publication access (Institution Access). All must login with their email and password on the HYPERLINK "http://www.swst.org" www.swst.org site, or use their ip authentication if they have a site license.

As an added benefit to our current subscribers, you can now access the electronic version of every printed article along with exciting enhancements that include:

- IP authentication for institutions (only with site license)
- Enhanced search capabilities
- Email alerting of new issues
- Custom links to your favorite titles

(ISSN 0735-6161)
CODEN WOOFAJ

WOOD AND FIBER SCIENCE

JOURNAL OF THE SOCIETY OF WOOD SCIENCE AND TECHNOLOGY

VOLUME 56 OCTOBER 2024 NUMBER 3

CONTENTS

EVALUATION OF RELATIONSHIPS BETWEEN CAMBIAL AGE-RELATED CHANGES IN RADIAL GROWTH INCREMENTS OF STEMS AND WOOD PROPERTIES IN *PAULOWNIA TOMENTOSA* TREES GROWN IN FUKUSHIMA, JAPAN

I. Nezu
Project Research Associate
E-mail: inezu@cc.utsunomiya-u.ac.jp

*F. Ishiguri**†*
Associate Professor
E-mail: ishiguri@cc.utsunomiya-u.ac.jp

J. Ohshima
Associate Professor
E-mail: joshima@cc.utsunomiya-u.ac.jp

S. Yokota
Professor
School of Agriculture, Utsunomiya University,
Utsunomiya 321-8505, Japan
E-mail: yokotas@cc.utsunomiya-u.ac.jp

(Received 13 April 2024)

Abstract. Information on the relationship between cambial age-related changes in stem size and wood properties is essential for promoting plantation forestry and utilization of fast-growing tree species. In this study, cambial age-related changes in radial growth increments of stems and wood properties were preliminarily examined using mixed-effects modeling of ∼25-yr-old *Paulownia tomentosa* trees planted in Fukushima, Japan. A Gompertz model was well-fitted to cambial age-related changes in stem diameter. The cambial ages showing the maximum current annual increment and mean annual increment estimated by the radial growth model were 5.4 and 7.3 yr, respectively. Although radial growth decreased after a certain cambial age, the mean annual increment value was still more than 2 cm per year until 25 yr. Most anatomical characteristics increased from the pith and stabilized toward the cambium. On the other hand, physical and mechanical properties were stable from the pith toward the cambium: the fixed-effect parameter estimates in the selected *y*-intercept model were 0.29 g·cm^{-3} for air-dry density, 4.02 GPa for MOE, and 40.3 MPa for MOR. Thus, a large volume of xylem with low and stable physical and mechanical properties values was produced for more than 20 yr, suggesting that the rotation age of plantations of this species can be determined from the viewpoint of wood quantity. In addition, the wood can be used where low density, but stable properties is an advantage at any age in this species.

Keywords: Anatomical characteristics, physical properties, mechanical properties, mixed-effects modeling, *Paulownia tomentosa*.

INTRODUCTION

Woody biomass production from fast-growing plantations is desirable to meet the increasing demands for wood resources. Because fast-growing trees can store massive carbon from the atmosphere in a short time, planting these trees also has merit for solving environmental issues. Therefore, promoting the establishment of plantations and wood utilization of fast-growing tree species is important not only to sustainable wood resources but also to minimize global warming by sequestering atmospheric carbon dioxide. At present, among several fast-growing tree species

* Corresponding author
† SWST member

including *Melia azedarach* L., *Cunninghamia lanceolata* (Lamb.) Hook., *Liriodendron tulipifera* L., and *Eucalyptus* spp. have been considered as candidates for plantations in Japan (Hirohashi et al 2012; Yokoo et al 2021; Nezu et al 2022; Ido et al 2023).

The relationships between radial growth increments of the stem and anatomical characteristics have been examined in several broad-leaved tree species concerning trade-offs between quantity and quality of wood (Tsuchiya and Furukawa 2008, 2009a, 2009b, 2009c). Generally, the growth stages of trees can be divided into young, middle, and old based on the cambial age-related changes in radial growth increments of the stem (Fig 1, Kataoka 1992; Salas-Eljatib et al 2021). The young stage occurs from the beginning of the radial stem increments to the age t_1 at the point of the maximum current annual increment (CAI). The middle stage is from age t_1 to age t_2 at the point of the mean annual increment (MAI). The old stage is over age t_2. Age t_1 corresponds to the inflection point of the S-shaped growth curve of the radial stem increment, and age t_2 is when CAI equals MAI (Kataoka 1992). To estimate the cambial age at the maximum point of CAI and MAI, the regression model based on the Gompertz growth function is fitted to the stem diameter or cumulative ring width over time in several broad-leaved tree species (Tsuchiya and Furukawa 2008, 2009a, 2009b, 2009c). On the other hand, a nonlinear regression model based on a quadratic function with a plateau was applied to describe cambial age-related changes in anatomical characteristics (Tsuchiya and Furukawa 2008, 2009a, 2009b, 2009c). The maturation age of each anatomical characteristic was regarded as the cambial age reaching a plateau value in the regression model. As a result, the maturation age of anatomical characteristics, such as wood fiber length and vessel lumen diameter, is similar at ages t_1 or t_2 in broad-leaved tree species (Tsuchiya and Furukawa 2009a). Tsuchiya and Furukawa (2009b) also investigated the relationships between the maturation ages of the wood fiber length, vessel element length, and vessel lumen diameter and the boundary age between the stages

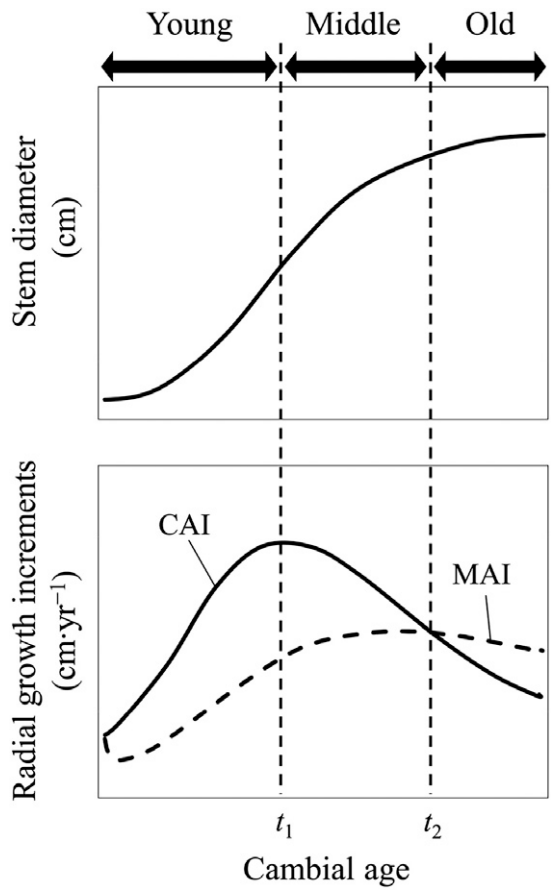

Figure 1. Schematic of the developmental stage of radial growth increment (modified from Kataoka 1992; Salas-Eljatib et al 2021): Upper graph, S-shaped growth curve fitted to the radial growth; lower graph, curves of the current annual increment (CAI) and mean annual increment (MAI); t_1, age showing maximum CAI; t_2, age showing maximum MAI.

of diameter growth in *Populus simonii* and *Populus* × *beijingensis* planted in China. In addition, the relationship between the maturation age of vessel lumen diameter and radial growth was also elucidated in 30 different broad-leaved tree species grown in Japan (Tsuchiya and Furukawa 2009c). The 30 species were classified into three types: 1) maturation age similar to age t_1 rather than age t_2 (13 species), 2) maturation age similar to age t_2 rather than age t_1 (15 species), and 3) no relationships between cambial age-related changes in vessel lumen diameter and radial

growth (two species). Studies of several broad-leaved tree species (Tsuchiya and Furukawa 2008, 2009a, 2009b, 2009c) suggest that there is a trade-off between radial growth increments of the stem and anatomical characteristics: the wood with mature anatomical characteristics might be formed after radial growth rate slows. Suppose this trade-off is adapted for the fast-growing tree species used for plantation development. In that case, the balance between the quantity and quality of wood obtained from the fast-growing tree plantations may be controlled by some silvicultural treatments. In addition, to utilize the wood obtained from the fast-growing tree plantations for value-added products, such as solid wood, the trade-off concepts should be evaluated for the other qualities of wood, such as density and strength properties.

Recently, the relationships between radial growth increments of stems and multiple wood properties were clarified in a fast-growing tree species, *L. tulipifera* planted in Japan using mixed-effect modeling of cambial age-related changes in these properties (Nezu et al 2022). The maximum CAI and MAI determined by stem diameter were found at 4.9 and 7.4 yr, respectively. In addition, all measured wood properties changed near the pith before becoming stable toward the cambium (Nezu et al 2022). The changing ratio of multiple wood properties at 1-yr intervals became stable after a cambial age of 9 yr (Nezu et al 2022). These results suggest a trade-off between radial growth increments of stems and wood properties in *L. tulipifera*: the tree produces a large volume of wood with lower wood properties, and the wood with greater and more stable properties forms as growth slows compared with the initial growth. The trade-offs in this species suggest that wood that forms before a cambial age of nine can be used for utility applications and wood thereafter can be used for structural applications (Nezu et al 2022). Thus, wood utilization based on this trade-off concept should be evaluated for other fast-growing tree species.

Trees in the genus *Paulownia* are native to East Asia, where they are particularly widespread in South Korea, China, and Japan (Young and Lundgren 2023). They also have been introduced to many other areas globally, including the United States and Europe in the mid-19th century (Young and Lundgren 2023). *Paulownia tomentosa* (Thunb.) Steud. has historically been planted for furniture and musical instruments in Japan (Kumakura 1957; Nagata et al 2013). For example, a tree of this species was planted at the birth of a daughter and harvested for making chests of drawers when she married in Japan (Kumakura 1957; Nagata et al 2013). This old custom indicates not only the cultural importance of *Paulownia* in Japan but also the fast-growth characteristics that produced enough wood to make chests of drawers. The Japanese Forestry Agency, Ministry of Agriculture, Forestry, and Fishery considers the wood of *P. tomentosa* a 'special forest products': wood from this species has not been recognized as wood produced from forestry species in Japan. Recently, the declining number of traditional provenances of *P. tomentosa* has been a serious problem in Japan. Focusing on the fast-growth characteristics of *P. tomentosa* might allow this species to be used as a plantation tree species to produce wood for construction and interior uses as well as biomass for fuel helping to achieve both sustainable wood production and the traditional uses of *Paulownia*.

Many researchers have reported MAIs of stems and wood properties of *P. tomentosa* (Kitamura and Imata 1955; Kitamura 1956; Wood Mechanics of Wood Technology Division 1957; Takashima et al 1959; Olson and Carpenter 1985; Nasir and Mahmood 2000; Koman et al 2017; Tomczak et al 2023). Kitamura and Imata (1955) reported that MAI, air-dry density, MOE, MOR, and compressive strength were 1.9 $cm \cdot yr^{-1}$, 0.253 $g \cdot cm^{-3}$, 5.18 GPa (52,900 $kg \cdot cm^{-2}$), 36.3 MPa (370 $kg \cdot cm^{-2}$), and 20.4 MPa (208 $kg \cdot cm^{-2}$) in three trees of 6-yr-old *P. tomentosa* planted in Niigata, Japan. In 7- and 12-yr-old *P. tomentosa* trees grown in the United States, MAI, basic density, and wood fiber length were 1.85 $cm \cdot yr^{-1}$, 0.274 $g \cdot cm^{-3}$, and 0.81 mm, respectively (Olson and Carpenter 1985). Koman et al (2017) reported that air-dry density, MOE, MOR, and compressive strength were 0.30 $g \cdot cm^{-3}$,

3.49 GPa, 41.5 MPa, and 22.1 MPa in *P. tomentosa* at the age of less than 10 planted in Hungary. They also reported cambial age-related changes in wood properties in young (less than ca. 10 yr) *P. tomentosa* trees (Kitamura and Imata 1955; Olson and Carpenter 1985; Koman et al 2017). However, the cambial age-related changes in radial growth increments of stems and wood properties estimated using the modeling approaches, and their relationship have not been elucidated yet in *P. tomentosa*.

In the present study, radial growth increments of stems and wood properties (anatomical characteristics, and physical and mechanical properties) were measured in *P. tomentosa* planted in Fukushima, Japan. The objectives of this study were 1) to evaluate the cambial age-related changes in these properties using linear or nonlinear mixed-effects modeling and 2) to clarify whether the trade-off between radial growth increments of the stems and wood properties in *L. tulipifera* is adapted in *P. tomentosa*.

MATERIALS AND METHODS

Materials

Four trees of *P. tomentosa* (Thunb.) Steud. were used in the present study. The trees were grown in Kaneyama, Fukushima, Japan (37°21′62″N, 139°26′84″E, and 412 m above sea level), which is a traditional *Paulownia* wood production site. Seed origin and age were unknown. The annual ring number at 0.4 m above the ground was 24 or 25 (Table 1). Disks (about 30 cm long) were collected from 0.1 to 0.4 m above the ground in each tree. Bark-to-bark radial strips with pith (about 5 cm in width) were collected from a random position (without any eccentric growth) on each disk. The radial strips were cut again into two strips (1 cm thickness in the longitudinal direction) for measuring annual ring width and anatomical characteristics with the remaining (∼) 16 cm section used for preparing specimens for static bending properties and compressive strength parallel to the grain.

Annual Ring Width and Anatomical Characteristics

The radial strips were sanded, and then transverse images of the strips were obtained by an 800 dpi image scanner (GT-9300; Epson, Nagano, Japan) (0.032 mm·pixel^{-1}). Annual ring width was measured from the pith to the bark side using ImageJ (National Institute of Health, Bethesda, MD). The cumulative ring width was calculated using the annual ring width.

Table 1. Anatomical, physical, and mechanical properties of four *P. tomentosa* trees.

	Tree no.						
Property	1	2	3	4	Mean	SD	CV (%)
Number of annual rings	24	25	25	24	25	1	4.0
Annual ring width (mm)	8.15	9.79	9.77	10.06	9.44	0.87	9.2
Stem diameter (cm)	39.1	49.0	48.9	48.3	46.3	4.8	10.4
Wood fiber length (mm)	1.01	1.05	0.97	1.01	1.01	0.03	3.0
Vessel element length (mm)	0.81	0.85	0.77	0.80	0.81	0.04	4.9
Vessel frequency (No·mm^{-2})	7.3	6.1	6.4	5.8	6.4	0.6	9.4
Vessel diameter (μm)	128	134	132	143	134	6	4.5
Wood fiber diameter (μm)	26.5	28.2	26.4	28.6	27.4	1.1	4.0
Wood fiber wall thickness (μm)	1.7	1.5	1.5	1.5	1.6	0.1	6.3
Air-dry density (g·cm^{-3})	0.32	0.28	0.27	0.29	0.29	0.02	6.9
MOE (GPa)	4.42	3.81	3.93	3.96	4.03	0.27	6.7
MOR (MPa)	44.1	40.4	39.7	37.1	40.3	2.9	7.2
Compressive strength parallel to grain (MPa)	14.3	14.6	17.1	15.6	15.4	1.2	7.8

SD, standard deviation; CV, coefficient of variation; MOE, modulus of elasticity; MOR, modulus of rupture. Number of annual rings, annual ring width, and stem diameter were measured at 0.4 m above the ground. To calculate each statistical value in a wood property, the individual mean was obtained by averaging the value at each cambial age within an individual.

To determine the anatomical characteristics, transverse sections (20 μm in thickness and 10 mm in tangential direction) were successively obtained at 5-cm intervals from pith to bark by a core microtome (WSL, Birmensdorf, Switzerland). The sections were stained with safranin, dehydrated through an ethanol series, dipped into xylene, and then put on slide glasses and mounted with a few drops of 75% glycerol and a coverslip. Transverse images were taken by a digital camera (CD-30C; Mitutoyo, Kanagawa, Japan) and a microscope (V-12B; Nikon, Tokyo, Japan). Photomicrographs of transverse images at the cambial ages of 2 and 24 in tree no. 2 are shown in Fig 2. The xylem of this species consisted of vessels, wood fibers, axial parenchyma, and ray parenchyma (Fig 2). The wood is semi-ring-porous (Fig 2). In this study, the anatomical characteristics (vessel frequency, vessel diameter, wood fiber diameter, and wood fiber wall thickness) were determined in every annual ring by ImageJ. Small wood specimens (1 [R] × 1 [T] × 10 [L] mm) were collected from each annual ring from the pith in the strips. Sticks from the innermost and outermost positions within an annual ring were macerated with Schultze's solution (100 mL of 35% nitric acid containing 6 g of potassium chloride). The macerated vessel elements in the pore zone and wood fiber in the outer pore zone were projected on a profile projector (V-12B; Nikon, Tokyo, Japan), and then cell length was measured by a digital caliper (CD-30C; Mitutoyo). A total of 30 vessels and 50 wood fibers were measured in each annual ring.

Physical and Mechanical Properties

Bending and compression tests were conducted according to the method described in Nezu et al (2022), which was partially modified from JIS Z 2101:2009 (Japanese Industrial Standards 2009). Bending (10 [R] × 10 [T] × 160 [L] mm) and compression test specimens (10 [R] × 10 [T] × 20 [L] mm) were successively collected from pith

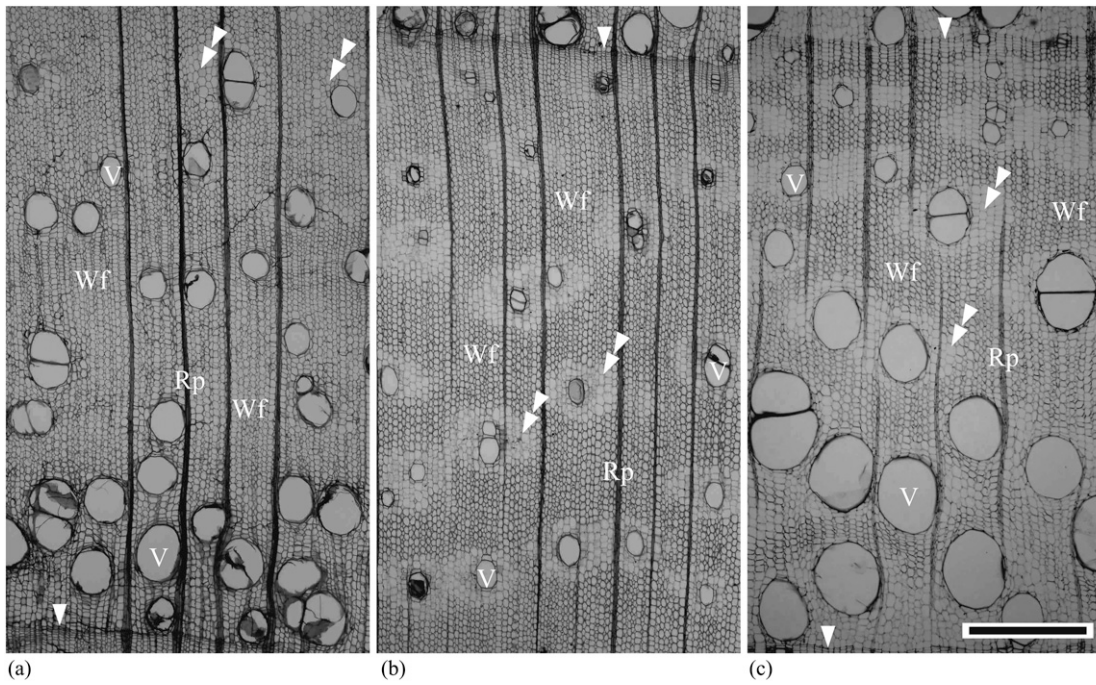

Figure 2. Photomicrographs of transverse sections: (a) the pore zone at the cambial age of two; (b) the outer-pore zone at the cambial age of two; (c) the cambial age of 24. V, vessel; Wf, wood fiber; Rp, ray parenchyma; arrowhead, annual ring boundary; double arrowheads, axial parenchyma; bar, 500 μm.

to bark from the strip. The specimens were conditioned to constant weight at 24°C and 65% RH for around 2 wk. The static bending test was conducted on a universal testing machine (MSC-5/200-2; Tokyo Testing Machine, Tokyo, Japan). The load was applied at the center of the radial section of the specimen with 140 mm of span at 2 mm/min. After the bending test, a block (10 [R] × 10 [T] × 10 [L] mm) without any visual defects, such as knots or cracks, was cut from each specimen and oven-dried to determine MC and air-dry density. The compression test was also conducted by the same testing machine with a 0.3 mm/min load speed. The average MC was 9.1 ± 1.7% in the static bending test and 9.6 ± 1.7% in the compression tests, respectively. The MOE, MOR, and compressive strength parallel to the grain were calculated using load–deflection data (Nezu et al 2022).

Statistical Analysis

Statistical analysis was conducted using R (Version 4.2.2) (R Core Team 2022). Cambial age-related changes in stem diameter and wood properties were evaluated using regression models developed based on the linear mixed-effect model using the packages "lmer" and "lmerTest" (Bates et al 2015) or nonlinear mixed-effects models using the package "nlme" (Pinheiro and Bates 2000).

The stem diameter (excluding bark) in relation to cambial age was regarded as twice the value of the cumulative ring width at 0.4 m above the ground in each individual tree. The regression model of cambial age-related change in stem diameter was developed based on the Gompertz function (Table 2). In each model, stem diameter was the response variable, cambial age was the explanatory variable, and the individual tree was the random effect. The best of the three models was selected based on the Akaike information criterion (AIC) (Akaike 1998). Based on the selected model, the CAI and MAI were calculated by Eqs 1 and 2:

$$\mathrm{CAI}\ \left(\mathrm{cm}\cdot\mathrm{yr}^{-1}\right) = \alpha_0\alpha_2 e^{\alpha_1-\alpha_2 \mathrm{CA}} e^{-e^{\alpha_1-\alpha_2 \mathrm{CA}}} \quad (1)$$

$$\mathrm{MAI}\ \left(\mathrm{cm}\cdot\mathrm{yr}^{-1}\right) = \frac{\alpha_0 e^{-e^{\alpha_1-\alpha_2 \mathrm{CA}}}}{\mathrm{CA}} \quad (2)$$

where α_0, α_1, and α_2 are parameters obtained from the selected model for radial growth model, and CA is cambial age. The cambial age showing maximum CAI and MAI was calculated.

The cambial age-related changes in wood properties were evaluated using regression models based on only *y*-intercept (Eq 1), linear (Eqs 2 and 3), logarithmic (Eqs 4 and 5), or quadratic functions (Eqs 6-8) with the explanatory variable of cambial age, response variable of each wood property, and random effect of the individual tree (Table 3). The model with the lowest AIC value was considered the best model. In the selected model for cambial age-related changes in stem diameter and wood properties, the ratio of the variance component of random-effect parameters to the total variance was calculated (Nakagawa and Schielzeth 2010).

The relationships between cambial age-related changes in radial growth increments of stems and wood properties between *P. tomentosa* and another fast-growing tree species *L. tulipifera*

Table 2. Comparison of AIC values among three models for cambial age-related change in stem diameter.

Eq	Formula	Explanation about random-effect parameter	AIC
I	$D_{ij} = (\alpha_0 + \mathrm{Tree}_{0j})e^{-e^{\alpha_1-\alpha_2 \mathrm{CA}_{ij}}} + \varepsilon_{ij}$	Asymptotic value	**365.53**
II	$D_{ij} = \alpha_0 e^{-e^{\alpha_1+\mathrm{Tree}_{1j}-\alpha_2 \mathrm{CA}_{ij}}} + \varepsilon_{ij}$	Start position of the curve	477.62
III	$D_{ij} = \alpha_0 e^{-e^{\alpha_1-(\alpha_2+\mathrm{Tree}_{2j})\mathrm{CA}_{ij}}} + \varepsilon_{ij}$	Slope	416.35

D_{ij}, stem diameter at 0.4 m above the ground at the *i*th cambial age of the *j*th individual tree; CA_{ij}, the *i*th cambial age of the *j*th individual tree; α_0, α_1, and α_2, fixed-effect parameters; Tree_{0j}, Tree_{1j}, and Tree_{2j}, random-effect parameters at the *j*th individual tree level; ε_{ij}, residuals. The bold value represents the minimum AIC value among the developed models.

Table 3. Comparison of AIC values among eight models in each wood property.

Eq	Formula	Explanation about random-effect parameter	Wood fiber length	Vessel element length	Vessel frequency	Vessel diameter	Wood fiber diameter	Wood fiber wall thickness	Air-dry density	MOE	MOR	Compressive strength
1	$WP_{ij} = \beta_0 + Tree_{0j} + \varepsilon_{ij}$	*y*-Intercept	−192.00	−434.80	363.94	748.21	328.07	−4.978	**−258.04**	**135.03**	**393.27**	288.63
2	$WP_{ij} = (\beta_0 + Tree_{0j})CA_{ij} + \beta_1 + \varepsilon_{ij}$	Slope	−240.87	−441.43	**335.90**	702.80	338.60	−35.102	—	—	—	—
3	$WP_{ij} = \beta_0 CA_{ij} + \beta_1 + Tree_{1j} + \varepsilon_{ij}$	*y*-Intercept	−247.01	−442.62	339.56	697.85	315.94	−36.642	—	—	—	**287.60**
4	$WP_{ij} = (\beta_0 + Tree_{0j})\ln(CA_{ij}) + \beta_1 + \varepsilon_{ij}$	Slope	−261.36	−446.53	—	696.70	**315.41**	−77.056	—	—	—	—
5	$WP_{ij} = \beta_0 \ln(CA_{ij}) + \beta_1 + Tree_{1j} + \varepsilon_{ij}$	*y*-Value at 1st annual ring from the pith	**−263.82**	**−447.27**	338.56	**694.83**	—	**−77.955**	—	—	—	—
6	$WP_{ij} = (\beta_0 + Tree_{0j})CA_{ij}^2 + \beta_1 CA_{ij} + \beta_2 + \varepsilon_{ij}$	Opening quadratic parabolas	—	−421.71	—	—	348.45	−54.392	—	—	—	—
7	$WP_{ij} = \beta_0 CA_{ij}^2 + (\beta_1 + Tree_{1j})CA_{ij} + \beta_2 + \varepsilon_{ij}$	Slope of the tangent line at the *y*-intercept	−236.21	−421.67	—	—	341.92	−63.422	—	—	—	—
8	$WP_{ij} = \beta_0 CA_{ij}^2 + \beta_1 CA_{ij} + \beta_2 + Tree_{2j} + \varepsilon_{ij}$	*y*-Intercept	—	−422.77	—	—	—	−72.292	—	—	—	—

MOE, modulus of elasticity; MOR, modulus of rupture; WP_{ij}, wood properties at the *i*th cambial age of the *j*th individual tree; CA_{ij}, the *i*th cambial age of the *j*th individual tree; β_0, β_1, and β_2, fixed-effect parameters; $Tree_{0j}$, $Tree_{1j}$, and $Tree_{2j}$, random-effect parameters at the *j*th individual tree level; ε_{ij}, residuals; —, the model failed to converge or the model with *p*-values of the fixed-effect parameters more than 0.05. The bold value represents the minimum AIC value among the developed models.

were examined for physical and mechanical properties estimated at 1-yr intervals based on the optimum radial variation models with only fixed-effect parameters (Nezu et al 2022). The specific MOE and MOR were calculated by dividing the estimated MOE and MOR by air-dry density from the pith toward the cambium at 1-yr intervals.

RESULTS

The mean stem diameter of sample trees was 46.3 cm with about 25 annual rings (Table 1). Table 2 shows the comparison of AIC values in the models for cambial age-related change in stem diameter. The model with random effects of the individual tree on asymptote value (Eq I) was optimum among the three models. Figure 3 shows the regression curves of cambial age-related changes in stem diameter, CAI, and MAI based on the selected model (Table 2) with only fixed-effect parameters (Table 4). CAI increased until the cambial age of 5.4 yr, and MAI increased with increasing cambial age until 7.3 yr (Fig 3) then both indicators decreased toward the cambium. The stem diameters were around 17 and 23 cm at the cambial age showing maximum CAI and MAI values, respectively. Values were more than 2 $cm \cdot yr^{-1}$ until 25 yr (Fig 3), especially for MAI.

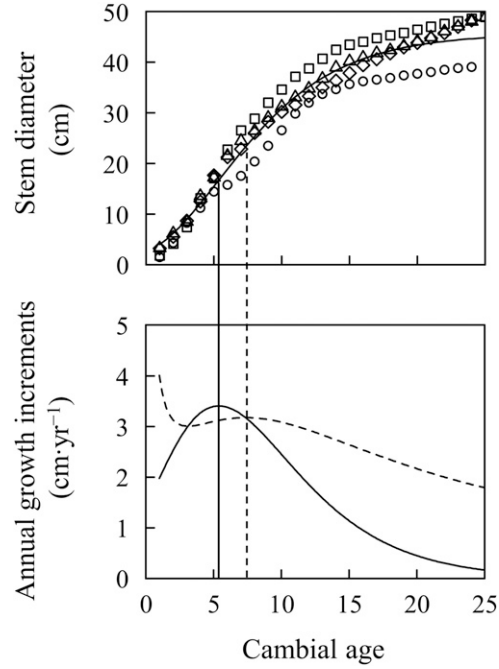

Figure 3. Cambial age-related changes in stem diameter and annual increment: Circles, squares, triangles, and diamonds represent measured values of the stem diameter in each individual tree. The solid curve in the upper figure represents the regression curve based on the selected model with only the fixed-effect parameters (Tables 2 and 4). Solid and dashed curves in the lower figure indicate CAI and MAI based on the selected model (Model I in Table 2) with only fixed-effect parameters. Solid and dashed lines in the vertical direction indicate cambial age showing maximum CAI (5.4 yr) and MAI (7.3 yr).

Individual mean anatomical, physical, and mechanical properties from pith to cambium were 1.01 mm in wood fiber length, 0.81 mm in vessel element length, 6.4 $No \cdot mm^{-2}$ in vessel frequency, 134 μm in vessel diameter, 27.4 μm in wood fiber diameter, 1.6 μm in wood fiber wall thickness, 0.29 $g \cdot cm^{-3}$ in air-dry density, 4.03 GPa in MOE, 40.3 MPa in MOR, and 15.4 MPa in compressive strength parallel to the grain, respectively (Table 1). Among the eight developed models for radial variation of wood properties, the logarithmic model (Eq 4 or 5) was well-fitted for all anatomical characteristics except for vessel frequency (Table 3). The *y*-intercept model (Eq 1) was an optimum model for explaining the radial variation of physical and mechanical properties except for compressive strength (Table 3). The linear model (Eq 2 or 3) fitted well for vessel frequency and compressive strength (Table 3). The selected model included a random intercept of individual trees for almost all wood properties, whereas the model with the random slope was selected for vessel frequency and wood fiber diameter. Based on the model selection, radial variations of measured anatomical characteristics and wood properties are shown in Fig 4 with regression lines or curves of only fixed-effect parameters (Table 4). For the selected models about cambial age-related changes in stem diameter and wood properties, the highest variance component ratio for individual trees was obtained for stem diameter (88.6%), followed by air-dry density (84.1%), MOE (49.1%), wood fiber wall thickness (30.7%), wood fiber length (26.6%), MOR

Table 4. Estimated values of the fixed-effect parameters of the selected models in each property in relation to cambial age.

Property	Eq	Parameter	Estimates	SE	*t*-value	*p*-value
Stem diameter	I	α_0	45.686	1.828	24.988	<0.001
		α_1	1.092	0.031	35.695	<0.001
		α_2	0.203	0.005	36.992	<0.001
Wood fiber length	5	β_0	0.0814	0.0070	11.615	<0.001
		β_1	0.8215	0.0220	37.295	<0.001
Vessel element length	5	β_0	0.0133	0.0025	5.308	<0.001
		β_1	0.1717	0.0062	27.511	<0.001
Vessel frequency	2	β_0	0.16	0.04	4.389	0.003
		β_1	4.39	0.34	12.744	<0.001
Vessel diameter	5	β_0	16.45	1.95	8.421	<0.001
		β_1	95.73	5.28	18.123	<0.001
Wood fiber diameter	4	β_0	1.110	0.245	4.532	<0.001
		β_1	24.855	0.474	52.457	<0.001
Wood fiber wall thickness	5	β_0	0.235	0.020	11.583	<0.001
		β_1	1.022	0.067	15.321	<0.001
Air-dry density	1	β_0	0.2930	0.0130	22.500	<0.001
MOE	1	β_0	4.0150	0.1873	21.430	<0.001
MOR	1	β_0	40.250	1.444	27.870	<0.001
Compressive strength	3	β_0	0.133	0.048	2.769	0.007
		β_1	14.002	0.723	19.357	<0.001

SE, standard error; MOE, modulus of elasticity; MOR, modulus of rupture. Fixed-effect parameters were estimated by the selected model (Tables 2 and 3).

(20.3%), compressive strength (15.2%), vessel diameter (12.3%), wood fiber diameter (4.9%), vessel element length (2.7%), and vessel frequency (0.1%) (Table 5).

Figure 5 shows the cambial age-related changes in MOE, MOR, AD, specific MOE, and specific MOR based on the selected radial variation model with only fixed-effect parameters listed in Table 4 for *P. tomentosa* and a reference for *L. tulipifera* (Nezu et al 2022). The air-dry density, MOE, and MOR in *P. tomentosa* were lower from the pith to the cambium and almost half of the values in the outermost compared with *L. tulipifera*. On the other hand, the specific MOE and MOR values were almost the same between these species over the time.

DISCUSSION

Cambial Age-Related Changes in Wood Properties

The mean values of wood properties in the present study (Table 1) were within the range of those in the previous studies (Kitamura and Imata 1955; Olson and Carpenter 1985; Tomczak et al 2023), although the tree age and sampling place differed among studies.

Several studies have examined radial variations of anatomical characteristics and wood properties at young ages (less than ca. 10 yr) of *P. tomentosa* planted in several countries (Kitamura and Imata 1955; Olson and Carpenter 1985; Tomczak et al 2023). Kitamura and Imata (1955) investigated air-dry density, MOE, MOR, and compressive strength of heartwood and sapwood in 6-yr-old plantation trees of *P. tomentosa* grown in Niigata, Japan. MOE and MOR did not differ between heartwood and sapwood, although heartwood had lower air-dry density and higher compressive strength than sapwood. Wood fiber length increased from the pith toward the cambium, reaching a length of 0.85-0.90 mm at 8 yr, and then decreased until 12 yr at 0.1 m above the ground in *P. tomentosa* naturally grown in southern Kentucky, United States (Olson and Carpenter 1985). Tomczak et al (2023) reported that wood fiber length, vessel element length, and vessel

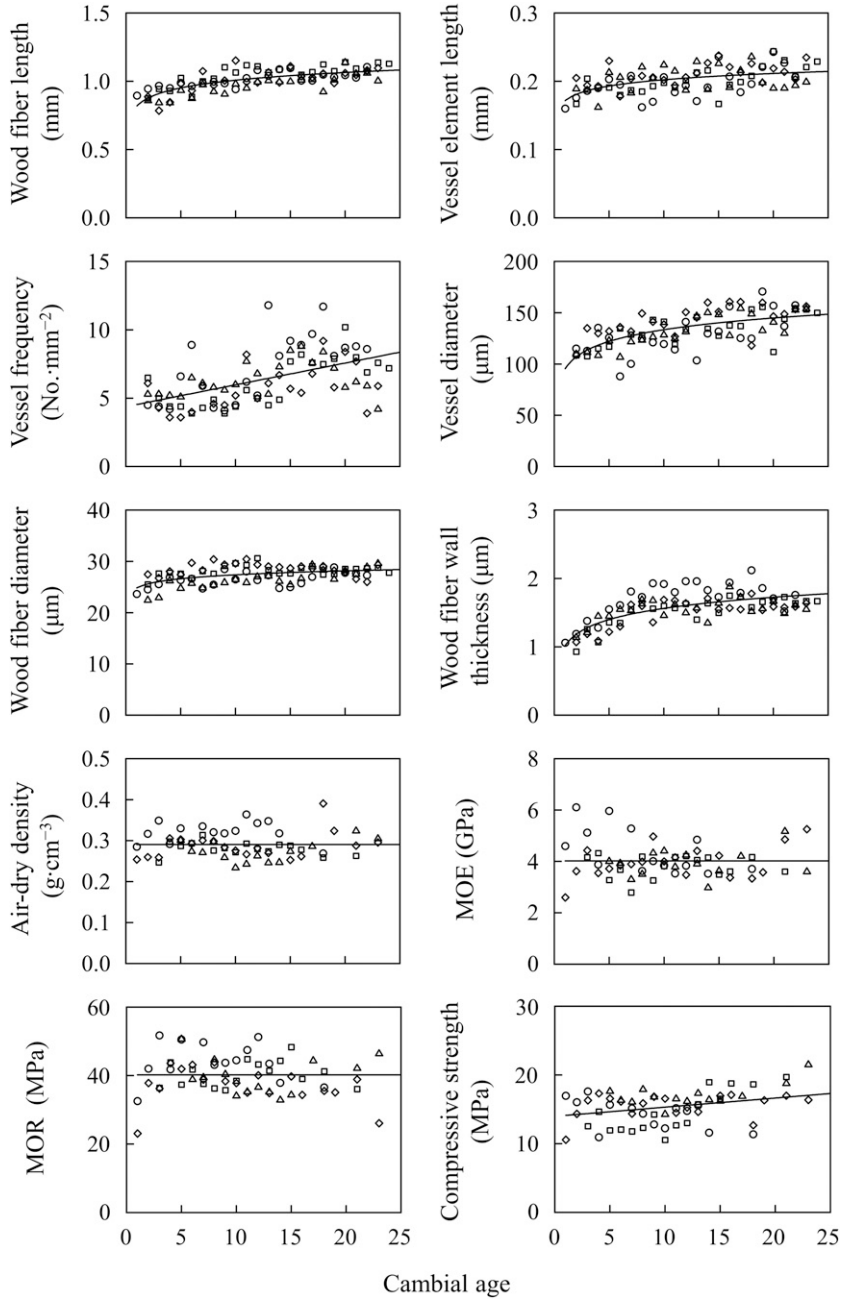

Figure 4. Cambial age-related changes in anatomical, physical, and mechanical properties: MOE, modulus of elasticity; MOR, modulus of rupture. Circles, squares, triangles, and diamonds represent measured values of each wood property. The solid line or curve represents the regression line or curve based on the fixed-effect parameters in the selected model (Tables 3 and 4).

Table 5. Variance component ratios of individual trees of the selected models in each property.

Property	V_{Tree}	V_E	V_{Tree} (%)
Stem diameter	12.888	1.662	88.6
Wood fiber length	0.7875×10^{-3}	0.2169×10^{-2}	26.6
Vessel element length	0.7826×10^{-5}	0.2794×10^{-4}	2.7
Vessel frequency	0.29×10^{-2}	2.14	0.1
Vessel diameter	20.83	149.13	12.3
Wood fiber diameter	0.087	1.699	4.9
Wood fiber wall thickness	0.811×10^{-2}	0.183×10^{-1}	30.7
Air-dry density	0.6704×10^{-3}	0.1269×10^{-3}	84.1
MOE	0.1319	0.1365	49.1
MOR	6.660	26.150	20.3
Compressive strength	0.795	4.429	15.2

V_{Tree}, variance component of individual tree; V_E, residual variance; V_{Tree} (%), variance component ratio of the individual tree to the total variance. MOE, modulus of elasticity; MOR, modulus of rupture. Fixed-effect parameters were estimated by the selected model (Tables 2 and 3).

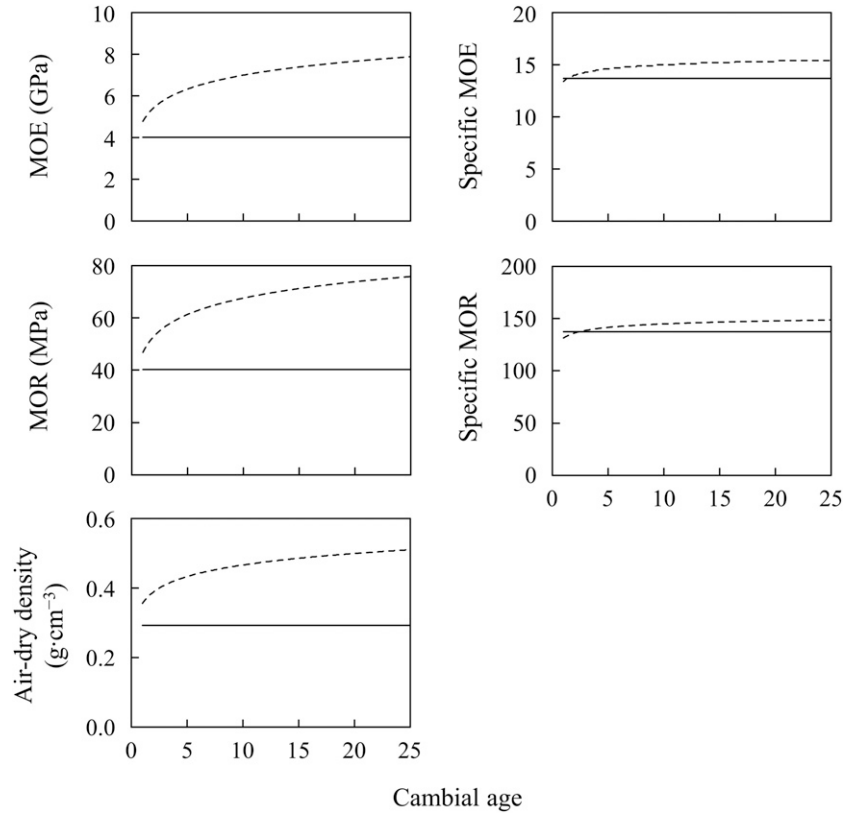

Figure 5. Cambial age-related changes in estimated physical and mechanical properties in *P. tomentosa* and *L. tulipifera*: MOE, modulus of elasticity; MOR, modulus of rupture; solid line, *P. tomentosa*; dotted curve, *L. tulipifera*. The MOE, MOR, and AD were estimated by the selected model with only fixed-effect parameters (Table 4 in this study for *P. tomentosa* and Nezu et al (2022) for *L. tulipifera*). Specific MOE and MOR were calculated by dividing MOE and MOR by estimated air-dry density.

diameter increased from the 1st to 4th annual rings in 4-yr-old *P. tomentosa* planted in Poland. In the present study, the model selected showed that all anatomical characteristics, except for vessel frequency, increased near the pith and then became stable toward the cambium (Fig 4). Vessel frequency and compressive strength gradually increased from the pith toward the cambium, while air-dry density, MOE, and MOR did not change with increased cambial age. The radial variation patterns of anatomical characteristics, MOE, and MOR in aged trees in the present study were similar to those previously found in younger trees (Kitamura and Imata 1955; Olson and Carpenter 1985; Tomczak et al 2023). On the other hand, radial trends in air-dry density and compressive strength differed between the present study and those by Kitamura and Imata (1955). However, the ratios of mean values in heartwood to sapwood for air-dry density and compressive strength were 1.00:0.96 (0.259 and 0.249 $g \cdot cm^{-3}$ in heartwood and sapwood) and 1.00:1.05 (19.6 and 18.6 MPa [200 and 190 $kg \cdot cm^{-2}$] in heartwood and sapwood), respectively, in the previous study (Kitamura and Imata 1955). The results suggest that there might be small differences in air-dry density and compressive strength among different radial positions. The result is similar to that of the present study (Fig 4). In summary, the xylem with uniform density and strength properties might be formed over the time in this species.

The selected model for explaining cambial age-related changes in wood properties included a random intercept of individual trees for almost all wood properties (Table 3). In addition, high variance component ratios (around 50% and more) of individual trees were found with air-dry density and MOE (Table 5). These findings suggest that although the patterns in all wood properties over the time were among individual trees, density and MOE might differed at the individual tree levels in *P. tomentosa*.

Ishiguri et al (2024) found that the MOR of 2 × 4 *P. tomentosa* lumber (38 × 89 mm × 1820 mm) from Tochigi, Japan with a 5% lower tolerance limit with a 75% confidence level was 12.1 MPa. MOR values of 2 × 4 lumber for construction, standard, and utility grades in the Notification of Ministry of Land, Infrastructure, Transport and Tourism No. 910 were 14.8, 8.2, and 3.9 MPa, respectively, in JS-II (*Cryptomeria japonica*), which is the most common plantation species in Japan (Japan 2 × 4 Lumber JAS Council 2023). Thus, the MOR values for *P. tomentosa* reported by Ishiguri et al (2024) exceeded values for utility grade but were lower than those for construction grade in JS-II. Since the MOR was stable from the pith to the cambium (Fig 4), wood for utility applications might be obtained at any radial positions in the stem.

Specific MOE and MOR values from pith toward the cambium were almost the same between *P. tomentosa* and *L. tulipifera* (Fig 5) suggesting a common ratio of xylem strength values to unit xylem volume among fast-growing tree species. To clarify this hypothesis, exploring cambial age-related changes should be conducted for other fast-growing tree species.

Relationships between Cambial Age-Related Changes in Radial Growth Increments of Stems and Wood Properties

We previously examined the relationships between the cambial age-related changes in radial growth increments of stems and wood properties in fast-growing tree species, *L. tulipifera* has grown in Japan (Nezu et al 2022). As a result, xylem maturation started at 9 yr after reaching the maximum CAI and MAI at 4.9 and 7.4 yr, respectively: a trade-off between radial growth rate and wood properties existed in *L. tulipifera* (Nezu et al 2022). Cambial ages showing the maximum CAI and MAI in *P. tomentosa* were similar to those in *L. tulipifera* (Nezu et al 2022)(Fig 3). To compare the volume at the same age between these two species, stem diameter at 15 yr (the maximum age of sampled trees for *L. tulipifera* in the previous study [Nezu et al 2022]) was estimated by substituting 15 for the explanatory variables in the best model with only the fixed-effect parameters for cambial age-related changes in stem diameter in each species. The estimated values of stem diameter at 15 yr were around 40 cm in

P. tomentosa and 20 cm in *L. tulipifera*, respectively. Therefore, the time to maximum CAI and MAI were almost the same between these species, but the stem diameter of *P. tomentosa* might be twice that of *L. tulipifera*.

Based on the radial variation modeling for each wood property, radial variations for anatomical characteristics, except for vessel frequency, were similar for both species (Fig 3, Nezu et al 2022), with each characteristic increasing from the pith outward and then stabilizing. On the other hand, the radial variations of air-dry density, MOE, and MOR in *P. tomentosa* (Fig 5) were stable from the pith toward the cambium, while they increased and then became stable in *L. tulipifera*. In addition, these properties in *P. tomentosa* were lower than those in *L. tulipifera*. Larjavaara and Muller-Landau (2010) stated that wood density generally mediates a trade-off between strength and economy of construction, with higher wood density providing higher strength but at a higher cost. They also hypothesized that a large trunk of low-density wood could achieve greater strength at a lower construction cost than a thin trunk of high-density wood. The trade-off supposed by Larjavaara and Muller-Landau (2010) might be related to the ability of *P. tomentosa* consistently form xylem with lower wood density, MOE, and MOR to achieve a faster radial growth compared with *L. tulipifera*.

CONCLUSIONS

In this study, cambial age-related change in stem diameter was well-fitted to the model with the Gompertz function. CAI and MAI reached their maximum at 5.4 and 7.3 yr, respectively. Based on the model selection for cambial age-related changes in wood properties, most anatomical characteristics increased from the pith and stabilized toward the cambium. On the other hand, air-dry density, MOE, and MOR did not change with increase in cambial age. The estimated fixed-effect parameters in the selected model were 0.29 $g \cdot cm^{-3}$ for air-dry density, 4.03 GPa for MOE, and 40.3 MPa for MOR, respectively. These results suggest that xylem with low but stable values of air-dry density, MOE, and MOR is formed for more than 20 yr in *P. tomentosa*. On these findings, in contrast to *L. tulipifera*, there might not be a trade-off between quantity and quality of wood for *P. tomentosa*: xylem with low and stable physical and mechanical properties is produced to keep a faster radial growth rate. Thus, the physical and mechanical properties of this species might be uniform regardless of whether the tree is in the young, middle, or old stages. Therefore, the rotation age of plantations of this species can be decided from the viewpoint of the quantity of wood. In addition, the wood obtained from the plantation can be used for the same final products (ie utility applications) at any growth stage. Based on the results of the present study, plantation forestry and wood utilization using fast-growing tree species are recommended based on the relationships between cambial age-related changes in quantity and quality of wood at the species level.

ACKNOWLEDGMENTS

Part of this research was financially supported by "Demonstration Project on Development of New Fuel Sources such as fast-growing trees" in "Support Project for Creating Stable and Effective Supply Systems of Woody Biomass Fuels (P21002)", New Energy and Industrial Technology Development Organization (NEDO), Japan. The authors would like to thank Ms. Akimi Fujita, Kaneyama Town Hall, Kaneyama, Fukushima, Japan, Ms. Norie Igarashi, Ai Power Forest, Mishima, Fukushima, Japan, and Sakuma Kensetsu Kogyo Ltd. Co., Mishima, Fukushima, Japan for helping wood sample collection. The authors would also like to thank Dr. Shigeru Kato and Mr. Masashi Nihei, Kankyo Kogai Bunseki Center, Utsunomiya, Tochigi, Japan, for helping with laboratory experiments.

REFERENCES

Akaike H, (1998) Information theory and an extension of the maximum likelihood principle. Pages 199-213 *in* E Parzen, K Tanabe, and G Kitagawa, eds. Selected papers of Hirotugu Akaike. Springer, New York.

Bates D, Mächler M, Bolker BM, Walker SC (2015) Fitting linear mixed-effects models using lme4. J Stat Soft 67(1):1-48.

Hirohashi A, Kojima M, Yoshida M, Yamamoto H, Watanabe Y, Inoue H, Kamoda S (2012) Wood properties of 6 fast-growing *Eucalyptus* species grown in Japan. Mokuzai Gakkaishi 58(6):339-346.

Ido H, Kojima E, Nagao H, Kato H, Matsumura Y, Matsuda Y (2023) Strength properties of Chinese fir timber collected from multiple sites. Bull FFPRI 21: 247-259.

Ishiguri F, Nezu I, Nihei M, Kato S, Otani N, Ohshima J, Yokota S (2024) Preliminary evaluation of bending properties in dimension lumber of *Paulownia tomentosa* as a fast-growing tree species in Japan. For Prod J 74(2): 159-164.

Japan 2 × 4 Lumber JAS Council (2023) https://www.2x4lumber.jp/about/04.html (8 June 2023).

Japanese Industrial Standards (2009) JIS Z 2101:2009. Methods of testing for woods. Japanese Standards Association, Tokyo.

Kataoka H, (1992) Shinrin to zouringaku [Forest and silviculture]. Pages 7–14 *in* Kawana A and Kataoka H eds. Zouringaku [Silviculture]. Asakura Publishing, Tokyo. (In Japanese).

Kitamura H (1956) Studies on the "kiri" (*Paulownia tomentosa* Steud.) wood (5) on the quality of wood from the natural forest in Fukushima Prefecture: Comparative note between the samples from Fukushima and Niigata Prefectures. J Jpn For Soc 38:400-408.

Kitamura H, Imata J (1955) Studies on the "kiri" (*Paulownia tomentosa* Steud) wood (report 3) wood study of *Paulownia tomentosa* Steud in Niigata Prefecture. Bull Agri Niigata Univ 7:122-129.

Koman S, Feher S, Vityi A (2017) Physical and mechanical properties of *Paulownia tomentosa* wood planted in Hungaria. Wood Res 62:335-340.

Kumakura K, (1957) Kiri saibai no Sankou [Reference for cultivation of *Paulownia*]. Kawaguchi Shoten, Niigata. 197 pp. (In Japanese).

Larjavaara M, Muller-Landau HC (2010) Rethinking the value of high wood density. Funct Ecol 24(4):701-705.

Nagata T, Du Val A, Schmull M, Tchernaja TA, Crane PR (2013) *Paulownia tomentosa*: A Chinese plant in Japan. Curtis's Bot Mag 30(3):261-274.

Nakagawa S, Schielzeth H (2010) Repeatability for Gaussian and non-Gaussian data: A practical guide for biologists. Biol Rev Camb Philos Soc 85(4):935-956.

Nasir GM, Mahmood I (2000) Preliminary study on wood properties of *Paulownia* species grown in Peshawar. Pakistan J For 50(1-2):49-55.

Nezu I, Ishiguri F, Ohshima J, Yokota S (2022) Relationship between the xylem maturation process based on radial variations in wood properties and radial growth increments of stems in a fast-growing tree species, *Liriodendron tulipifera*. J Wood Sci 68(1):48.

Olson JR, Carpenter SB (1985) Specific gravity, fiber length, and extractive content of young *Paulownia*. Wood Fiber Sci 17:428-438.

Pinheiro JC, Bates DM, (2000) Mixed-effects models in S and A-PLUS. Springer, New York. 528 pp.

R Core Team (2022) R: A language and environment for statistical computing. R Foundation for Statistical Computing, Vienna, Austria. https://www.R-project.org/ (1 October 2022).

Salas-Eljatib C, Mehtätalo L, Gregoire TG, Soto DP, Vargas-Gaete R (2021) Growth equations in forest research: Mathematical basis and model similarities. Curr For Rep 7(4):230-244.

Takashima T, Kawaguchi M, Miyake Y (1959) On the strength of kiri wood I: Bending strength and tensile strength. Mokuzai Gakkaishi 5:18-23.

Tomczak K, Mania P, Jakubowski M, Tomczak A (2023) Radial variability of selected physical and mechanical parameters of juvenile *Paulownia* wood from extensive cultivation in central Europe: Case study. Materials 16(7): 2615.

Tsuchiya R, Furukawa I (2008) The relationship between radial variation of wood fiber length, vessel lumen diameter, and the stage of diameter growth in *Castanea crenata*. Mokuzai Gakkaishi 54(3):116-122.

Tsuchiya R, Furukawa I (2009a) Radial variation in the size of axial elements in relation to stem increment in *Quercus serrata*. IAWA J 30(1):15-26.

Tsuchiya R, Furukawa I (2009b) The relationship between the maturation age in the size of tracheary elements and the boundary age between the stages of diameter growth in planted poplars. Mokuzai Gakkaishi 55(3):129-135.

Tsuchiya R, Furukawa I (2009c) Radial variation of vessel lumen diameter in relation to stem increment in 30 hardwood species. IAWA J 30(3):331-342.

Wood Mechanics of Wood Technology Division (1957) Comparisons of the strength and related properties of kokonoe-kiri and nippon-kiri grown in Japan. Bull Gov For Exp Sta 97:83-111.

Yokoo K, Koga Y, Sakagami H, Matsumura J (2021) Within-stem variation of wood properties in bud-pruned *Melia azedarach*. Mokuzai Gakkaishi 67(4):197-207.

Young SN, Lundgren MR (2023) C_4 photosynthesis in *Paulownia*? A case of inaccurate citations. Plants People Planet 5(2):292-303.

PERFORMANCE OF BAMBOO FIBER CORE BOARD AS SOFA CUSHION MATERIAL

Zhongyu Luo
Master's Degree Student
E-mail: luozhongyu@njfu.edu.cn

Ran Peng
Master's Degree Student
E-mail: 1020155332@qq.com

*Wei Xu**
Professor
E-mail: xuwei@njfu.edu.cn

Shuangshuang Wu
PhD Student
E-mail: wushuangshuang@njfu.edu.cn

Xiaoying Zhang
Master's Degree Student
College of Furnishings and Industrial Design
Nanjing Forestry University
Nanjing 210037, China
E-mail: zxy000221@163.com

(Received September 2024)

Abstract. Bamboo fiber is an environmentally friendly elastic material and its application in sofa upholstery material could minimize the environmental problems associated with traditional polyurethane foam. To explore the feasibility of bamboo fiber core board (BFCB) as a sofa cushion material, the indentation hardness, support factor, deformation recovery, and constant-load impact fatigue loss of two types of BFCBs were analyzed. The mechanical properties of BFCBs were compared with polyurethane foam commonly used as padding material for sofa upholstery. Yellow-BFCBs (Y-BFCBs) had better resilience, lower indentation hardness, better support performance, and less performance loss after fatigue than Moso bamboo. In addition, the thickness loss of Y-BFCB after fatigue treatment was greater than that of PU foam, while the loss of hardness was lower, and the loss of elasticity performance was the same as that of medium-soft foam. Moreover, the resilience of the Y-BFCB was the same as that of medium-soft sofa foam with a density of 35 kg/m^3. Y-BFCB has the potential to replace sofa polyurethane foam cushion material in practical applications. This study analyzed the mechanical properties of BFCBs and provided a theoretical basis for the application of bamboo fibers in sofa cushion materials.

Keywords: Bamboo fiber core board, compressive properties, resilience, fatigue loss.

INTRODUCTION

Sofas are an indispensable part of the living and socializing environment, and the type and combination of cushion material directly affect the mechanical properties and durability of the sofa. Polyurethane (PU) foam is the main raw material used in the production of sofa cushions due to its excellent mechanical properties and comfort (Chen et al 2017; Liu et al 2021). However, PU foam undergoes creep behavior under prolonged use, which leads to defects such as collapse and deformation of sofa cushions (Xu et al 2015). The main components of PU foam include polyols,

* Corresponding author

isocyanates, foaming agents, and catalysts that can potentially release hazardous gases. While closed-loop recycling and biodegradation of PUs have been extensively researched, they are still unsolved (Liu et al 2023). Therefore, it is important to explore environmentally friendly materials with favorable properties to replace traditional PU foam for sofa padding.

Numerous studies have been conducted on the application of plant fiber materials such as jute, bamboo, straw, luffa, and latex as padding materials in upholstered furniture. The majority of plant fiber cushions require adhesives to bond the dispersed fibers, which gives the cushions a high degree of hardness, poor ventilation, and incorporation of harmful substances such as formaldehyde (Chen et al 2018a, 2018b; Richely et al 2022). The use of thermoplastics as adhesives in cushion production reduces the use of chemical adhesives. Bamboo fibers showed promise in combination with thermoplastics in polymer composites, resulting in superior mechanical and physical properties of bamboo fibers (Yeh and Yang 2020). In addition, China is rich in bamboo resources, with 6.42 million hectares of bamboo forests producing more than 150 million tons of bamboo timber annually (Xiong et al 2020). Bamboo fiber composites have seen applications in mattresses, vehicle interiors, decoration, textiles, and other fields (Rocky and Thompson 2020).

Bamboo fiber core board (BFCB) is a newly developed composite material produced from raw bamboo fiber and low-melting-point polyester staple fiber (4080) by thermal pressing. Raw bamboo fiber obtained by milling and separating bamboo material retains the structure of bamboo fiber and has excellent thermal, antibacterial, and moisture absorption properties (Chan et al 2023). Low-melting-point fibers have excellent melt bonding and thermal stability and can be recycled by melt regeneration. Numerous studies have advanced the development of bamboo-fiber-reinforced thermoplastic polymer composites to improve the properties of bamboo fiber materials (Mahmud et al 2021; Radzi et al 2022). Yu et al (2023) evaluated bamboo-based upholstery blended with Ethylene-propylene side by side fibers and found that the modulus of elasticity of the unit had a significant effect on the change in the static seating pressure distribution of the upholstery and the subjective comfort. Wang and Young (2022) examined the mechanical properties of woven bamboo fiber-reinforced polypropylene composites and found that the tensile strength of composites increased after alkali treatment of bamboo fibers, while moisture-heat aging reduced the mechanical properties of the composites. Jitkokkruad et al (2023) investigated the effect of bamboo leaf fiber content on foam structure, mechanical properties, cushioning properties, and biodegradability of eco-friendly foam mats made of bamboo leaf fiber and natural rubber latex. Variations in fiber content affected the bulk density, indentation hardness, deformation characteristics, compressive properties, and cushioning coefficient of the foam mat. Bamboo fiber composites have great potential for application as sofa padding materials. Most of the above studies were related to the preparation process and properties of bamboo fibers; however, feasibility studies on the application of bamboo fibers in sofa cushions are almost nonexistent. The objective of this work was to develop bamboo fiber cushions as an alternative to PU foam.

In this study, the mechanical properties of two types of BFCB were tested for resilience, indentation hardness, support factor (SF), deformation recovery, and constant-load impact fatigue loss compared with those of PU foam. The possibility of replacing PU foam with BFCB as a sofa cushion was analyzed. The preferred material parameters for BFCB application to sofa cushions were identified.

MATERIALS AND METHODS

Materials

BFCB made from Yellow BFCB (Y-BFCB) and Moso BFCB (M-BFCB), are commonly produced in the Chinese market (Fig 1). Moso bamboo fibers are slender and stiff, with small cavities thick walls, and smooth inner and outer walls (Fig 1; Lian et al 2021; Li et al 2023).

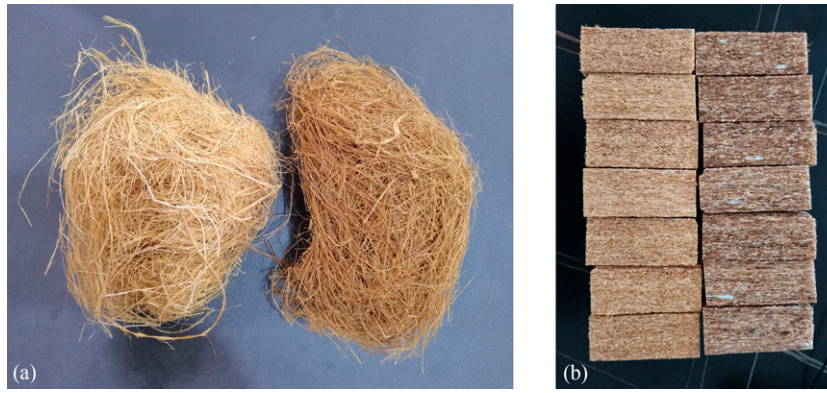

Figure 1. Examples of (a) yellow bamboo fiber (left); and Moso bamboo fiber (right).

BFCB and PU foam used for mechanical properties testing in this study were provided by Changsheng New Material Technology Co., Ltd. (Sichuan, China). BFCBs were prepared by hot pressing bamboo fibers and 4080 fibers at a 2:1 ratio. 4080 fiber is a low melting point fiber that mainly plays the role of bonding and curing bamboo fibers. This fiber can maintain the original network structure and physical and chemical properties of bamboo fibers. The fibers were uniformly blended, and the large clumps of fibers were loosened into smaller pieces. A carding machine was used to comb the small pieces of fiber into reticulated fiber layers. The fiber layers were evenly laid by a mesh-laying machine and repeatedly stacked to form a nonwoven blanket of a certain thickness. The nonwoven mats were thermoformed in a hot press at 180°C and 50 KPa for 5 min. The molded BFCBs were cut into pattern sizes for specific tests.

The densities and types of PU materials commonly used in the production of sofa padding layer materials in the enterprise were selected. Y-BFCBs and M-BFCBs with an apparent density of 80 kg/m^3 were selected. PU samples were selected as 35 kg/m^3 medium-soft foam (M-PU) and 37 kg/m^3 high-resilience foam (H-PU). According to the test standard GB/T 10807 (2006); the test specimen sizes were $100 \times 100 \times 50$ mm. All specimens were conditioned at 21-25°C and 45-55% RH before testing. Three blocks of each sample were tested, and each block was tested three times.

Experimental Design and Statistical Analysis

A one-way analysis of variance general linear model was used to analyze the mechanical properties of BFCBs. All significance levels were set at $p < 0.05$.

Load-Strain Curve and Indentation Hardness Test

Load-strain curves and indentation hardness of the materials were tested according to Chinese standard GB/T 10807 (2006) on a HD-F750A Foam Indentation Hardness Tester (Guangdong Province Dongguan Haida Instrument Co., Ltd., China). The specimen was positioned in the center of the support plate, aligned with the circular indenter above. The indenter descended on the upper surface of the specimen applying a force of 3-5 N. The preliminary thickness of the specimen was measured and recorded. The indenter continued to descend at a uniform speed of 100 mm/min.

The test concluded when the indentation thickness reached 95% of the original specimen thickness. The results were used to construct a load-displacement curve. Values were specifically recorded at 25%, 40%, and 65% of the original specimen thickness. The force value F_{40}, measured at 40% deformation was the indentation hardness index of the material. After unloading, the samples were allowed to recover in the experimental environment for 24 h. The SF and

deformation recovery (ε) of the material were calculated by Eqs 1 and 2.

$$SF = F_{65}/F_{25} \quad (1)$$

$$\varepsilon = (D_2 - D_1)/(D_0 - D_1) \times 100\% \quad (2)$$

where F_{25} is the value of the indentation force measured when the specimen is deformed by 25%; F_{65} is the value of the indentation force measured when the specimen is deformed by 65%; ε is the rate of shape recovery after 24 h; D_2 is the thickness of the specimen after 24 h of recovery from deformation (mm); D_1 is the thickness of the specimen after deformation (mm); and D_0 is the initial thickness of the specimen (mm).

Resilience Tests

The resilience test was conducted on a HD-F754 Foam Ball Rebound Tester (Dongguan Haida Instrument Co., Ltd.) by Chinese standard GB/T 6670 (2008). The test standard specifies that each sample is tested three times and the median is selected as the final resilience result for that sample. Three samples were evaluated for each material, and the mean value of the three samples was selected for statistical analysis. The specimen was positioned in the built-in groove of the Ball Rebound Tester to ensure that both the specimen and the instrument's transparent tube were placed horizontally. A 16 mm diameter steel ball (16.8 ± 1.5 g) was placed 500 mm vertically from the center of the test sample. The ball was released, and the value of the initial rebound height was recorded. The data were invalidated if the rebound hit the inner wall of the transparent tube. Resilience (R) was calculated by Eq 3.

$$R = \frac{H}{H_0} \times 100\% \quad (3)$$

where H is the bounce height of the ball (mm). H_0 is the height of the ball drop (mm).

Constant Load Impact Fatigue Test

Constant load impact fatigue of the sample material was determined by Chinese standard GB/T 18941 (2003). The sample was placed on the platform with ventilation holes of the HD-F750-1 Foam Fatigue Tester (Dongguan Haida Instrument Co., Ltd.). The vertical distance between the indenter and the upper surface of the specimen was adjusted to be the same as the thickness of the specimen. The indentation parameter was set at 750 ± 20 N. The specimen was subjected to impact testing at a rate of 70 cycles per minute. The test was terminated after 80,000 load cycles provided the sample remained centered on the circular indenter within the test period. The specimens were removed for 10 min of natural recovery under stress-free conditions. The test standard specifies that each sample is tested three times and the median is selected as the final resilience result for that sample. As the initial properties of the BFCB and PU foam materials differed widely, the absolute value of the performance reduction after testing also differed. The visual differences in fatigue loss were difficult to accurately measure. We compared the percentage of material fatigue loss. The fatigue loss rate for thickness, indentation hardness, and resilience were calculated from Eqs 4 to 6.

$$l = (L - L_0)/L \times 100\% \quad (4)$$

$$f = (F - F_0)/F \times 100\% \quad (5)$$

$$r = (R - R_0)/R \times 100\% \quad (6)$$

where l is the fatigue loss rate of the thickness of the sample; f is the fatigue loss rate of the hardness of the sample; r is the fatigue loss rate of the resilience of the sample; L is the initial thickness of the sample measured by vernier calipers(mm); L_0 is the thickness of the sample after constant load impact fatigue(mm); F is the initial indentation hardness value of the sample (N); F_0 is the indentation hardness value of the sample after constant load impact fatigue (N); R is the initial resilience of the sample (%); and R_0 is the resilience of the material after constant load impact fatigue (%).

RESULTS AND DISCUSSION

Load-Strain Curves

Figure 2(a) and (b) illustrate load-strain curves for the two types of BFCBs. Similar to latex and palm fiber mats, the stress-strain curve of BFCB displayed two stages (the plateau phase and the

densification phase; Liu et al 2022). The stress-strain curves of Y-BFCB samples had a narrower range and more consistent compression characteristics. Load-strain curves of M-BFCBs tended to be dispersed, and the test results obtained from different samples varied considerably. M-BFCB will require further stabilization before utilization as an elastic padding material due to the poor stability of its compressive mechanical properties.

Indentation performance was more uniform for high-resilience foam compared with medium-soft foam (Fig 2[c]), and the trend of stress increase during compression was stronger for high-resilience foam (Fig 2[d]). In comparison with BFCBs, the stress-strain curve of PU foam displayed three phases (linear, plateau, and densification phases). Due to the softness of the two PUs in the study, the PU samples underwent low stress at the start of the compression phase. Compressive stress progressively increased after the sample reached the plateau stage. The results revealed that the stress-strain curves of the BFCBs exhibited patterns similar to those of the foam materials and that the degree of deformation was linearly correlated with the magnitude of the force. The pore space of the fibers shrank as the degree of deformation rose, and the material eventually moved into the densification phase. The internal fiber structure was destroyed as a result of the indentation deformation, which also caused a substantial rise in stress. M-BFCBs contain more and finer bamboo fibers than Y-BFCBs at the same density. M-BFCBs entered the densification stage early due to the greater resistance between the fibers during compression.

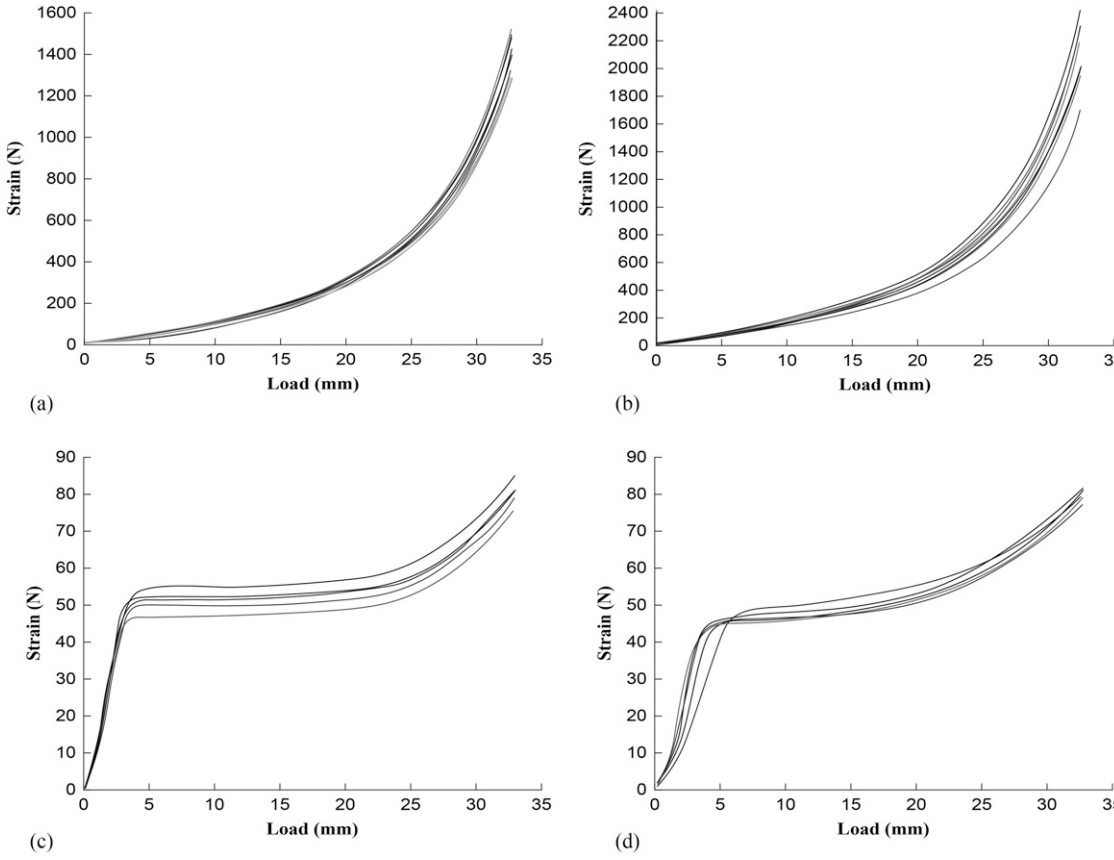

Figure 2. Stress-strain curves of (a) yellow bamboo fiber core boards, (b) Moso bamboo fiber core boards, (c) medium-soft foam, and (d) high-resilience foam.

Indentation Hardness

An independent samples t-test for the indentation hardness of the two types of BFCBs is shown in Table 1. The mean indentation hardness of Y-BFCBs was 229.14 N, and that of M-BFCBs was 322.17 N. The indentation hardness of M-BFCB was significantly higher than that of Y-BFCB (p-value < 0.001), and its mean indentation hardness value was 1.41 times higher than that of Y-BFCB. The type of raw bamboo material had a significant effect on the indentation hardness of BFCB. Yeh and Yang (2020) studied the effects of different bamboo-fiber-reinforced PP composites and also showed that bamboo species influenced the mechanical properties of composites and attributed the effects to differences in crystallinity and lignin content.

The average indentation hardness of the 35 kg/m^3 medium soft foam was 42.7 N, and that of the 37 kg/m^3 high resilience foam was only slightly lower at 41.2 N (Fig 3). The indentation hardness of both Y-BFCBs and M-BFCBs was higher than those of the two PU foam materials. M-BFCB had the highest indentation hardness, which was 7.61 times higher than that of medium-soft foam. The indentation hardness of the Y-BFCB was 5.20 times higher than the medium-soft foam. Indentation hardness is a visual reflection of the load-bearing properties and surface softness of flexible porous materials. Indentation hardness reflects the compactness and firmness of the buffer layer in compression. Gu et al (2016) used 25% and 65% indentation hardness and SFs to evaluate the mechanical properties of rattan cushions. The higher the indentation hardness value of the material, the higher the support capacity, but with less softness.

Table 1. The independent sample t-test results for indentation hardness and support factor of BFCB.

	Mean (SD)			
	M-BFCB (N = 9)	Y-BFCB (N = 9)	t-test	p-value
F_{40}	322.17 (32.67)	229.14 (12.98)	8.034	0.000**
SF	8.13 (0.72)	8.82 (0.62)	−2.594	0.018*

*$p < 0.05$.
**$p < 0.01$.
BFCB, bamboo fiber core board; M-BFCB, Moso-BFCB; Y-BFCB, yellow-BFCB.

Comparative analysis of BFCB and PU foam indicated that the indentation hardness of the two types of BFCBs was greater than PU foam, which was mainly due to the internal fiber structure of the BFCBs. The BFCB had higher indentation hardness and better load-bearing capacity than PU. The development of padding material for sofa cushions made of BFCB provides increased support capacity and meets the comfort needs of sofas for some populations. BFCBs need to be softened before application.

Support Factor

The SF gauges the ability of a material to support people using the furniture, which is directly proportional to the support force and the resistance against deformation. The SF of comfortable upholstery material is required to be greater than 2.8. As shown in Fig 3, the average SF values of M-BFCB, Y-BFCB, medium-soft foam, and high-resilience foam samples were 8.13, 8.82, 1.55, and 1.62, respectively. The average SF of the overall BFCB was 5.35 times higher than that of the PU foam. The mean SF of Y-BFCBs was significantly higher than that of M-BFCBs (Table 1). The SF of the BFCB was considerably higher than that of the foam material, which satisfied the support requirements of the sofa production standard for padding material. The BFCB was still in the linear phase when it was compressed to 25% of its thickness. The larger pores in the material were not completely compressed, with relatively minor values of F_{25}. The material entered the densification stage when the compression thickness of the BFCB reached 65%. The pores between the fibers were fully compressed, the force required for indentation increased dramatically, and the value of F_{65} far exceeded the value of F_{25}. Yu et al (2023) analyzed the hardness and supported the performance of the PU by using the indentation hardness and SF. The results showed that the PU samples were in the stabilization stage when compressed to 25% and 65% of their thickness. Due to the uniformity of PU materials, the difference between the values of F_{25} and F_{65} of PU samples was relatively minor, which made the SF values of the PU foam relatively small.

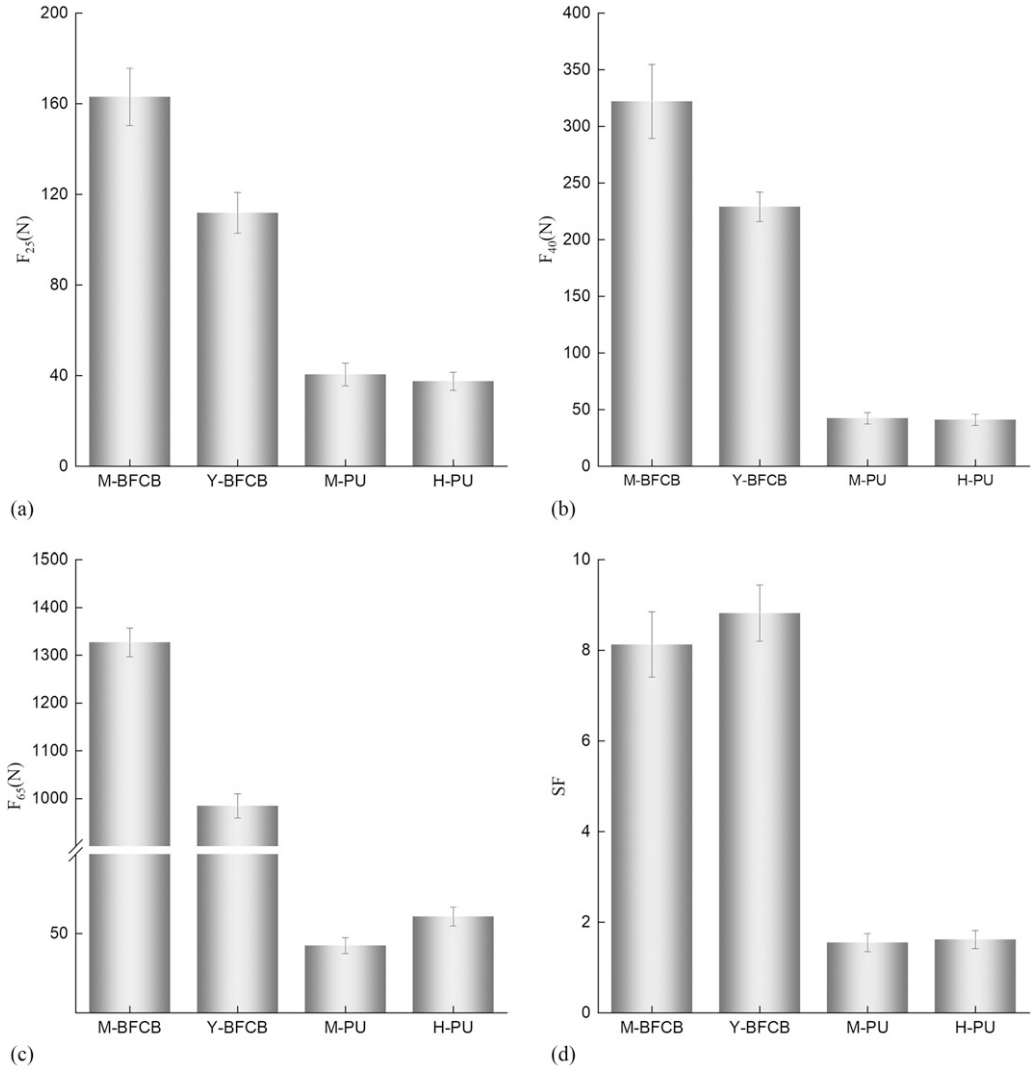

Figure 3. The mean F_{25}, F_{40}, and F_{65} values of BFCB and PU foam samples (a-c) and (d) mean SF of BFCB and PU foam samples. BFCB, bamboo fiber core board; H-PU, high-resilience foam; M-BFCB, Moso-BFCB; M-PU, medium-soft foam; PU, polyurethane; SF, support factor; Y-BFCB, yellow-BFCB.

Therefore, the support performance of BFCB was better than the medium-soft and high-resilience foam used in the test.

Deformation Recovery Rate

The deformation recovery rate reflects the ability of a material to regain its shape after use. The higher the deformation recovery rate, the better the ability of the sample to regain its shape after loading. The deformation recovery rates of different BFCBs and PU foam samples are shown in Fig 4(a). The mean deformation recovery rates of M-BFCB and Y-BFCBs were 29.6% and 40.5%, respectively. The mean deformation recovery rates of medium-soft PU foam and high-resilience PU foam were 56.2% and 63.2%, respectively. Table 2 summarizes the independent sample t-test results for the deformation recovery rate of BFCBs. Which showed significant

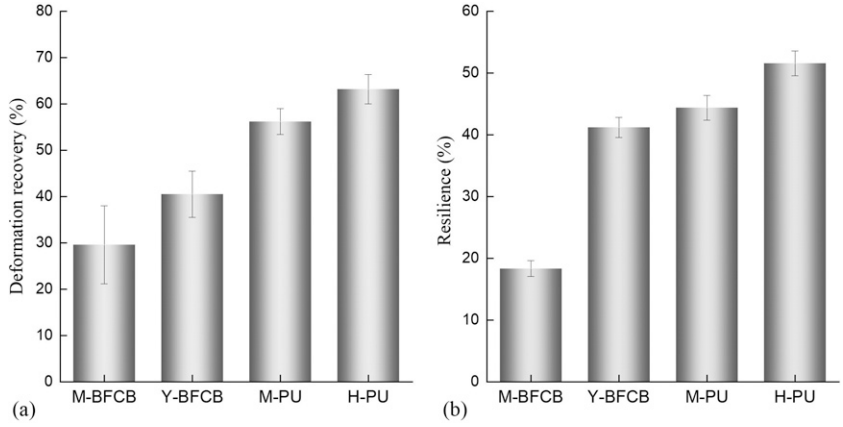

Figure 4. The mean (a) deformation recovery and (b) resilience of BFCB and PU foam samples. BFCB, bamboo fiber core board; H-PU, high-resilience foam; M-BFCB, Moso-BFCB; M-PU, medium-soft foam; PU, polyurethane; Y-BFCB, yellow-BFCB.

differences in the deformation recovery rates of the two types of BFCBs (p-value < 0.001). This is attributable to the fact that the BFCB had entered the densification stage; the pores between the fibers were compressed, and internal fiber deformation occurred when the sample was compressed to 65% of its thickness. After stress unloading, the bamboo fibers in compression slowly recovered from the deformation of the sample due to its internal stress. During the pressurization process, M-BFCBs were comparatively less able to recover from deformation due to the distortion of the fibers inside the boards. This was mainly due to the development of numerous microcracks as well as larger cracks appearing on the surface of fiber bundles and between fiber cells when bamboo fibers were compressed to the dense stage. These cracks would loosen the structure of bamboo fiber bundles (Chen et al 2017).

The lowest deformation recovery rate in the test samples was obtained from the M-BFCB, and the highest was obtained from the high-resilience PU foam. The average deformation recovery rate of medium-soft foam was 1.39 times higher than that of Y-BFCB and 1.90 times higher than that of M-BFCB. The overall deformation recovery rate of BFCB material was lower than that of PU foam, and the ability to return to shape after force was weaker than that of PU foam. The deformation recovery ability of BFCB was higher and closer to PU. Therefore, it has more potential to replace PU as cushion-filling material.

Resilience

The difference in the resilience of BFCB and PU foam was investigated in Fig 4(b). The average resilience of Y-BFCB, M-BFCB, medium-soft foam, and high-resilience foam was 41.2%, 18.6%,

Table 2. The independent sample t-test results for deformation recovery and resilience of BFCB.

	Mean (SD)			
	M-BFCB	Y-BFCB	t-test	p-value
Deformation recovery	29.60 (8.4)	40.50 (5.00)	−6.113	0.000**
Resilience	18.35 (1.30)	41.2 (1.61)	−33.073	0.000**

**$p < 0.01$.

BFCB, bamboo fiber core board; M-BFCB, Moso-BFCB; Y-BFCB, yellow-BFCB.

44.4%, and 51.6%, respectively. The resilience of M-BFCB with a density of 80 kg/m^3 was considerably lower than that of the other three materials. The content of 4080 fibers in M-BFCB was slightly higher than that in Y-BFCB. Compared with yellow bamboo, Moso bamboo had denser interfiber pores and a larger volume of individual pores. The interior of the large-volume pores was not supported by a fibrous structure. As a result, the Moso bamboo fibers were unable to provide sufficient resistance to the reaction force when impacted, and the M-BFCB was less resilient. Y-BFCB had a higher resilience, which was similar to that of medium-soft foam with a density of 35 kg/m^3, and the value was only 6.10% lower than that of medium-soft foam.

Table 2 shows the results of the independent sample t-tests for the resilience of BFCBs. The variety of raw materials used in BFCBs had a significant effect on resilience. The resilience of the Moso fiber core board was significantly lower than that of Y-BFCB (p-value < 0.001). According to Chinese industry standard QB/T 1952.1 2012 for the manufacture of upholstered furniture, the resilience performance of Grade A foam used in sofas should exceed 45%, that of Grade B foam should exceed 40%, and that of Grade C foam is supposed to exceed 35%. The resilience of Y-BFCB satisfied the standard of sofa padding, whereas the resilience of M-BFCB failed to reach the standard of sofa padding material. Y-BFCB was more applicable to upholstered sofa cushion material.

Constant-Load Impact Fatigue Loss

The mean loss of properties after constant load fatigue for the BFCB and PU foam samples are shown in Fig 5, while Table 3 illustrates the results of independent sample t-tests on the post-fatigue performance loss of BFCBs.

The rate of thickness reduction for M-BFCB was 4.0 times higher than that for medium-soft foam, while that for Y-BFCB was 4.6 times higher than that for medium-soft foam (Fig 5). The thickness reduction value of Y-BFCB was 1.2 times higher than that of M-BFCB, and the thickness reduction rate of medium soft foam was 1.4 times higher

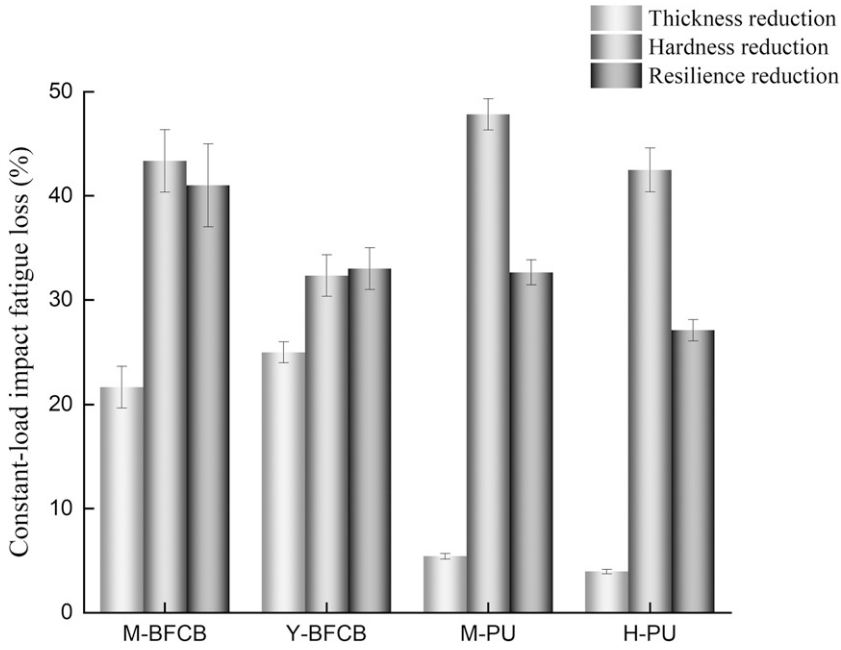

Figure 5. Mean constant load impact fatigue loss of BFCB and PU foam samples. BFCB, bamboo fiber core board; H-PU, high-resilience foam; M-BFCB, Moso-BFCB; M-PU, medium-soft foam; PU, polyurethane; Y-BFCB, yellow-BFCB.

Table 3. The independent sample t-test results for constant load impact fatigue loss of BFCB.

	Mean (SD)			
	M-BFCB	Y-BFCB	t-test	*p*-value
Thickness reduction	0.21 (0.02)	0.25 (0.01)	2.612	0.059
Indentation hardness reduction	0.43 (0.03)	0.32 (0.02)	4.928	0.008*
Resilience reduction	0.41 (0.04)	0.33 (0.02)	3.235	0.032*

*$p < 0.05$.

than that of high-resilience foam. There were no significant differences in the postfatigue thickness reduction of the two types of BFCBs (Table 3). Thickness reduction after the fatigue of BFCB was greater than that of PU foam material. BFCB specimens entered the densification stage under the repeated extrusion of the instrument indenter and the internal fiber structure was severely damaged. The internal force direction of the fibers of BFCB was complicated, making it difficult to return to the initial form after testing.

Hardness reduction rates of M-BFCB, Y-BFCB, medium-soft foam, and high-resilience foam were 43.6%, 32.3%, 47.8%, and 42.5%, respectively (Fig 5). There were significant differences between the hardness reduction values of the two types of BFCBs (p-value = 0.008; Table 3). The hardness reduction value of M-BFCB was 1.34 times higher than that of Y-BFCB. The hardness reduction values were the highest for medium-soft foam while those for Y-BFCB were the lowest, which was 0.67 times the hardness reduction value of medium-soft foam. The analysis revealed that the Y-BFCBs had the least hardness loss and outperformed the other three materials.

Resilience reductions of M-BFCB, Y-BFCB, medium soft foam, and high resilience foam were 40.7%, 33.0%, 32.6%, and 27.1%, respectively. There were significant differences in postfatigue resilience reduction of the two types of BFCBs (p-value = 0.032; Table 3). Resilience loss after fatigue treatment of M-BFCB material was 1.23 times higher than the Y-BFCB while that for Y-BFCB was slightly higher than that of PU foam material, which was 1.01 times higher than that of medium-soft foam.

Y-BFCB performed better than the M-BFCB after being fatigued. The Y-BFCB had a slightly higher rate of thickness loss than the two types of PU foam that are frequently used in sofa cushions, a lower rate of hardness loss than the PU foam, and a resilience performance loss that was equivalent to the medium-soft foam. The deformation rate of BFCB was smaller than that of Moso bamboo fiber after long-term use. Y-BFCB represents a better choice than M-BFCB for the development of bamboo fiber cushions. The production process of BFCB should be improved to reduce the fatigue loss rate.

CONCLUSIONS

1. Resilience, indentation hardness, compression deformation characteristics, deformation recovery, and constant-load impact fatigue loss of BFCBs were significantly influenced by bamboo species. The mechanical properties of Y-BFCB were better than those of M-BFCB.
2. The indentation hardness and SF of Y- and M-BFCB were noticeably higher than those of the PU foam, indicating that the BFCBs had better support properties but lower surface softness.
3. The thickness loss rate of Y-BFCB after constant load impact fatigue was greater than that of PU foam commonly used for sofa filler layers, but the loss of hardness was less than that of the PU foam, and resilience loss was comparable to medium-soft PU. In addition, the resilience of Y-BFCB complied with the standards for cushion-filling materials in the sofa manufacturing industry and had the potential to be applied as a sofa cushion-filling material.
4. Deformation recovery of BFCBs was lower than PU foam. Further studies are needed to produce softer BFCBs and analyze the dynamic

cushioning properties of these upholstery materials to model pressure and human comfort.

ACKNOWLEDGMENTS

The authors are grateful to Changsheng New Material Technology Co., Ltd. (Sichuan, China) for providing the experimental material. We also thank the College of Furnishings and Industrial Design of Nanjing Forestry University for supplying laboratories and equipment for this experiment. Last, but not least, we thank the International Cooperation Joint Laboratory for Production, Education, Research, and Application of Ecological Health Care on Home Furnishing; and the Ministry of Education Industry-University Cooperation Collaborative Education Project (202101148004) for supporting the project.

REFERENCES

Chan C-H, Wu K-J, Young W-B (2023) The effect of densification on bamboo fiber and bamboo fiber composites. Cellulose 30(7):4575-4585.

Chen Y, Su N, Zhang K, Zhu S, Zhao L, Fang F, Ren L, Guo Y (2017) In-depth analysis of the structure and properties of two varieties of natural luffa sponge fibers. Materials 10(5):479.

Chen Y, Yuan F, Guo Y, Hu D, Zhu Z, Zhang K, Zhu S (2018a) A novel mattress filling material comprising of luffa fibers and EVA resin. Ind Crops Prod 124:213-215.

Chen Y, Zhang K, Yuan F, Zhang T, Weng B, Wu S, Huang A, Su N, Guo Y (2018b) Properties of two-variety natural luffa sponge columns as potential mattress filling materials. Materials 11(4):541.

GB/T 6670 (2008) Flexible cellular polymeric materials—Determination of resilience by ball rebound. Standardization Administration of China, Beijing, China.

GB/T 10807 (2006) Flexible cellular polymeric materials—Determination of hardness (indentation technique). Standardization Administration of China, Beijing, China.

GB/T 18941 (2003) Flexible cellular polymeric materials—Determination of fatigue by constant-load pounding. Standardization Administration of China, Beijing, China.

Gu Y, Wu Z, Zhang J (2016) Load-deflection behavior of rattan chair seats. Wood Fiber Sci 48(1):13-24.

Jitkokkruad K, Jarukumjorn K, Raksakulpiwat C, Chaiwong S, Rattanakaran J, Trongsatitkul T (2023) Effects of bamboo leaf fiber content on cushion performance and biodegradability of natural rubber latex foam composites. Polymers (Basel) 15(3):654.

Li H, Xu W, Chen C, Yao L, Lorenzo R (2023) Temperature influence on the bending performance of laminated bamboo lumber. J Mater Civ Eng 35(5):04023072.

Lian C, Chen H, Zhang S, Liu R, Wu Z, Fei B (2021) Characterization of ground parenchyma cells in Moso bamboo (*Phyllostachys edulis*-Poaceae). IAWA J 43(1-2): 92-102.

Liu Q, Gu Y, Xu W, Lu T, Li W, Fan H (2022) Compressive properties of polyurethane fiber mattress filling material. Appl Sci 12(12):6139.

Liu B, Huang X, Wang S, Wang D, Guo H (2021) Performance of polyvinyl alcohol/bagasse fibre foamed composites as cushion packaging materials. Coatings 11(9):1094.

Liu B, Westman Z, Richardson K, Lim D, Stottlemyer AL, Farmer T, Gillis P, Vlcek V, Christopher P, Omar MMA (2023) Opportunities in closed-loop molecular recycling of end-of-life polyurethane. ACS Sustainable Chem Eng 11(16):6114-6128.

Mahmud S, Hasan KMF, Jahid MA, Mohiuddin K, Zhang R, Zhu J (2021) Comprehensive review on plant fiber-reinforced polymeric biocomposites. J Mater Sci 56(12): 7231-7264.

Radzi AM, Zaki SA, Hassan MZ, Ilyas RA, Jamaludin KR, Daud MYM, Aziz SA (2022) Bamboo-fiber-reinforced thermoset and thermoplastic polymer composites: A review of properties, fabrication, and potential applications. Polymers (Basel) 14(7):1387.

Richely E, Bourmaud A, Placet V, Guessasma S, Beaugrand J (2022) A critical review of the ultrastructure, mechanics and modelling of flax fibres and their defects. Prog Mater Sci 124:100851.

Rocky BP, Thompson AJ (2020) Production and modification of natural bamboo fibers from four bamboo species, and their prospects in textile manufacturing. Fibers Polym 21(12):2740-2752.

Wang B-J, Young W-B (2022) The natural fiber reinforced thermoplastic composite made of woven bamboo fiber and polypropylene. Fibers Polym 23(1):155-163.

Xiong X, Ma Q, Yuan Y, Wu Z, Zhang M (2020) Current situation and key manufacturing considerations of green furniture in China: A review. J Clean Prod 267: 121957.

Xu W, Wu Z, Zhang J (2015) Compressive creep and recovery behaviors of seat cushions in upholstered furniture. Wood Fiber Sci 47(4):431-444.

Yeh C-H, Yang T-C (2020) Utilization of waste bamboo fibers in thermoplastic composites: Influence of the chemical composition and thermal decomposition behavior. Polymers 12(3):636.

Yu Y, Zheng J, Pu H, Zhu C, Wu Q (2023) Preparation and evaluation of an elastic cushion with waste bamboo fiber based on sitting pressure distribution of the human body. Sustainability 15(9):7462.

TREATMENTS TO IMPROVE THE DIMENSIONAL STABILITY OF WHITE SPRUCE CLADDING

Diane Schorr
Scientist
E-mail: diane.schorr@fpinnovations.ca

Gabrielle Boivin
Scientist
FPInnovations
1055, rue du P.E.P.S.
Quebec City, Quebec, Canada G1V 4C7
E-mail: gabrielle.boivin@fpinnovations.ca

*Rod Stirling**
Manager, Biomaterials
FPInnovations
2665 East Mall
Vancouver, British Columbia, Canada V6T 1Z4
E-mail: rod.stirling@fpinnovations.ca

(Received February 2024)

Abstract. Most wood cladding, in North America, is coated with paint or stain. Key performance parameters include durability, dimensional stability of the wood, and adhesion and color stability of the coating. Changes in wood MC below the FSP result in dimensional changes. This creates stresses in the wood which may manifest as checks and cracks. These impact the appearance of wood products and limit the use of wood in some applications. Many chemical treatments to improve wood stability have been developed, though they are generally only applied to wood species with high permeability. The present work investigates several commercial-scale and lab-scale modification treatments for their ability to stabilize white spruce, a refractory softwood species typically produced as boards containing both sapwood and heartwood for cladding applications. Modified white spruce was evaluated for weight percent gain after treatment, dimensional stability in humidity and immersion, total color change after accelerated UV exposure, and coating adhesion before and after UV exposure. All treatments improved stability with antiswelling efficiency between 11 and 59%. However, these treatments were also associated with increased color change after accelerated UV exposure and poorer adhesion of an acrylic water-based stain. The improvements in dimensional stability were generally lower than those reported for permeable species, and it is unclear if they would meet end-user expectations for cladding performance. Additional research is needed to further enhance performance and overcome the resulting photostability and coating adhesion challenges.

Keywords: Cladding, dimensional stability, spruce, wood modification.

INTRODUCTION

Dimensional stability is particularly important in exterior applications, such as cladding and decking, where wood is exposed to large and rapid changes in MC, and for which checking and cracking negatively impact the esthetic value of the wood. In eastern Canada, white spruce (*Picea glauca* (Moench) Voss) is commonly used for exterior cladding applications. Refractory softwoods are the most abundant wood products in Canada and make up a significant proportion of the fiber available in many parts of the world. Many of these species, including most *Abies* and *Picea* species, have heartwood with low natural durability (Scheffer and Morrell 1998). These wood species are less competitive in certain exterior above-ground applications such as cladding,

* Corresponding author

due to their low natural durability and stability, and the difficulty of applying preservatives or chemical modification treatments. Anatomically, spruce differs from pine by its pit structure and by the diameter of its resin canals. Indeed, the piceoid pits found in spruces are a lot smaller than the pinoid pits of yellow pines (Wheat et al 1996), and the diameter of the resin canals of spruces are also a lot smaller than those of pines (Panshin and de Zeeuw 1980). In addition, the epithelial cells located inside the longitudinal and transverse resin canals of pines have thin walls (possibly nonlignified), whereas those of spruce have thick walls (more lignified). Together, these factors explain why liquid diffusion is more difficult in refractory species compared with permeable ones.

Wood stability is influenced by physical, ultrastructural, and chemical factors that affect wood–water relationships (Hillis 1984). Wood has a dynamic and complex relationship with water, continually absorbing and desorbing water as environmental conditions change. Moisture gain associated with exposure to liquid water or water vapor results in swelling until the FSP is reached. Similarly, wood shrinks as it dries below the FSP. This fundamental behavior limits the applications where wood can be used and impacts performance (Sargent 2019). This dimensional instability must be considered in applications where wood may be exposed to liquid water or significant changes in humidity. Fluctuating MC creates stresses in the wood that can result in checks and cracks. These checks and cracks affect the appearance of wood and can also lead to changes in mechanical properties. Wood that is naturally more stable, or treated to be more stable, may have a more natural uniform appearance valued by end users (Høibø and Nyrud 2010).

Treatments to improve the dimensional stability of wood have been studied for many years (Tarmian et al 2020). Physical approaches, such as kerfing or incising, do not alter the stability of the wood material but they can relieve moisture-induced stresses that lead to checking and cracking. These approaches have been shown to work on railway ties (Brentlinger 1960) and deck boards (Cheng and Evans 2018), but they are not applicable to all products.

Thermal modifications have been extensively studied for their ability to improve wood material properties (Stamm and Hansen 1937; Hill et al 2021). Improved dimensional stability is consistently reported for several different modification processes and species (Esteves and Pereira 2008; Militz and Altgen 2014; Sandberg and Kutnar 2016). This improvement is caused by chemical reactions in hemicellulose and lignin that result in increased crosslinking (Tjeerdsma et al 1998). One of the advantages of thermal modification is that it is not dependent on chemicals moving into the wood. This enables the stabilization of larger dimension pieces of refractory wood species (Zelinka et al 2022). Researchers have also explored chemical treatments to catalyze the thermal degradation reactions and enable them to occur at lower temperatures (Qu et al 2021; Wang et al 2022). Pretreatments with different aluminum solutions before thermal treatment were shown to significantly improve the dimensional stability of Chinese fir (*Cunninghamia lanceolata* (Lamb.) Hook) and Chinese white poplar (*Populus* × *tomentosa* Carrière) wood at relatively low temperatures (130-160°C). The stability achieved was similar or better than the dimensional stability achieved with only thermal treatment under high temperatures. Nevertheless, such pretreatments require penetration into the wood and may not be as effective on refractory species.

Water-repellent coatings or surface treatments that enhance hydrophobicity can improve dimensional stability by reducing the uptake of liquid water or atmospheric moisture. However, this is a potentially risky approach as any damage to the coating will expose wood that is susceptible to moisture and movement. Some coatings may also inhibit the drying of wood once it gets wet, which can create conditions that increase the risk of decay (Norton and Francis 2008; Schauwecker et al 2010).

Cell wall bulking treatments have been explored to stabilize wood. Rowell (1988) describes three types of chemical bulking treatments: nonbonded

and leachable, nonbonded and nonleachable, and bonded and nonleachable. Sugars, salts, and polyethylene glycol (PEG) are nonbonded and leachable. PEG has been extensively studied for its ability to stabilize wood (Stamm 1959; Schneider 1969) but has limited applications due to its leachability and hygroscopicity. Nonbonded and nonleachable treatments include treatments that form polymers in the wood, such as phenol-formaldehyde (Furuno et al 2004). Bonded and nonleachable treatments include chemical reactions with the cell wall. These include well-known chemical modification techniques, such as acetylation and furfurylation (FUR).

Acetylation results from the reaction of acetic anhydride with the hydroxyl groups in wood. The acetyl groups are less hygroscopic and leave the wood in a permanently swollen state. This reduces the ability of wood to absorb water. A 20% acetyl content has been reported to reduce shrinkage by about 70% (Stamm and Tarkow 1947). Acetylation of spruce has been reported, though test materials were limited to 1/8 in. (3.2 mm) thick (Tarkow et al 1955). Baird (1969) found vapor phase treatments with acetic anhydride and butyl isocyanate that could modify and stabilize wood, though it was noted that these would likely only be effective on thin materials.

Treatment of wood with furfuryl alcohol resin, catalysts, and heat has been reported to stabilize and enhance the properties of several wood species (Stamm 1977; Schneider 1995). The properties of furfurylated wood depend on the uptake and reaction of the furfuryl alcohol polymer with the wood cell wall. At high modification levels there is increased dimensional stability, mechanical properties, and resistance to biodegradation (Lande et al 2004). Detailed studies on the reactions between furfuryl alcohol polymer and the wood cell wall found evidence of condensation reactions between uncrowded ring positions and lignin side chains (Shen et al 2021).

Wood modification with dimethyloldihydroxyethyleneurea (DMDHEU) has been used to enhance wood properties, including dimensional stability (Militz 1993; Emmerich et al 2019). Research on DMDHEU treatments has focused on relatively permeable species (Militz and Norton 2013; Derham et al 2017).

Several organosilane treatments have been applied to permeable species (Schneider and Brebner 1985; Sèbe and Jéso 2000; Mai and Militz 2004). These treatments are associated with improved antishrink efficiency, lower moisture uptake, and increased durability (Donath et al 2004). Research into the mode of action has found that organosilanes influence the rate of moisture uptake, but do not reduce the maximum swelling (De Vetter et al 2010). This explains some of their poor results in laboratory decay tests yet good performance in field tests where moisture conditions are variable (De Vetter et al 2009). Improvements in the dimensional stability of white spruce impregnated and reacted with organosilanes have been reported (Schorr and Blanchet 2020).

More recently, wood modification with citric acid and sorbitol has been shown to improve dimensional stability and biological resistance (Larnøy et al 2018; Mubarok et al 2020). Lower EMC has been associated with covalent bonding and cross-linking of the polyesters with wood polymer constituents (Kurkowiak et al 2021). High molecular weight sorbitol-citric acid polyesters in the wood result in cell wall bulking (Kurkowiak et al 2023). Studies on wood modification with citric acid and sorbitol have been largely limited to permeable species such as pine (*Pinus sylvestris* L.) and beech (*Fagus sylvatica* L.) (Beck 2020; Mubarok et al 2020).

Chemical modification methods for enhancing the dimensional stability of wood have been extensively reviewed (Mai and Militz 2004; Rowell 2006; Kocaefe et al 2015; Gérardin 2016; Sandberg et al 2017; Sargent 2019). Most stabilization treatments, particularly those involving chemical impregnation, have focused on permeable woods or very thin specimens. It is unclear to what extent refractory wood species' anatomy affects the capacity of chemical treatment to improve dimensional stability.

This paper reports on selected modifications of white spruce lumber. White spruce is a North American softwood that generally has a thin band (approximately 3 cm, Quiñonez-Piñón and Valeo 2017) of relatively permeable sapwood surrounding larger volumes of refractory heartwood. Thin white spruce boards (>25 mm) milled for cladding or decking applications are often cut from the outer parts of the log and contain a mixture of sapwood and heartwood. This can manifest as sapwood corners, a sapwood edge, or a sapwood face depending on the cutting pattern employed. It is generally not feasible to cut pure sapwood boards from white spruce due to the relatively low volumes of sapwood present. The present work evaluated the dimensional stability and coating performance of commercially milled mixed sapwood-heartwood white spruce boards, modified with a series of commercial-scale and lab-scale treatments.

MATERIALS AND METHODS

Kiln-dried boards from a mix of heartwood and sapwood of white spruce (*Picea glauca* (Moench) Voss) without any knots or defects from Bois d'oeuvre Cedrico (Quebec, Canada) were used for this study.

Commercial Treatments

For all these commercial treatments, the processes are proprietary and some information cannot be disclosed.

Furfurylation treatment. FUR treatment parameters were described by Boivin and Schorr (2022). Ten white spruce boards (5.9 mm × 127 mm × 1219 mm) were treated by FUR using a commercial process. This process used furfuryl alcohol, which is manufactured industrially by catalytic reduction of furfural. It included a wood impregnation step with furfuryl alcohol and catalysts, followed by a curing step where the furfuryl alcohol was polymerized within the wood cell walls. The treatment is a vacuum pressure process and a heating treatment.

Citric acid: sorbitol treatment. Treatment parameters were described by Schorr et al (2024). Ten white spruce boards (19 mm × 152 mm × 1200 mm) were vacuum-treated for 1 h at 40 mb and then pressure-treated for 2 h at 8 bars with an aqueous citric acid and sorbitol solution in a pilot plant in Norway. Heat treatment at 140°C for 12 h was then initiated.

Thermal modification. The thermal modification was performed by a commercial producer in Quebec, Canada on five white spruce boards (25.6 mm × 152 mm × 2438 mm) in a closed system (atmospheric pressure and oxygen-free) with a maximum temperature of 220°C. After modification, the wood was steam conditioned to a final MC between 3 and 7%.

Laboratory Treatments

Organosilanes and metal treatments. Four laboratory treatments were evaluated in this work. These included an organosilanes treatment (SiTT) and organosilanes treatment followed by impregnation with aluminum (SiTT + Al), as the literature suggests that inorganic solutions, in particular aluminum solutions, can be used as thermal catalysts (Ximenes and Evans 2006; Qu et al 2021; Wang et al 2022). Two inorganic treatments were also evaluated without organosilanes treatment: aluminum treatment alone (Al) and magnesium treatment alone (Mg). Methyltrimethoxysilane (MTMS) (>98%) and hexadecyltrimethoxysilane (HDTMS) (95%) were provided by Gelest, Inc. (Morrisville, PA) and glacial acetic acid (>99%), ethyl alcohol, and aluminum sulfate ($Al_2(SO_4)_3$) (>97%) were provided by Sigma-Aldrich (Toronto, Canada) and magnesium chloride ($MgCl_2$) (>99%) by Laboratoire MAT (Quebec, Canada). The organosilanes solution was prepared by mixing MTMS, ethyl alcohol, glacial acetic acid, and HDTMS in a 1:3.9:0.05:0.33 mass ratio, respectively. First MTMS was mixed with ethanol, then, glacial acetic acid was slowly added to the solution, which was stirred at 60°C for 30 min. Finally, HDTMS was added, and the solution was stirred for 60 min. Treatment parameters are described by Schorr et al (2022).

Inorganic treatment alone with aluminum or magnesium cycle impregnation was also evaluated on white spruce wood to assess the possibility of using these inorganic treatments along with mild temperature thermal treatment instead of higher temperature thermal treatment. For the aqueous inorganic treatment, the solution was prepared with $Al_2(SO_4)_3$ or $MgCl_2$ in distilled water. The concentration of the $Al_2(SO_4)_3$ was 0.44 M. The concentration of the $MgCl_2$ solution was 1.57 M.

Fifteen white spruce boards of 19 mm × 88.9 mm × 254 mm were subjected, for each laboratory treatment, to a 20-min vacuum and then 2 h pressure treatment cycle with organosilanes solutions and/or aluminum or magnesium solutions (see sequence in Table 1). After 24 h at ambient temperature, all treated samples were heat treated at 120°C for 24 h.

Weight Percent Gain

All boards before and after treatment were conditioned at 20°C and 50% RH. The weight of the boards before and after treatment was measured, and weight percent gain (WPG) was calculated using the following equation:

$$\mathrm{WPG} = \frac{\boldsymbol{W_1} - \boldsymbol{W_0}}{\boldsymbol{W_0}} \times 100 \qquad (1)$$

where W_0 is the weight of the samples before treatment (stabilized in a conditioning room at 20°C and 50% humidity) and W_1 is the weight of the samples after treatment and after stabilization in a conditioning room at 20°C and 50% humidity.

Dimensional Stability

Humidity. Fifteen specimens were taken from the boards of each treatment. For laboratory treatments, one specimen was cut from each board treated. For commercial treatments, two or three specimens were cut from each board (three samples from each thermally treated boards of 2438 mm long and two samples from each chemically treated boards of 1219 mm long). All test specimens (50 mm × 50 mm × 16 mm) were placed in a conditioning chamber at 20°C/50% RH until mass was constant (difference of less than 0.2% after 24 h) and dimensions constant (difference of less than 0.1 mm after 24 h). Once stable, the mass of the samples was recorded, and radial, tangential, and longitudinal dimensions were measured using a caliper. The same specimens were then placed in a conditioning chamber at 20°C/90% RH. When the masses were constant, the radial, tangential, and longitudinal dimensions were measured using a caliper. The samples were then returned to 20°C/50% RH. This cycle was repeated three times.

Dimensional stability was determined by anti-swelling efficiency (ASE). A higher ASE indicates greater dimensional stability. ASE is calculated from the swelling coefficients of treated and untreated samples, subjected to different conditions, according to equations taken from DIN 52184 (DIN 1979)

$$\mathrm{Sw_{ctrl}} = \left(\frac{V_{\mathrm{ctrl90}} - V_{\mathrm{ctrl50}}}{V_{\mathrm{ctrl50}}}\right) \times 100 \qquad (2)$$

$$\mathrm{Sw_{tr}} = \left(\frac{V_{\mathrm{tr90}} - V_{\mathrm{tr50}}}{V_{\mathrm{tr50}}}\right) \times 100 \qquad (3)$$

$$\mathrm{ASE}\ (\%) = \left(\frac{\mathrm{Sw_{ctrl}} - \mathrm{Sw_{tr}}}{\mathrm{Sw_{ctrl}}}\right) \times 100 \qquad (4)$$

where V_{ctrl90} is the volume of the sample untreated at 90% RH; V_{ctrl50} is the volume of the sample untreated at 50% RH; V_{tr90} is the volume

Table 1. Details of the different impregnation cycles done with organosilanes, aluminum, or magnesium solution on white spruce wood for each treatment.

Treatments	Cycle with organosilanes	Cycle with aluminum	Cycle with magnesium
SiTT (organosilanes)	✓	—	—
SiTT + Al (organosilanes + aluminum)	✓	✓	—
Al (aluminum)	—	✓	—
Mg (magnesium)	—	—	✓

of the sample treated at 90% RH; and V_{tr50} is the volume of the sample treated at 50% RH.

Immersion. Fifteen specimens were taken from the boards of each treatment. For laboratory treatments, one specimen was cut from each board treated. For commercial treatments, two or three specimens were taken from each board (three specimens from each thermally treated boards of 2438 mm long and two specimens from each chemically treated boards of 1219 mm long). All test specimens (50 mm × 50 mm × 16 mm) were placed in a conditioning chamber at 20°C/50% RH until mass was constant (difference of less than 0.2% after 24 h) and dimensions constant (difference of less than 0.1 mm after 24 h). Once stable, the mass of the samples was recorded, and radial, tangential, and longitudinal dimensions were measured using a caliper. The same samples were then immersed in a distilled water bath at 22°C. When the masses were constant (difference of less than 0.2% of mass after 24 h), the radial, tangential, and longitudinal dimensions were measured using a caliper. The samples were then returned to 20°C/50% RH. The immersion cycle was repeated twice. Dimensional stability was calculated based on initial and final dimensions, compared with those obtained for untreated samples using the same calculations presented above for dimensional stability.

Preparation of Finished Samples

Three treated and untreated samples (76.2 mm × 76.2 mm) were finished with a semitransparent acrylic stain. Two coats of stain were applied in accordance with the manufacturer's recommendations. Specimen surfaces were previously sanded with P80 abrasive paper. For specimens placed in an accelerated UV exposure chamber, the sides and back were sealed with epoxy.

Accelerated UV Exposure

Accelerated UV exposure tests were conducted over a period of 2000 h on three unfinished and three finished specimens (76.2 mm × 76.2 mm) per series (untreated, organosilanes, organosilanes + aluminum treated, furfurylated, and esterified white spruce). The samples were placed in a Q-Sun from Q-Lab (Westlake, OH) according to ASTM G155-21 (ASTM 2021). Cycle 1 was followed based on the parameters listed in Table 2.

Color measurements were taken initially, after 250, 500, 1000, and 2000 h of accelerated UV exposure using a Check3 Spectrophotometer from Datacolor (Lawrenceville, NJ), which was quantified using the CIE L*a*b* color space coordinates (Eq 5). The samples were scanned at the same intervals.

$$\begin{aligned} \Delta L^* &= L_1^* - L_0^* \\ \Delta a^* &= a_1^* - a_0^* \\ \Delta b^* &= b_1^* - b_0^* \end{aligned} \tag{5}$$

The total color change (ΔE*ab) was calculated using the equation as follows:

$$\Delta E_{ab}^* = \left[(\Delta L^*)^2 + (\Delta a^*)^2 + (\Delta b^*)^2 \right]^{1/2} \tag{6}$$

Crosshatch Test

Coating adhesion performance was assessed before and after accelerated UV exposure, pursuant to ASTM D3359-2023 method B (ASTM 2023) using a precision knife (X-Acto® knife) and a Gardco Temper II template. Three replicates were performed per series. This test was performed on the finished samples only. The samples were rated (from 0B, no adhesion to 5B, perfect adhesion) based on the classification presented in Table 3. Visibility of the underlying wood structure indicates poor coating adhesion.

RESULTS AND DISCUSSION

Application of Stabilization Technologies to White Spruce

White spruce boards were modified with seven treatments to find which treatment is the most suitable to improve the durability and stability of this refractory species for cladding applications. Some treatments are commercially available, such as thermal modification, FUR, and citric

Table 2. Cycle 1 parameters following standard ASTM G155-21.

Exposure duration (h)	2000
Filter	Daylight
Irradiance W/(m^2 • nm)	0.35
Wavelength (nm)	340
Step 1	102 min light, 50% RH at 63°C (black panel temperature), air chamber temperature at 44°C
Step 2	18 min light, water spray at a rate of 5 s/min. RH and black panel not controlled. Air chamber temperature at 44°C

acid sorbitol esterification (SOR), which are mostly used on permeable species. White spruce boards were also treated, at the lab scale, with different noncommercial treatments; organosilanes (SiTT), a combination of aluminum and organosilanes (SiTTAl), aluminum aqueous solution (Al), magnesium aqueous solution (Mg).

Table 4 presents the WPG after treatment on white spruce. Lab scale treatments all showed a WPG of 15% or lower. Low WPG was expected for all laboratory treatments, as the solution strengths were low. Moreover, treatments were not meant to fill the lumen. The low WPG for the aluminum aqueous solution can be explained by the fact that it is mostly used as a thermal catalyst, so it does not react to the wood (Qu et al 2021). Indeed, in Schorr and Boivin (2023), the leaching test on aluminum-treated wood showed that it was leachable.

Commercial treatments with a vacuum-pressure process (FUR and SOR) show similar WPG of 26 and 25%, respectively. For FUR treatment, studies on permeable species, such as Scots pine, have shown that WPG could vary between 15 and 47% depending on the properties needed (Westin et al 2004). For pine (*Pinus pinaster*), a WPG of 38% was obtained (Esteves et al 2011). For Norway spruce, an average WPG of 63% was observed with FUR treatment, but this is due to the small size of the 14 mm diameter cylindrical samples or $1 \times 40 \times 40$ mm^3 samples used (Thygesen et al 2010). For citric acid SOR treatment, permeable species, such as Scots pine, showed a high WPG of 62%. For another refractory species (Norway spruce, *Picea abies* (L.) H. Karst.), a similar WPG as white spruce was obtained (24%) (Schorr et al 2024). Higher WPG was observed for commercial treatments for white spruce in comparison with one obtained with the laboratory scale treatments. This can be explained by the fact that the commercial treatments are meant to fill the lumens and create cross-linking within the wood, which results in a weight increase. WPG for the thermal modification process was not presented as this is not an impregnation process.

Table 3. Classification of adhesion test results according to ASTM D3359-23 (method B).

Classification	Description
5B	The edges of the cuts are completely smooth; none of the squares of the lattice is detached.
4B	Small flakes of the coating are detached at intersections; less than 5% of the area is affected.
3B	Small flakes of the coating are detached along the edges and at intersections of cuts. The area affected is 5-15% of the lattice.
2B	The coating has flaked along the edges and on parts of the squares. The area affected is 15-35% of the lattice.
1B	The coating has flaked along the edges of cuts in large ribbons and whole squares have detached. The area affected is 35-65% of the lattice.
0B	Flaking and detachment are worse than grade 1.

Table 4. Average weight percent gain (WPG) in white spruce after each treatment.

	Chemical treatment	WPG after treatment (%)[a]
Lab scale treatment	Al (aluminum)	4 (5)
	Mg (magnesium)	15 (4)
	SiTT (organosilanes)	11 (5)
	SiTTAl (organosilanes + aluminum)	12 (6)
Commercial treatment	FUR (furfurylation)	26 (7)
	SOR (esterification)	25 (19)

[a]Standard deviations appear in parentheses.

Dimensional stability. Figure 1 shows the humidity and immersion volumetric dimensional stability (ASE) of white spruce samples treated with each of the lab scale and commercial treatments (FUR, SOR, and thermal modification). Organosilanes lab scale treatments had a WPG of 11% and showed the lowest dimensional stability (between 21 and 33%). Donath et al (2004) evaluated the stability of wood modified with several organosilanes and found WPG between about 10 and 25% and ASE values up to approximately 30% in treated beech wood. This is comparable to the values found in the present study. The inorganic lab scale treatments (Al and Mg) are the ones that show the highest humidity and immersion ASE (>50%) with a WPG of 4% for aluminum and 15% for magnesium treatment. Ximenes and Evans (2006) reported high ASE (between 45 and 105%) for Scots pine (*Pinus sylvestris* L.) sapwood treated with aluminum hydroxide and magnesium aluminate . Wang et al (2022) observed, for Chinese white poplar (*Populus* × *tomentosa* Carrière), dimensional stability in the radial and tangential direction of between 35 and 62% depending on the concentration of aluminum chloride ($AlCl_3$) used. These authors

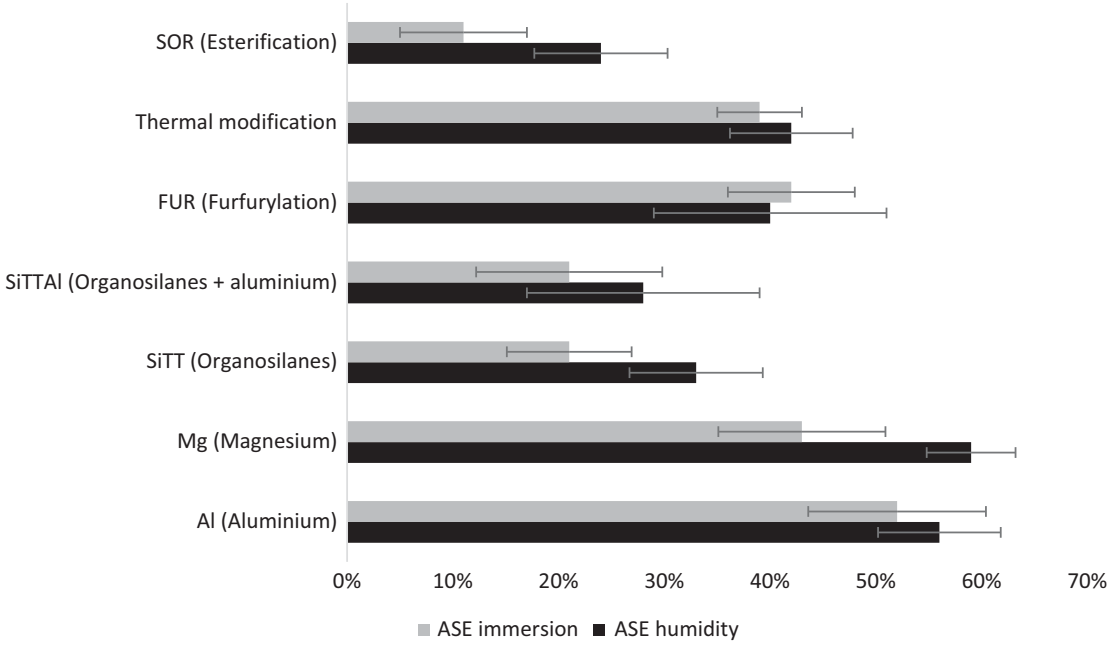

Figure 1. Average volumetric antiswelling efficiency (ASE) under humidity conditions and after immersion for white spruce treated with different treatments.

explained that the aluminum solution impregnated into the wood before treatment was used as a thermal catalyst. They concluded that the hydrolysis of polysaccharides was accelerated by $AlCl_3$ acid. Depolymerization and repolymerization of lignin in this $AlCl_3$ environment during heat treatment could be promoted. The high antiswelling efficiency observed for magnesium and aluminum treatment (43-59%) under humidity and immersion conditions for white spruce mixed heartwood and sapwood is similar to the results obtained in those studies.

For the commercial treatments, the highest stability was obtained with the FUR treatment and thermal modification (around 40%). The FUR modification of white spruce had an average WPG of 26% with volumetric ASE of 40% with changes in RH. There was considerable variability likely due to variation in the proportion of sapwood and heartwood within this specimen. In previous work on *Cryptomeria japonica* sapwood, Baysal et al (2004) reported an ASE of 85% at a WPG of 122%. In previous work on *Pinus pinaster*, Esteves et al (2011) reported an ASE of 46% at a WPG of 40%. Westin et al (2004) reported an ASE of 30-35% at a WPG of 15% for Scots pine sapwood. By increasing the WPG up to 47% in the furfurylated Scots pine, the ASE was up to 70% (Westin et al 2004). For Scots pine sapwood, Lande et al (2004) reported an ASE of approximately 50% at a WPG of 32%. Lande et al (2004) evaluated ASE at four different WPG levels and observed a correlation between WPG and ASE with higher uptakes associated with higher degrees of stabilization. The limited uptake achievable with white spruce will likely limit the degree to which the wood can be stabilized. However, based on the reported uptake, the ASE obtained for white spruce was slightly lower than that reported on other species. The present study did not control for the source of the white spruce evaluated. Previous research on Norway spruce has shown significant differences in furfuryl alcohol uptake based on the growth conditions, tree characteristics, location within the stem, and drying method (Lande et al 2010). Similar variations in white spruce may occur but were not assessed as part of the present work. The SOR modification of white spruce had an average WPG of 25% with volumetric ASE of 24% with changes in RH. Studies on European beech (*Fagus sylvatica*) sapwood at comparable WPG (22%) found ASE between 44 and 52% (Mubarok et al 2020). For Scots pine sapwood with sorbitol and citric acid, the ASE was 72% with a WPG of 62% (Schorr et al 2024). These are approximately double the ASE that we found in this study for the white spruce, which is explained because of the mixed sapwood and heartwood present in the white spruce samples studied.

Thermal modification showed slightly lower stability than the FUR treatment for refractory species but is still at 42% (humidity) and 39% (in immersion). Thermal modification is one of the most promising technologies for refractory species because it does not require the penetration of chemicals into the wood. The dimensional stability of refractory species can be significantly improved by thermal modification (Bekhta and Niemz 2003; Lekounougou and Kocaefe 2014). However, improvements in decay resistance are limited to above-ground applications, and the wood remains susceptible to termites (Shi et al 2007; Candelier et al 2017; Mubarok et al 2019).

Combined thermal modification and chemical treatments have been studied (Salman et al 2014; Wang et al 2018; Qu et al 2021) and may be able to overcome these technical challenges, though lower-cost solutions may be needed to commercialize this approach. Moreover, this approach would likely not be suitable for refractory species as the chemical pretreatments would still require deep penetration into the wood.

The use of chemical modification technologies remains confined to a few species with wide, permeable sapwood. The present work has shown that chemical modification technologies can improve wood properties in refractory species where full penetration is not achieved. However, this improvement may not be sufficient to meet end-user expectations or to compete with chemically modified permeable wood species. There is

a lack of information on the degree of stabilization that is required for various applications. The development of performance-based standards for material stability could help to identify appropriate technologies for specific end users, and spur innovation of new products to meet these specifications.

Accelerated UV exposure. Wood surfaces are susceptible to photochemical degradation when exposed to weathering. Stable wood color is one of the most important requirements for cladding in North America. Figure 2 presents the Δa* for treated and untreated, finished, and unfinished samples from 0 h to 2000 h of accelerated UV exposure. Unfinished untreated and organosilanes-treated samples showed an increase in Δa* up to 250 h compared with the other samples, then a decrease in Δa*, becoming negative after 2000 h. In fact, all unfinished treated samples showed a lower negative Δa* after 2000 h than unfinished untreated wood, becoming greener with accelerated UV exposure. The finished esterified samples (SOR) also showed a negative Δa* after 2000 h compared with all other finished treated and untreated samples which maintained a Δa* greater than 0. Table 5 shows the total color change (ΔE*ab), ΔL*, Δa*, Δb* for treated and untreated, finished and unfinished samples after 2000 h of accelerated UV exposure. Tables 6 and 7 show the pictures of the unfinished and finished, treated and untreated white spruce samples. Most of the treatments studied resulted in a darkening of the wood. However, after accelerated aging, most materials had a similar color and appearance. The larger color changes associated with many of the treatments reflects the loss of color associated with the treatment rather than a greater change in the color of the underlying wood.

All treatments applied to white spruce negatively impacted the ΔE*ab when the samples were not finished with a stain. Unfinished samples show

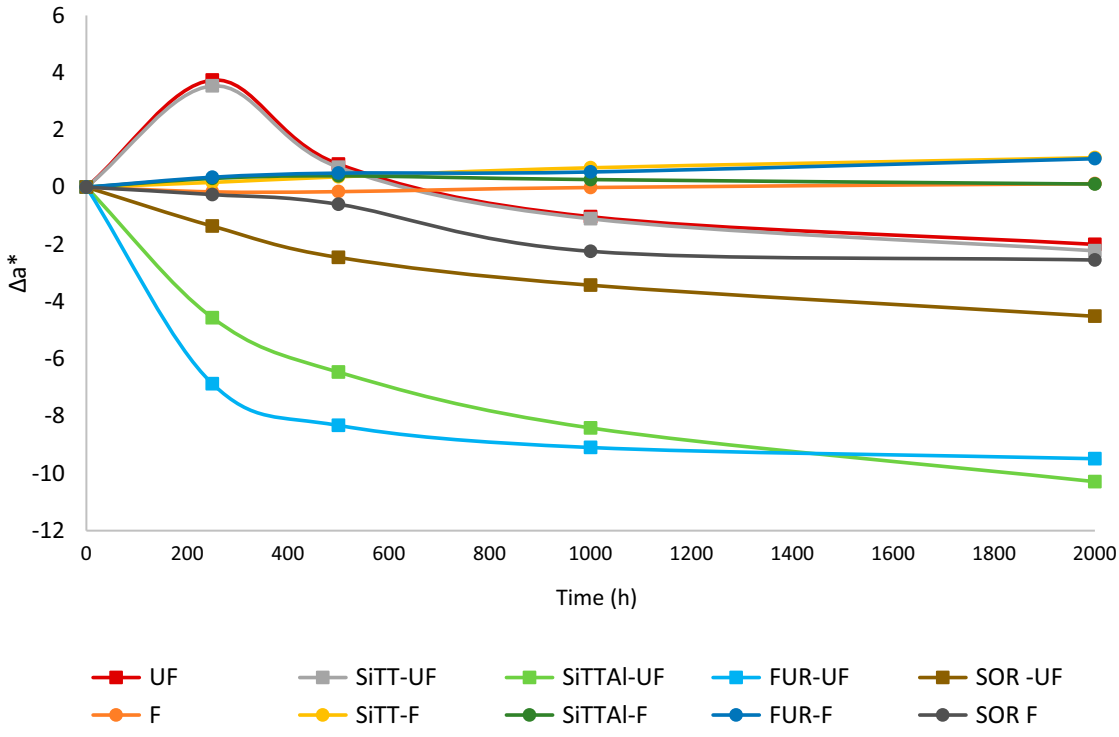

Figure 2. Δa* evolution for treated and untreated, finished (F) and unfinished (UF) white spruce samples over a period of 2000 h of accelerated UV exposure.

Table 5. Total color change (ΔE*ab), ΔL*, Δa*, Δb* for treated and untreated, finished and unfinished white spruce samples after 2000 h of accelerated UV exposure.

		Unfinished				Finished			
	Treatment	ΔEab*	ΔL*	Δa*	Δb*	ΔEab*	ΔL*	Δa*	Δb*
	Untreated	16.3	2.1	−2	−15.8	0.9	0.4	0.1	0.1
Lab scale treatment	Al (aluminum)	No data				No data			
	Mg (magnesium)	No data				No data			
	SiTT (organosilanes)	22.0	4.7	−2.2	−21.4	1.4	−0.4	1.0	0.3
	SiTTAl (organosilanes + aluminum)	39.5	31.2	−10.3	−21.4	1.5	−0.1	0.1	−0.2
Commercial treatment	FUR (furfurylation)	44.7	40.8	−9.5	−29.2	4.4	0.1	1.0	9.4
	Thermal modification	No data				No data			
	SOR (esterification)	21.4	13.8	−4.5	−15.5	3.3	−0.03	−2.6	−1.4

high ΔE*ab with values higher than 16. The highest ΔE*ab was obtained with the FUR treatment with a value of 44.7. Since the North American cladding market values color stability, even after UV exposure, the use of a semitransparent stain was important to assess whether the color change was limited to coated treated wood. The use of a semitransparent stain helped slow down the effect of photodegradation on treated and untreated samples and reduce ΔE*ab, especially for untreated

Table 6. Pictures of treated and untreated white spruce unfinished before and after 2000 h of accelerated UV exposure without semitransparent stain.

	Initial pictures	Pictures after 2000 h of UV exposure
Untreated		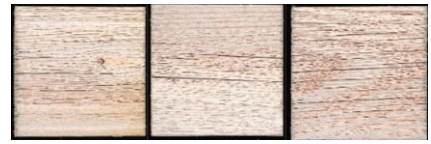
Aluminum		
Magnesium		
SiTT (organosilanes)		
SiTTAl (organosilanes aluminum)		
Furfurylation		
Thermal modification		
SOR (esterification)	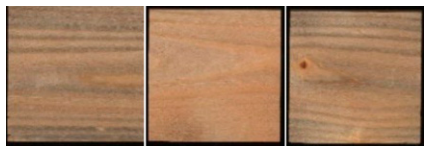	

Table 7. Pictures of treated and untreated white spruce coated with a semitransparent stain before and after accelerated UV exposure.

	Initial pictures	Pictures after 2000 h of UV aging exposure
Untreated		
Aluminum Magnesium SiTT (organosilanes)	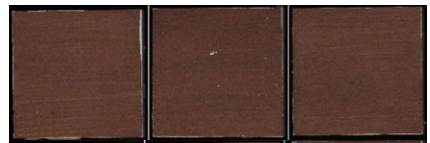	
SiTTAl (organosilanes + aluminum)		
Furfurylation		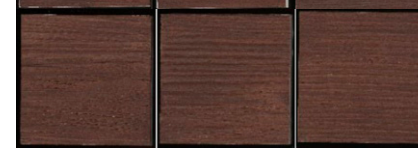
Thermal modification SOR (esterification)		

and organosilanes treatment with ΔE*ab of 1 or 2. However, even with the semitransparent stain, both commercially finished treated wood (FUR and SOR) show a ΔE*ab $>$ 3 that may be visible to the naked eye.

Coating adhesion. As accelerated UV exposure tests have shown in this study, all the treated white spruce wood studied should be finished to retain its color unchanged to the naked eye after at least 2000 h of accelerated UV exposure. However, to maintain good finish protection, coating adhesion must be good after application and after aging. For this reason, coating adhesion was an important test to perform on finished treated wood. Table 8 presents the stain adhesion values obtained for the various coated, treated white spruce samples. The untreated samples present the highest adhesion value. The only treatment that had fair adhesion, before UV exposure, was the FUR. Poor adhesion was obtained with the organosilanes treatment, as well as for thermal modification. All other treatments show no stain adhesion, even before exposure to UV. There was no value presented for the magnesium treatment as the stain was not adhering to the sample surface during sample preparation. After 2000 h of accelerated UV exposure, all treated samples showed no coating adhesion, whereas untreated samples still had fair adhesion. The treatments investigated may have increased the hydrophobicity of the wood surface which could reduce adhesion with the water-based semitransparent stain. In addition, mechanical anchoring may have been hampered by changes in lumen filling and, as Jaic et al (2014) presented in their study, adhesion

Table 8. Average adhesion of a semitransparent stain applied on treated and untreated white spruce.

	Average initial adhesion	Example of pictures before 2000 h of UV aging exposure	Average adhesion after 2000 h of UV aging exposure	Example of pictures after 2000 h
Untreated	4B	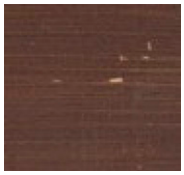	3B	
Aluminum	0B		—	—
Magnesium	—	—	—	—
SiTT (organosilanes)	2B		0B	
SiTTAl (organosilanes + aluminum)	0B		0B	
Furfurylation	3B	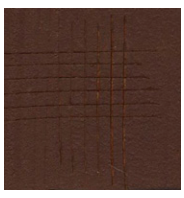	0B	
Thermal modification	2B	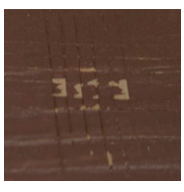	—	—
SOR (esterification)	0B		0B	

between an aqueous-phase coating and the wood substrate is primarily based on mechanical bonding (entanglement) compared with a solvent-based coating whose adhesion may be based on other bonding mechanisms.

CONCLUSIONS

The dimensional stability of white spruce boards containing a mixture of sapwood and heartwood was improved following cyclical exposure to high humidity and water immersion. The degree of stabilization varied within and between treatments and was generally lower than reported values for more permeable wood types, such as pine sapwood. All treatments were associated with greater color change than unmodified wood following accelerated UV exposure. The application of a semitransparent stain reduced the color change of the modified materials. However, all modifications were associated with greatly reduced stain adhesion. The limited improvement in stability and poor performance as a coating substrate limit the commercial applications for these technologies on white spruce. Further work is required to enhance the permeability of refractory species that resist chemical modification. Additionally, there is a need to identify or develop coatings that can adhere effectively to the wood modified by these treatments.

ACKNOWLEDGMENTS

The authors acknowledge financial support from Natural Resources Canada, NRCan, under the Transformative Technologies Program. The authors would also like to thank Erik Larnøy and Stig Lande for their support and collaboration in these experiments.

REFERENCES

ASTM (2021) Standard G155. Standard practice for operating xenon arc light apparatus for exposure of nonmetallic materials. ASTM, West Conshohocken, PA.

ASTM (2023) Standard D3359. Standard test methods for rating adhesion by tape test. ASTM, West Conshohocken, PA.

Baird BR (1969) Dimensional stabilization of wood by vapor phase chemical treatments. Wood Fiber Sci 1:54-63.

Baysal E, Ozaki SK, Yalinkilic MK (2004) Dimensional stabilization of wood treated with furfuryl alcohol catalysed by borates. Wood Sci Technol 38:405-415. https://doi.org/10.1007/s00226-004-0248-2.

Beck G (2020) Leachability and decay resistance of wood polyesterified with sorbitol and citric acid. Forests 11(6): 650. https://doi.org/10.3390/f11060650.

Bekhta P, Niemz P (2003) Effect of high temperature on the change in color, dimensional stability and mechanical properties of spruce wood. Holzforschung 57(5): 539-546. https://doi.org/10.1515/HF.2003.080.

Boivin G, Schorr D (2022) Effect of furfurylation treatment on the performance of three Canadian wood species. *in* Proceedings, International Research Group on Wood Protection. Document No. IRG/WP/22-40925, May 29-June 2, 2022, Bled, Slovenia.

Brentlinger PD (1960) Methods of retarding the mechanical wear of ties, including stabilization of wood, and the splitting of cross and switch ties. Pages 1-12 *in* Proceedings, Annual Convention American Railway Engineering Association, March 14-16, 1960, Chicago, IL.

Candelier K, Hannouz S, Thévenon MF, Guibal D, Gérardin P, Pétrissans M, Collet R (2017) Resistance of thermally modified ash (*Fraxinus excelsior* L.) wood under steam pressure against rot fungi, soil-inhabiting micro-organisms and termites. Eur J Wood Prod 75(2): 249-262. https://doi.org/10.1007/s00107-016-1126-y.

Cheng KJ, Evans PD (2018) Manufacture of profiled amabilis fir deckboards with reduced susceptibility to surface checking. J Manuf Mater Process 2(1):7. https://doi.org/10.3390/jmmp2010007.

Derham B, Singh T, Militz H (2017) Commercialisation of DMDHEU modified wood in Australasia. *in* Proceedings, International Research Group on Wood Protection. Document No. IRG/WP/17-40772, June 4-8, 2017, Ghent, Belgium.

De Vetter L, Stevens M, Van Acker J (2009) Fungal decay resistance and durability of organosilicon-treated wood. Int Biodeterior Biodegrad 63(2):130-134. https://doi.org/10.1016/j.ibiod.2008.08.002.

De Vetter L, Van den Bulcke J, Van Acker J (2010) Impact of organosilicon treatments on the wood-water relationship of solid wood. Holzforschung 64(4):463-468. https://doi.org/10.1515/hf.2010.069.

DIN (1979) Standard 52184. Testing of wood; determination of swelling and shrinkage. Deutsches Institut fur Normung, Berlin.

Donath S, Militz H, Mai C (2004) Wood modification with alkoxysilanes. Wood Sci Technol 38(7):555-566. https://doi.org/10.1007/s00226-004-0257-1.

Emmerich L, Bollmus S, Militz H (2019) Wood modification with DMDHEU (1.3-dimethylol-4.5-dihydroxyethyleneurea)–State of the art, recent research activities and future perspectives. Wood Mater Sci Eng 14(1):3-18. https://doi.org/10.1080/17480272.2017.1417907.

Esteves BM, Pereira HM (2008) Wood modification by heat treatment: A review. BioRes 4(1):370-404.

Esteves B, Nunes L, Pereira H (2011) Properties of furfurylated wood (*Pinus pinaster*). Eur J Wood Prod 69(4):521-525.

Furuno T, Imamura Y, Kajita H (2004) The modification of wood by treatment with low molecular weight phenol-formaldehyde resin: A properties enhancement with neutralized phenolic-resin and resin penetration into wood cell walls. Wood Sci Technol 37(5):349-361. https://doi.org/10.1007/s00226-003-0176-6.

Gérardin P (2016) New alternatives for wood preservation based on thermal and chemical modification of wood—A review. Ann For Sci 73(3):559-570. https://doi.org/10.1007/s13595-015-0531-4.

Hill C, Altgen M, Rautkari L (2021) Thermal modification of wood—A review: Chemical changes and hygroscopicity. J Mater Sci 56(11):6581-6614. https://doi.org/10.1007/s10853-020-05722-z.

Hillis WE (1984) High temperature and chemical effects on wood stability: Part 1: General considerations. Wood Sci Technol 18(4):281-293. https://doi.org/10.1007/BF00353364.

Høibø O, Nyrud AQ (2010) Consumer perception of wood surfaces: The relationship between stated preferences and visual homogeneity. J Wood Sci 56(4):276-283. https://doi.org/10.1007/s10086-009-1104-7.

Jaic M, Palija T, Djordjevic M (2014) The impact of surface preparation of wood on the adhesion of certain types of coatings. Zas Mat 55(2):163-169. https://doi.org/10.5937/ZasMat1402163J.

Lande S, Høibø O, Larnøy E (2010) Variation in treatability of Scots pine (*Pinus sylvestris*) by the chemical modification agent furfuryl alcohol dissolved in water. Wood Sci Technol 44(1):105-118. https://doi.org/10.1007/s00226-009-0272-3.

Lande S, Westin M, Schneider M (2004) Properties of furfurylated wood. Scand J For Res 19(sup5):22-30. https://doi.org/10.1080/0282758041001915.

Larnøy E, Karaca A, Gobakken LR, Hill CAS (2018) Polyesterification of wood using sorbitol and citric acid under aqueous conditions. Int Wood Prod J 9(2):66-73. https://doi.org/10.1080/20426445.2018.1475918.

Lekounougou S, Kocaefe D (2014) Effect of thermal modification temperature on the mechanical properties, dimensional stability, and biological durability of black spruce (*Picea mariana*). Wood Mater Sci Eng 9(2):59-66. https://doi.org/10.1080/17480272.2013.869256.

Kocaefe D, Huang X, Kocaefe Y (2015) Dimensional stabilization of wood. Curr Forestry Rep 1(3):151-161. https://doi.org/10.1007/s40725-015-0017-5.

Kurkowiak K, Emmerich L, Militz H (2021) Sorption behavior and swelling of citric acid and sorbitol (SorCA) treated wood. Holzforschung 75(12):1136-1149. https://doi.org/10.1515/hf-2021-0068.

Kurkowiak K, Hentges D, Dumarçay S, Gérardin P, Militz H (2023) Understanding the mode of action of sorbitol and citric acid (SorCA) in wood. Wood Mater Sci Eng 18(1):67-75. https://doi.org/10.1080/17480272.2022.2125340.

Mai C, Militz H (2004) Modification of wood with silicon compounds. Treatment systems based on organic silicon compounds—A review. Wood Sci Technol 37(6):453-461. https://doi.org/10.1007/s00226-004-0225-9.

Militz H (1993) Treatment of timber with water soluble dimethylol resins to improve their dimensional stability and durability. Wood Scitechnol 27(5):347-355. https://doi.org/10.1007/BF00192221.

Militz H, Altgen M (2014) Processes and properties of thermally modified wood manufactured in Europe in deterioration and protection of sustainable biomaterials. Am Chem Soc 16:269-285. https://doi.org/10.1021/bk-2014-1158.ch016.

Militz H, Norton J (2013) Performance testing of DMDHEU-modified wood in Australia. *in* Proceedings, International Research Group on Wood Protection. Document No. IRG/WP/13-30613, June 16-20, 2013, Stockholm, Sweden.

Mubarok M, Dumarcay S, Militz H, Candelier K, Thévenon MF, Gérardin P (2019) Non-biocide antifungal and antitermite wood preservation treatments based on combinations of thermal modification with different chemical additives. Eur J Wood Prod 77(6):1125-1136. https://doi.org/10.1007/s00107-019-01468-x.

Mubarok M, Militz H, Dumarçay S, Gérardin P (2020) Beech wood modification based on in situ esterification with sorbitol and citric acid. Wood Sci Technol 54(3):479-502. https://doi.org/10.1007/s00226-020-01172-7.

Norton J, Francis LP (2008) Effect of surface-applied treatments on the above-ground performance of simulated timber joinery. Aust For 71(2):100-106. https://doi.org/10.1080/00049158.2008.10676276.

Panshin AJ, de Zeeuw C (1980) Textbook of wood technology: Structure, identification, properties, and uses of the commercial woods of the United States and Canada, 4th edition. Page 772 *in* McGraw-Hill Series in *Forest Resources.* McGraw-Hill Book Co., New York, NY.

Qu L, Wang Z, Qian J, He Z, Yi S (2021) Effects of aluminum sulfate soaking pretreatment on dimensional stability and thermostability of heat-treated wood. Eur J Wood Prod 79(1):189-198. https://doi.org/10.1007/s00107-020-01616-8.

Quiñonez-Piñón MR, Valeo C (2017) Allometry of sapwood depth in five boreal trees. Forests 8(11):457. https://doi.org/10.3390/f8110457.

Rowell RM (1988) Can the cell wall be stabilized. Pages 53-63 *in* Wood Science Seminar: Stabilization of the Wood Cell Wall, December 15-16, 1988. Michigan State University, East Lansing, MI.

Rowell RM (2006) Chemical modification of wood: A short review. Wood Mater Sci Eng 1(1):29-33. https://doi.org/10.1080/17480270600670923.

Salman S, Pétrissans A, Thévenon MF, Dumarçay S, Perrin D, Pollier B, Gérardin P (2014) Development of new wood treatments combining boron impregnation

and thermo modification: Effect of additives on boron leachability. Eur J Wood Prod 72(3):355-365. https://doi.org/10.1007/s00107-014-0787-7.

Sandberg D, Kutnar A (2016) Thermally modified timber: Recent developments in Europe and North America. Wood Fiber Sci 48:28-39.

Sandberg D, Kutnar A, Mantanis G (2017) Wood modification technologies - A review. iForest 10(6):895-908. https://doi.org/10.3832/ifor2380-010.

Sargent R (2019) Evaluating dimensional stability in solid wood: A review of current practice. J Wood Sci 65(1): 1-11. https://doi.org/10.1186/s10086-019-1817-1.

Schauwecker CF, Zahora A, Preston AF (2010) The relative performance of an organic preservative system under UC3A and UC3B conditions using two test methods. *in* Proceedings, International Research Group Wood Protection. Document No. IRG/WP 10-20429, May 9-13, 2010, Biarritz, France.

Scheffer TC, Morrell JJ (1998) Natural durability of wood: A worldwide checklist of species. Research contribution 22, Forest Research Laboratory, Oregon State University. 58 pp. https://ir.library.oregonstate.edu/concern/technical_reports/dz010r37p

Schneider A (1969) Contributions on the dimensional stabilization of wood with polyethylene glycol—Part 1: Basic investigations on the dimensional stabilization of wood with polyethylene glycol. Holz Roh-Werkst 27: 209-224. https://doi.org/10.1007/BF02612917.

Schneider MH (1995) New cell wall and cell lumen wood polymer composites. Wood Scitechnol 29(2):121-127. https://doi.org/10.1007/BF00229341.

Schneider MH, Brebner KI (1985) Wood-polymer combinations: The chemical modification of wood by alkoxysilane coupling agents. Wood Sci Technol 19(1):67-73. https://doi.org/10.1007/BF00354754.

Schorr D, Blanchet P (2020) Improvement of white spruce wood dimensional stability by organosilanes sol-gel impregnation and heat treatment. Materials 13(4):973. https://doi.org/10.3390/ma13040973, May 19-23, 2024, Knoxville, TN.

Schorr D, Boivin G (2023) Influence of basic catalyst and organosilane types on dimensional stability and durability of exterior wood cladding. Wood Mater Sci Eng 18(1): 82-87. https://doi.org/10.1080/17480272.2022.2118073.

Schorr D, Boivin G, Stirling R (2022) Effect of a thermal catalyst on organosilanes treatment to improve durability and stability of Canadian wood. Coatings 12(12): 1867. https://doi.org/10.3390/coatings12121867.

Schorr D, Larnøy E, Stirling R, Boivin G (2024) Citric acid and sorbitol treatment: A comparative study of Canadian and Norwegian species. *in* Proceedings, International Research Group on Wood Protection. Document No. IRG/WP/24-30806.

Sèbe G, Jéso BD (2000) The dimensional stabilisation of maritime pine sapwood (*Pinus pinaster*) by chemical reaction with organosilicon compounds. Holzforschung 54(5):474-480. https://doi.org/10.1515/HF.2000.080.

Shen X, Guo D, Jiang P, Li G, Yang S, Chu F (2021) Reaction mechanisms of furfuryl alcohol polymer with wood cell wall components. Holzforschung 75(12): 1150-1158. https://doi.org/10.1515/hf-2020-0271.

Shi JL, Kocaefe D, Amburgey T, Zhang J (2007) A comparative study on brown-rot fungus decay and subterranean termite resistance of thermally-modified and ACQ-C-treated wood. Holz Roh Werkst 65(5):353-358. https://doi.org/10.1007/s00107-007-0178-4.

Stamm AJ, Hansen LA (1937) Minimizing wood shrinkage and swelling effect of heating in various gases. Ind Eng Chem 29(7):831-833. https://doi.org/10.1021/ie50331a021.

Stamm AJ, Tarkow H (1947) Dimensional stabilization of wood. J Phys Colloid Chem 51(2):493-505. https://doi.org/10.1021/j150452a016.

Stamm AJ (1959) The dimensional stability of wood. For Prod J 9(10):375-381.

Stamm AJ (1977) Dimensional stabilization of wood with furfuryl alcohol resin. Page 372 *in* IS Goldstein, ed. Wood technology: Chemical aspects, ACS Symposium series 43, Washington, DC. https://doi.org/10.1021/bk-1977-0043.ch009

Tarkow H, Stamm AJ, Erickson ECO (1955) Acetylated wood. United States Department of Agriculture, Forest Service, Forest Products Laboratory, Madison, WI.

Tarmian A, Zahedi Tajrishi I, Oladi R, Efhamisisi D (2020) Treatability of wood for pressure treatment processes: A literature review. Eur J Wood Prod 78(4):635-660. https://doi.org/10.1007/s00107-020-01541-w.

Thygesen L, Tang Engelund E, Hoffmeyer P (2010) Water sorption in wood and modified wood at high values of relative humidity. Part I: Results for untreated, acetylated, and furfurylated Norway spruce. Holzforschung 64 (3):315-323. https://doi.org/10.1515/hf.2010.044.

Tjeerdsma BF, Boonstra M, Pizzi A, Tekely P, Militz H (1998) Characterisation of thermally modified wood: Molecular reasons for wood performance improvement. Holz Als Roh-Und Werkstoff 56(3):149-153.

Wang W, Chen C, Cao J, Zhu Y (2018) Improved properties of thermally modified wood (TMW) by combined treatment with disodium octoborate tetrahydrate (DOT) and wax emulsion (WE). Holzforschung 72(3):243-250. https://doi.org/10.1515/hf-2017-0043.

Wang X, Luo C, Mu J, Qi C (2022) Effects of aluminum chloride impregnating pretreatment on physical and mechanical properties of heat-treated poplar wood under mild temperature. Forests 13(8):1170. https://doi.org/10.3390/f13081170.

Westin M, Lande S, Schneider M (2004) Wood furfurylation process and properties of furfurylated wood. *in*

Proceedings, International Research Group on Wood Protection. Document No. IRG/WP/04-40289, June 6-10, 2004, Ljubljana, Slovenia.

Wheat PE, Curtis KC, Chatrathi RS (1996) Ultrasonic energy in conjunction with the double-diffusion treating technique. Forest Prod J 46(1):43-48.

Ximenes F, Evans PD (2006) Protection of wood using oxy-aluminum compounds. Forest Prod J 56(11/12):116-122.

Zelinka SL, Altgen M, Emmerich L, Guigo N, Keplinger T, Kymäläinen M, Thybring EE, Thygesen LG (2022) Review of wood modification and wood functionalization technologies. Forests 13(7):1004. https://doi.org/10.3390/f13071004.

REVIEW ON WOOD PROPERTIES OF INDIGENOUS TREE SPECIES FOR PULP AND PAPER PRODUCTION IN TROPICAL REGIONS

*R. Rajaram**

Post Graduate
Forest Products and Utilisation,
Forest College and Research Institute,
Tamil Nadu Agricultural university, Mettupalayam, Tamil Nadu, India 641 301
E-mail: rajaram7204@gmail.com
and

*R. Ravi**

Assistant Professor (Forestry)
Forest Products and Wildlife, Forest College and Research Institute, Tamil Nadu Agricultural University, Mettupalayam, Tamil Nadu, India 641 301
E-mail: ravi.r@tnau.ac.in

K. Baranidharan

Professor (Forestry) and Head
Forest Products and Wildlife, Forest College and Research Institute, Tamil Nadu Agricultural University, Mettupalayam, Tamil Nadu, India 641 301
E-mail: baranidharan.k@tnau.ac.in

I. Sekar

Professor (Forestry)
Department of Agroforestry, Forest College and Research Institute, Tamil Nadu Agricultural University, Mettupalayam, Tamil Nadu, India 641 301
E-mail: sekar.i@tnau.ac.in

P. Hemalatha

Associate Professor (Horticulture)
Forest Products and Wildlife, Forest college and research institute,
Tamil Nadu Agricultural university, Mettupalayam, Tamil Nadu, India 641 301
E-mail: hemalatha.p@tnau.ac.in

S. Krishnamoorthi

Senior Research Fellow (Forestry)
Forest Products and Utilization, Forest College and Research Institute, Tamil Nadu Agricultural University, Mettupalayam, Tamil Nadu, India 641 301
E-mail: krishnamoorthik9725@gmail.com

(Received April 2024)

Abstract. This comparative review of the anatomical and chemical properties of indigenous tree species to determine their suitability for pulp and paper production, a sector crucial for industrial and economic development. Recognizing the critical gap in comprehensive documentation on the wood properties essential for paper production, this paper aims to serve as a benchmark for future research, guiding pulp, and paper producers in selecting the most appropriate materials. It delves into the global and Indian scenarios, highlighting the pressing need for sustainable materials in the face of escalating greenhouse gas emissions from the building sector and the burgeoning demand for wood amidst dwindling supplies. By examining a variety of species, such as

* Corresponding author

Albizia lebbeck, *Albizia falcataria*, *Gmelina arborea*, *Melia dubia*, *Leucaena leucocephala*, *Acacia auriculiformis*, and *Dalbergia sissoo*. The study not only explores their potential in pulp and paper production but also considers their ecological values, thereby emphasizing a holistic approach to resource utilization.

Keywords: Indigenous tree species, wood properties, sustainable utilization, anatomical and chemical composition.

INTRODUCTION

Various studies have extensively documented the crucial role of forests in maintaining ecological stability and preserving biodiversity, as well as the challenges they face due to deforestation. Forests play a vital role as habitats for diverse species and are indispensable for providing a wide array of ecosystem services essential for human well-being. Recent research increasingly demonstrates the importance of biodiversity in sustaining the functioning of forest ecosystems and the delivery of ecosystem services, including but not limited to biomass production, habitat provision, pollination, seed dispersal, and carbon sequestration (Brockerhoff et al 2017). Additionally, global forests, which are crucial for supplying resources like energy, building materials, and food, and for offering services such as carbon storage and climate regulation, are at risk due to factors such as climate change, air pollution, and the spread of invasive pests (Trumbore et al 2015).

In India, the situation reflects a global trend where deforestation has been a major concern until legislative actions, such as the Forest Conservation Act of 1980; helped to mitigate the loss. The reduction in forest cover not only jeopardizes ecological balance but also underlines the significant gap between the supply and demand for wood, leading to environmental instability. The Forest Policy of 1988 aimed to address these issues by mandating sustainable sourcing for forest-based industries, highlighting the need for sustainable forest management practices to reconcile the demand for forest products with the necessity of conserving forest resources

The invention of papermaking and the widespread use of paper products illustrate the critical role forests play beyond their ecological importance, influencing every aspect of human life from communication and information dissemination to personal hygiene. This underscores the challenge of balancing the demand for paper and other forest products with the imperative of conserving and sustainably managing forest resources to ensure their continuous ability to fulfill vital ecological functions and support economic prosperity (Liang et al 2016).

A thorough understanding of the properties of any material is crucial for optimizing its use, a principle that holds particularly true for wood due to its cellular composition and intricate cell wall structure. As stated eloquently by renowned architect Frank Lloyd Wright in 1928, "We may use wood with intelligence only if we understand wood" (Jozsa and Middleton 1994). Consequently, resource managers and foresters aiming to enhance forest values must grasp not only the fundamentals of tree growth but also the macroscopic and microscopic characteristics influencing wood quality (Jozsa and Middleton 1994).

Wood is most likely one of the first natural resources that have ever been used by humans (Anoop et al 2011). Wood, a dense fibrous substance present in numerous tree species, has served various purposes such as fuel, construction, and industrial resources for millennia. Comprising cellulose fibers intertwined with lignin, a sturdy compound resistant to compression, wood is often classified as the secondary xylem within tree stems (Riki et al 2019). Its significance lies in being the primary resource for pulp and paper production, thus contributing significantly to a nation's industrial and economic advancement.

Amidst numerous factors contributing to the significance of wood as a valuable raw material for pulp and paper production, particular emphasis is placed on its anatomical and chemical composition. While extensive research has explored the potential of various wood species for pulp and paper manufacturing, a comprehensive overview

of their anatomical and chemical characteristic, crucial for guiding researchers and industry professionals in material selection, remains lacking. This study aims to fill this gap by reviewing the principal anatomical and chemical properties of wood and their practical implications in pulp and paper production. It is anticipated that this review will serve as a valuable resource for pulp and paper producers, researchers, and aspiring scientists seeking guidance in the evaluation of lignocellulosic materials for papermaking purposes.

GLOBAL SCENARIO

The total global production of pulp for paper stood at 198.57 million metric tons in 2022—an increase of over 1% from the previous year. The annual production of pulp for paper has increased massively since the 1960s, though output has slowed in recent decades. The United States was the largest pulp for paper producer in 2022; accounting for roughly a quarter of global production. In 2022; worldwide pulp production for paper reached 198.57 million metric tons, marking a growth of more than 1% compared with the year before. Since the 1960s, there has been a significant rise in the production of paper pulp, although the rate of increase has decelerated in the later years. The United States emerged as the top producer of paper pulp in 2022; contributing approximately 25% to the global output paper in 2022; contributing approximately 25% to the global output (Statista 2024). In Europe, the production of

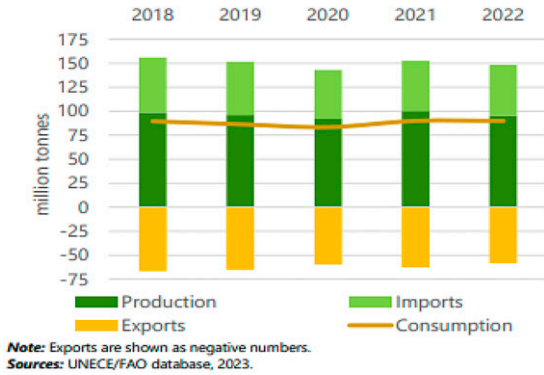

Figure 1. Europe: Paper production, trade and consumption 2018-2022 (FAO 2023).

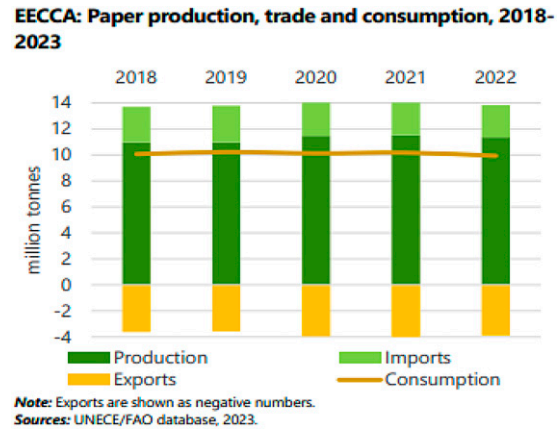

Figure 2. EECCA: Paper production, trade and consumption 2018-2022 (FAO 2023).

paper and paperboard saw a 4.9% decrease in 2022; dropping to 95.5 million tons due to the high costs of energy and raw materials affecting the region. Despite these challenges, the apparent consumption of paper and paperboard remained stable at 89.9 million tons. The latter part of 2022 witnessed several shutdowns of paper machines attributed to reduced demand, spurred by increased raw material costs and decreased advertising budgets for printed materials, with this trend extending into 2023 (FAO 2023).

Wood pulp production in 2022 decreased by 1.6% to 39.0 million tons, with a notable decline

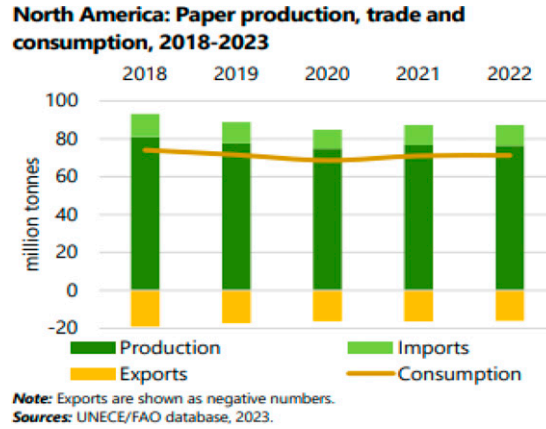

Figure 3. North America: Paper production, trade, and consumption 2018-2022 (FAO 2023).

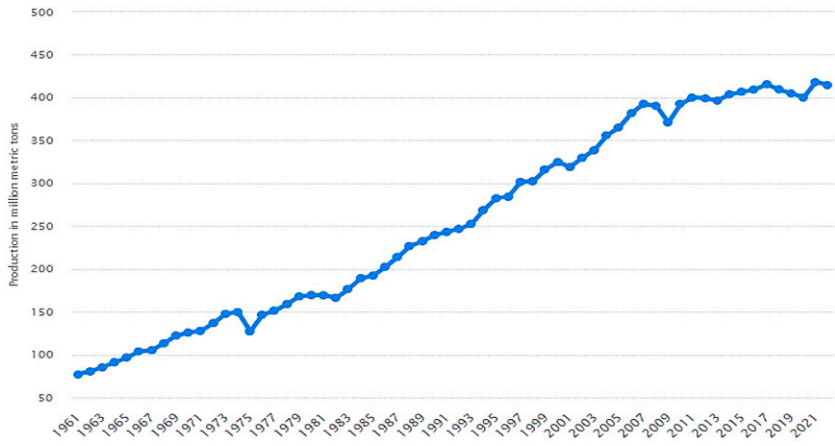

Figure 4. Production of pulp and paper worldwide from 1961 to 2021 (Statista 2024).

in chemical grades by 1.9%. Despite closures, many mills kept their integrated pulp lines operational, selling excess tonnage on the market. Market pulp production fell by 3.6% to 14.4 million tons, attributed to high energy prices and reduced log availability from the Russian Federation, prompting a 4.9% increase in woodpulp imports to 20.3 million tons. Woodpulp exports grew by 2.8% to 16.6 million tons, as mills without operational paper machines sold off their pulp. The apparent consumption of woodpulp slightly decreased by 0.1% to 43.0 million tons, whereas market pulp consumption saw a 3.1% rise to 16.9 million tons (FAO 2023).

The recycling sector also faced challenges in 2022; with a 6.4% reduction in paper recycling utilization to 47.5 million tons, driven by decreased packaging production and high costs for electricity, gas, and CO_2, which disproportionately impacted recycling mills. Paper collection dropped by 5.0% to 52.6 million tons, and the recycling rate decreased to 70.5% from 72.8% in the previous year. This underscores the ongoing need for substantial green investments to align with the EUs climate goals (FAO 2023).

In 2022, the Eastern Europe, Caucasus, and Central Asia (EECCA) region experienced a slight decline in paper and paperboard production, falling by 1.5% to 11.3 million tons, with apparent consumption also decreasing by 2.4% to 10 million tons. Notably, the production of sanitary and household papers saw a small increase of 1.3% to 893,000 t, and their consumption rose by 2.0% to 877,000 t. However, packaging material production dropped by 2.2% to 7.6 million tons, and its consumption decreased by 2.1% to 6.9 million tons. Specifically, case material production fell by 3.4% to 5.3 million tons, whereas carton board production barely decreased by 0.3% to 1.1 million tons. Consumption patterns reflected these production changes, with case materials consumption decreasing by 4.4% to 4.4 million tons, while carton board consumption grew by 3.7% to 1.8 million tons. Wood pulp production and consumption remained steady at 9.1 and 6.7 million tons, respectively. Exports stayed constant at 2.7 million tons, but imports saw a 4.6% reduction to 323,000 t, with significant trade focused between the Russian Federation, Belarus, China, and India (FAO 2023).

In North America, paper and paperboard production slightly declined by 0.3% to 76.5 million tons in 2022 due to market shifts and unplanned downtime, including the shutdown of high-cost facilities. Despite this, apparent consumption marginally increased by 0.3% to 71.2 million tons, spurred by postpandemic market recovery and the reopening of trade routes between Canada and the United States. Graphic grade production remained steady,

while there was a modest rise in uncoated wood free and coated papers, but newsprint and sanitary paper production declined. Packaging material production also saw a slight decrease. Interestingly, the consumption of graphic grades and uncoated wood-free paper increased, suggesting a recovery from the pandemic, though consumption of newsprint significantly dropped. Packaging materials consumption remained stable with a minor decrease, reflecting adjustments in the market. Wood pulp production decreased by 1.1%, but exports of chemical market pulp increased, indicating a shift toward selling pulp in the global market. Overall, the industry faced challenges from higher prices and shifting consumption patterns, leading to closures and adjustments in production strategies (FAO 2023).

Meanwhile, Brazil's pulp production rose by 10.9% to 25.0 million tons in 2022; fueled by capacity expansions, with exports climbing by 22.1% to 19.1 million tons, primarily of bleached eucalyptus kraft pulp. Conversely, Chile faced a competitive squeeze, notably from Brazil's capacity increase, leading to a 5% decline in market pulp exports to 4.1 million tons. However, exports of specific pulp types like bleached radiata pine and unbleached kraft saw increases, despite overall challenges including high prices and expansion projects affecting the market dynamics. This scenario underscores the competitive and rapidly evolving nature of the global pulp and paper industry, with significant developments in China, Brazil, and Chile impacting international market trends and trade flows (FAO 2023).

INDIAN SCENARIO

India's paper and pulp sector is witnessing the most rapid expansion globally. There is a consistent rise in the need for various paper commodities, encompassing packaging materials, writing and printing papers, as well as niche paper products. India's paper sector is at the forefront of recycling endeavors, advocating for the use of repurposed paper to safeguard natural assets and lessen ecological footprints. Renowned for its eco-friendly methods, the industry in India is also recognized for its commitment to sustainability and utilization of renewable resources. Globally, 410 million tons of paper are used each year, and India's usage accounts for 22.05 million tons of this total, representing 4.72% of worldwide paper consumption. India's paper usage has been on an upward trajectory, correlating with the country's economic growth starting in the early 1990s. From 2010-2011 to 2019-2020, paper consumption in India increased from 13.96 to 22.05 million tons. However, the international paper and pulp mills sector has seen a slight downturn in the last half-decade, largely due to the adoption

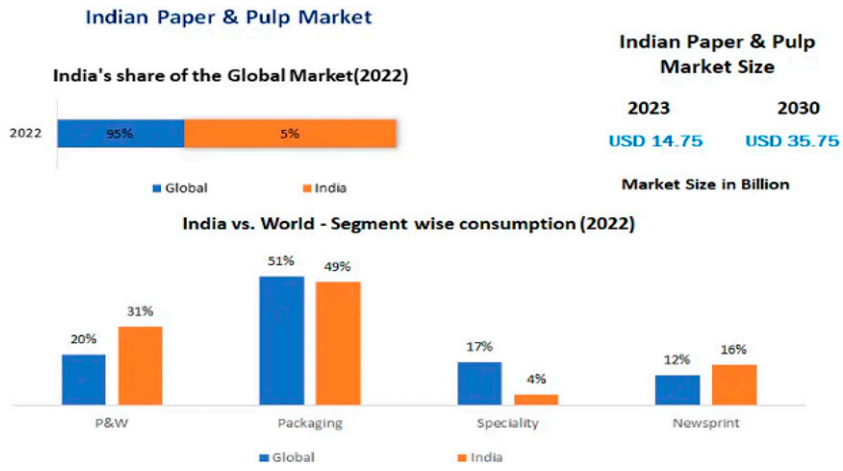

Figure 5. Indian vs World Pulp and Paper Market (MMR 2023).

Table 1. Location of large paper units (both integrated and nonintegrated) across different states in India (MMR 2023).

Name of state	No of units
Andhra Pradesh	4
Gujarat	10
Himachal Pradesh	1
Karnataka	1
Maharashtra	3
Odisha	2
Punjab	4
Tamil Nadu	7
Telangana	1
Uttar Pradesh	9
Uttarakhand	2
West Bengal	2

of digital media and a move toward paperless communication in many advanced economies. The market value of the Indian paper and pulp sector stood at USD 14.75 billion in 2023; and it is projected to grow to USD 35.57 billion by 2030. This growth is anticipated to occur at a compound annual growth rate (CAGR) of 13.4% throughout the forecast period (MMR 2023).

Figure 5 presents an overview of the Indian paper and pulp market within the global context for the year 2022; indicating India's modest but significant presence in the industry, with a particular emphasis on various market segments such as printing and writing, packaging, specialty papers, and newsprint. It shows India's market size for paper and pulp with an optimistic growth forecast, projecting a substantial increase in market value from 2023 to 2030; highlighting a robust CAGR, signaling a rapidly expanding sector within the Indian economy. The displayed data suggests a narrative of India as an emerging player in the paper and pulp industry with expectations of continued growth and increased influence on the global stage over the coming years.

Table 2. Showing the estimated number of wood-based industries in India (Kant and Nautiyal 2021).

Industry	Number of units
Sawmilling and planning industry	27,680
Veneer sheet, plywood, laminated board, particleboard, and other panels industry	47,403
Carpentry and joinery industry	2599
Packing case industry	16,580
Pulp, paper and paperboard industry	24,880
Corrugated paper and paperboard industry	92,871
Manufacture of other articles of paper and paperboard industry	26,894
Total	238,907

Table 3. Showing the annual estimated wood production in India (Shrivastava and Saxena 2017).

Source of wood production	Production (in million m^3)
Timber production from forest (excluding Forest Development Corporation [FDCs])	1.205
Timber production from FDCs	1.97
Annual production of timber from Tree outside the forest (TOF)	44.34
Bamboo production in India	5.38
Imports (all timber and allied products)	18.01
Fuel-wood production	385.25
Total	456.15

DEMAND AND SUPPLY

Since the conclusion of World War II, there has been a fluctuating demand for wood, reaching its zenith in 1973 at 120 million m^3 before declining to less than 95 million m^3 between 1981 and 1986. However, a resurgence occurred in 1987; attributed to a surge in new home construction driven by domestic economic policies and heightened paper demand stemming from increased office automation. Despite a temporary downturn due to economic recession, the demand rebounded to 111.93 million m^3 in 1995; primarily fueled by renewed paper and paperboard demand. Domestic wood supply dwindled to 22.92 million m^3, a mere fifth

Table 4. Showing the annual estimated wood consumption in India (Shrivastava and Saxena 2017).

Source of wood consumption	Consumption (in million m^3)
Construction, furniture, and agricultural implements	48.0
Plywood and panel	8.47
Paper, paperboard, and newsprint	12.52
Fuel wood consumption	333
Total	402

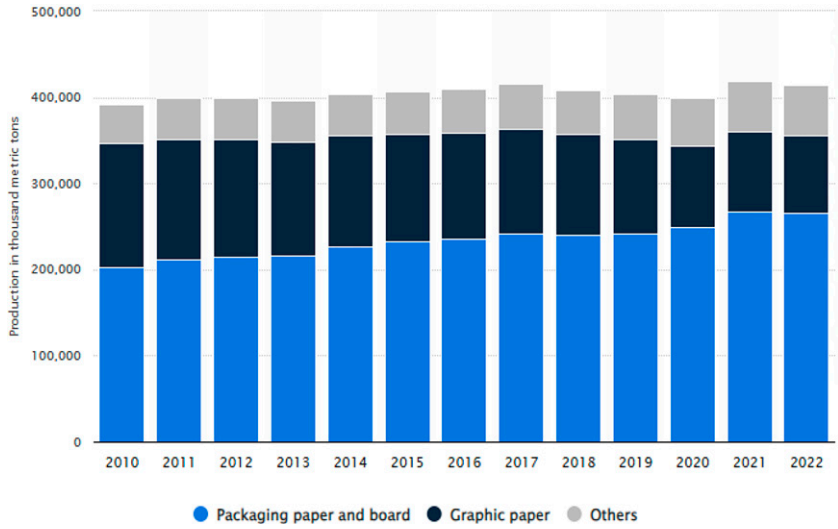

Figure 6. Production volume of paper and paperboard worldwide from 2010 to 2022; by type (in 1000 t) (Statista 2024).

of the total supply in 1995; owing to constraints in domestic forest resources and hindered supply capacity due to delays in wood production infrastructure development. The import share of wood surged from over 50% in 1969 to approximately 70% by 1979.

According to the economic survey by the Ministry of Finance in 2011; forestry and logging contributed 1.2% to India's GDP. In the same year, the Indian forest products industry generated a total revenue of $65,844.6 million, indicating a CAGR of 5.5% from 2007 to 2011. Consumption volumes within the industry saw a marginal increase, with a CAGR of 0.2% from 2007 to 2011; reaching 355.4 million m^3 in 2011. Projections suggest a further acceleration in industry performance, with an anticipated CAGR of 7.7% from 2011 to 2016; poised to elevate the industry's value to $95,467 million by the close of 2016. Annually, approximately 405 million tons of paper

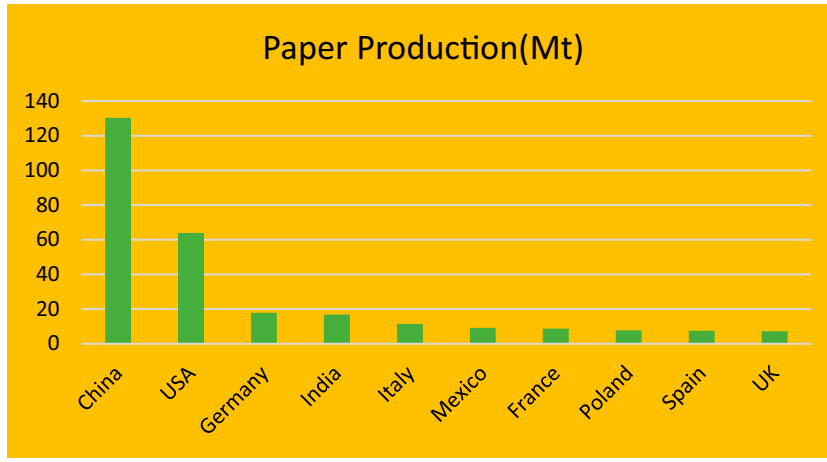

Figure 7. Production of paper and paperboard in selected countries worldwide in 2022 (in 1000 t) (Statista 2024).

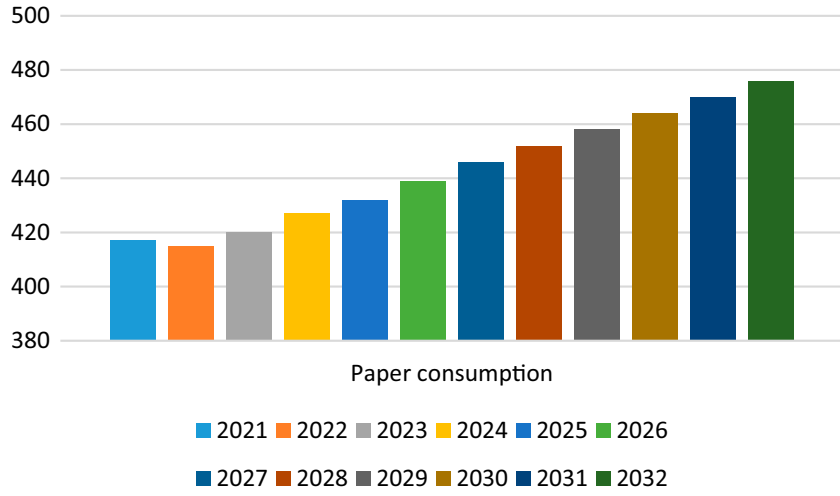

Figure 8. Paper consumption worldwide from 2021 to 2032*(in million metric tons) (Statista 2024).

and paperboard are manufactured, accounting for about 13-15% of the world's total wood usage. As the demand for paper goods rises, it is projected that worldwide output may reach twice the current amount by the year 2050. The paper manufacturing industry has a considerable environmental impact; it ranks as the fourth highest in terms of energy use. Furthermore, the production of paper necessitates a substantial volume of water, which varies with the mill's efficiency, and it exceeds the water consumption of other sectors such as steel and oil (Sunny 2018).

VARIOUS INDEGENIOUS WOOD

Albizia lebbeck

The *Albizia* genus encompasses around 150 taxonomically recognized species, found extensively across Asia, Africa, Australia, and tropical/subtropical regions of the Americas (He 2020). *Albizia lebbeck*, primarily found in the Indian subcontinent and Myanmar (Burma), has a broad distribution spanning Western and Southeast Asia, Australia, Northern and West Africa, the Caribbean, Central America, and parts of South America (Fig 1) (Parrotta 2006). In forestry, *A. lebbeck* plays a crucial role in reforestation and afforestation projects, especially in tropical and subtropical regions. Stems of *A. lebbeck* were easily pulped with Alkaline Sulphite Anthra quinone and Methanol, yielding high viscosities, low kappa numbers, good to exceptional physical characteristics, and high yields (Elzaki et al 2012).

The environmental benefits of *A. lebbeck* extend beyond its utility in paper production (Balkrishna et al 2022). Research on *A. lebbeck* has explored its potential in forestry and pulp and paper production, highlighting its versatility and benefits. One study explores the delignification of refiner mechanical pulp from *A. lebbeck* using the soda

Figure 9. *Albizia lebbeck* (CABI Digital library 2017).

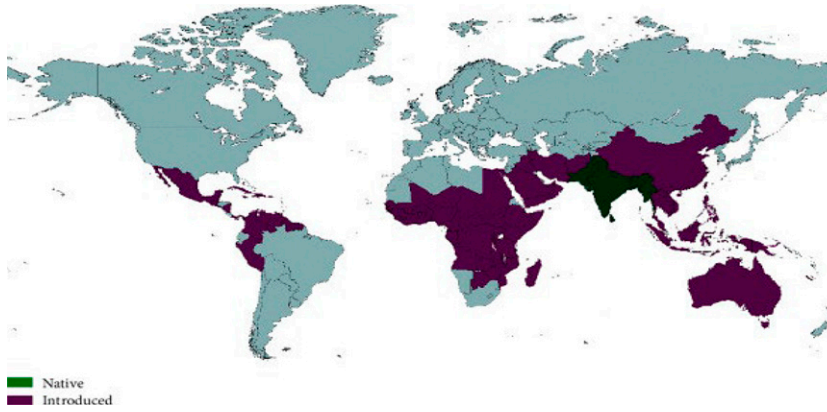

Figure 10. Global distribution of *Albizia lebbeck* (L.) Benth (Balkrishna et al. 2022).

process, demonstrating that high-yield pulps with comparable strength properties to conventional chemical pulps can be produced, highlighting the wood's potential for sustainable pulp production (Kalra 1990). Additionally, the restoration potential of *A. lebbeck* has been examined, showing its superior performance in improving soil properties, biomass accumulation, and net primary production in mine spoils, which could indirectly benefit forestry and pulp and paper industries by enhancing raw material quality and availability (Singh et al 2004).

Albizia falcataria

Albizia falcataria, also known as *Falcataria moluccana*, is a tropical hardwood tree extensively utilized in Southeast Asia for its significant value in timber production. It is renowned for its rapid growth and adaptability to a range of environmental conditions, making it an excellent candidate for reforestation and afforestation projects. Research highlights its wide adaptability and suitability for social forestry, particularly in areas with high rainfall, due to its minimal soil demands (Bahuguna et al 1989). The wood's physical properties have also been enhanced through densification, addressing its low-density limitations for commercial applications (Julian et al 2022). For the pulp and paper industry, *A. falcataria* presents a viable and sustainable raw material option. The tree's fast growth rate and high cellulose content make it an excellent source for pulp production, contributing to meeting the global demand for paper and paperboard products. The pulp derived from *falcataria* is known for its high quality, which is suitable for producing a wide range of paper products, including writing paper, packaging materials, and tissue papers. Heartwood is a commonly used material for lightweight packaging materials, lightweight buildings, paneling, cabinets, and furniture. It is also easily worked and ideal for pulping, paper, and matchsticks (Rojas-Sandoval 2009).

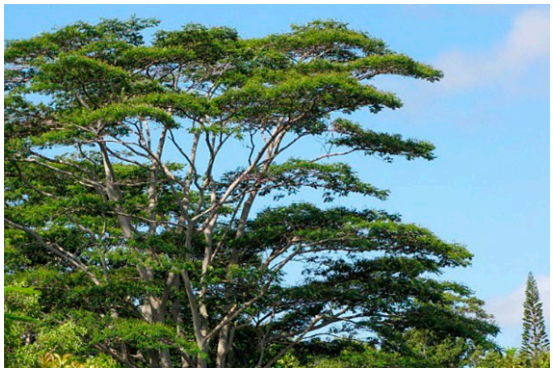

Figure 11. *Albizia falcataria* (https://www.ecured.cu/index.php/Falcata_*Albizia_falcataria*).

The utilization of *A. falcataria* in the pulp and paper industry also aligns with environmental sustainability goals. The cultivation of *A. falcataria* for pulp production can be integrated into agroforestry systems, promoting land use efficiency and providing additional income sources for farmers.

Furthermore, as the industry seeks to reduce its reliance on traditional wood sources and increase the use of more sustainable raw materials, *A. falcataria* offers a pathway to achieve these objectives without compromising on the quality of the final paper products (Setyawan et al. 2018). Studies on the utilization of *A. falcataria* specifically for forestry, pulp, and paper industries are not directly available. However, related research offers insights into the broader context of pulpwood plantation, genetic modifications for pulp production, and the use of hybrid species for increasing forest biodiversity and supporting the pulp/paper industry. For instance, Kröger and Nylund (2012) applied ethical analysis to assess conflicts in the expansion of pulpwood plantations in Brazil, highlighting the complexities of social, ecological, and economic dynamics in large-scale forestry investments. Unnikrishnan and Gurumurthy (2015) reviewed genetic modifications in major tree species used in India's pulp and paper industry, aiming to enhance growth, wood characteristics, and stress tolerance. Sunarti and Nirsatmanto (2021) discussed the use of interspecific *Acacia* hybrids in Indonesia for pulp/paper industry support and forest biodiversity increase, emphasizing the development of hybrids with fast growth, good wood properties, and tolerance to pests and diseases. These studies reflect the broader research efforts and considerations in the domain of forestry, pulp, and paper production, which may inform the utilization and management of *A. falcataria* in related contexts. *Albizia falcataria* can be employed in generating pulp and paper making (Olufunmilayo 2013). *Albizia falcataria* is one hardwood species that works well for producing high-quality, high-yield kraft pulp (Akhtaruzzaman and Chowdhury 1991).

These studies collectively underscore the multifaceted importance of *Albizia falcataria* in forestry, ecological studies, and industrial applications, highlighting its potential for future research and utilization.

Gmelina arborea

Gmelina arborea, commonly known as yemane, is a fast-growing hardwood species valued for its timber. It is extensively used in furniture, construction, and paper production due to its desirable properties. Research on *G. arborea* has highlighted its significant mechanical properties and adaptability, making it a preferred choice in forestry and agriculture. For instance, studies conducted on Nigerian-grown *G. arborea* revealed variations in wood properties with age and sampling position, indicating increases in strength properties with age, which is crucial for its utilization in construction and furniture making (Ogunsanwo and Akinlade 2011). In Bangladesh, designated forestlands are planted with Gamari (*G. arborea*) to produce pulpwood (Sarwar Jahan et al 2018). Similarly, extensive research on the mechanical properties of *G. arborea* for engineering design underscored its potential for load-bearing structures, comparing favorably with European softwood species and highlighting its suitability as a construction material (Iwuoha et al 2021). *Gmelina arborea* is one of the hardwoods found in Nigeria's forest reserves. About 50 yr ago, several plantations of the tree were planted, primarily in southern Nigeria, with the intention of providing pulp wood for the paper industry (Akeem Azeez et al 2016). Additionally, the impact of soil moisture regimes on the growth and wood properties of *G. arborea* seedlings has been studied, providing insights into its adaptability and the quality of paper produced from its wood, which is crucial for pulp and paper manufacturing (Ogbonnaya et al 1992). Studies on *G. arborea* have explored its significance in forestry and the pulp and paper industry, highlighting its utility based on geographical variations, growth characteristics, and suitability for pulp production. For instance, research by Soosai Raj et al (2017) examined the pulping properties of *G. arborea* from different regions in Tamil Nadu, India, identifying trees with favorable traits for pulp and paper manufacturing due to their superior slenderness ratio and fiber dimensions (Soosai Raj et al. 2017). Research by Olufunmilayo (2013) compared the pulp and paper-making suitability of *G. arborea* with other species, highlighting its advantages and proposing methods for identifying suitable hardwood species for the industry. *Gmelina arborea*

Roxb. deciduous tree species is indigenous to Bangladesh and grows quickly. It has been widely planted in Bangladesh's hilly regions for the commercial production of pulpwood since 1992 (Khushi et al 2019). These studies collectively underscore the potential of *G. arborea* in enhancing forestry, pulp, and paper production through genetic selection, growth modeling, and comparative analysis with other species.

Melia dubia

Melia dubia, also known as Malabar Neem, is a fast-growing tree species valued for its diverse applications ranging from agroforestry to the timber industry. Its wood properties, including basic density, fiber dimensions, and chemical composition, vary with age, influencing its suitability for pulp and paper production. Sinha et al (2019) highlighted that the wood's basic density, fiber length, cellulose, and lignin content increase with tree age, making it suitable for high-quality pulp and paper at ages 4 and 5. Moreover, Chavan et al (2021) discussed its economic viability in agroforestry systems in India, noting its high biomass production and profitability, making it a favored species for wood-based industries. Additionally, Gupta et al (2019) reported on the wood's working qualities, indicating its potential in the plywood industry due to its satisfactory planning and shaping properties. Goswami et al (2020) emphasized its rapid growth and high demand in various industries, alongside its notable medicinal and pharmacological properties. Research on *M. dubia* has highlighted its potential for forestry, pulp, and paper industries, with studies focusing on its growth performance, wood properties, and suitability for pulp production. *Melia dubia* is unique among traditional raw materials used in the pulp and paper industry because of its exceptional fiber strength and excellent pulp recovery (Dhaka et al 2020).

Figure 12. *Melia dubia* (IBDP 2015).

Sinha et al (2019) found that *M. dubia* exhibits favorable wood properties for pulp and paper quality, with basic density, fiber dimensions, and cellulose content improving with tree age, suggesting the optimal harvesting period for high-quality pulp is at 4 to 5 yr. *Melia dubia* is a species that can be used in agroforestry and farm forestry plantation programs due to its many uses, including pulpwood, timber, fuel wood, and plywood (Saravanan et al 2013). These studies collectively emphasize the significant potential of *M. dubia* in contributing to sustainable forestry practices and supporting the pulp and paper industries through its fast growth, quality wood properties, and versatility in applications. These studies collectively underscore. In India, the *Melia* genus is making a comeback and gaining popularity as a substitute for eucalyptus and poplar as an indigenous source of pulp and plywood (Chavan et al 2021).

Melia dubia significance in sustainable forestry and agroforestry practices, highlighting its potential for economic and environmental benefits.

Leucaena leucocephala

Leucaena leucocephala, commonly known as the White Leadtree, demonstrates versatile applications and environmental benefits, particularly in the contexts of agroforestry, phytoremediation, and material production. Its ability to rapidly metabolize soil and groundwater contaminants such as ethylene dibromide and trichloroethylene positions it as an effective tool for environmental cleanup, especially in tropical regions (Doty et al 2003). Additionally, *L. leucocephala* suitability for biomass and paper production, even from its varieties like giant leucaena, underscores its potential for sustainable agroforestry and as a renewable energy source, supporting industries

Figure 13. *Leuceana leucocephala* (Mónica Sánchez).

ranging from timber and paper pulp to biofuel production (Bageel et al 2020). Research on *L. leucocephala* has demonstrated its potential in the forestry and pulp and paper industries due to its rapid growth and suitable wood properties. López et al (2008) evaluated Leucaena species for biomass and paper production, finding *L. leucocephala* among others to show good adaptation and productivity, with properties favorable for papermaking, such as lower lignin content and suitable cellulose levels. Shaik et al (2009) focused on optimizing a regeneration system for *L. leucocephala*, which is crucial for genetic engineering aimed at modifying lignin content to improve paper quality. Bhola and Sharma (1982) demonstrated that *L. leucocephala* could produce high yields of unbleached kraft pulp with low alkali consumption, suggesting its suitability for sustainable pulp production. *Leucaena leucocephala* is a good choice for making unbleached kraft pulp because of its medium basic density and medium-sized fiber length (Gillah and Ishengoma 1993).

Kumar et al (2013) identified and characterized cinnamate 4-hydroxylase genes from *L. leucocephala,* providing insights into the genetic basis for its growth and wood properties, which are relevant for pulp and paper production. *Leucaena* has drawn a lot of attention due to its widespread use as a raw material in the pulp and paper industries as well as in the production of packaging materials (Pandey and Kumar 2013). *Leucaena leucocephala* is a versatile, quickly growing legume tree that can be used for pulp, paper, leaf compost, and fodder (Shaik et al 2009). These studies collectively underscore the versatility and potential of *L. leucocephala* in contributing to the forestry sector, particularly for pulp and paper manufacturing, through its favorable growth characteristics and wood properties.

Acacia auriculiformis

Acacia auriculiformis, commonly known as earleaf acacia, is recognized for its significant contribution to the timber and pulpwood industry due to its desirable wood properties. Research has highlighted the genetic variation in wood stiffness and strength, which are crucial for structural and appearance-grade timber applications. Studies from southern Vietnam demonstrate significant variation among clones in static bending stiffness and strength, indicating the potential for genetic improvement (Hai et al 2010). Additionally, investigations into the wood property variation in 11-yr-old *A. auriculiformis* grown in Bangladesh revealed that basic density, fiber length, and compressive strength increase with radial distance from the pith, suggesting the potential for tree selection to enhance wood quality through breeding (Chowdhury et al 2009). Moreover, the anatomical and physico-mechanical properties of the species to age and soil type in Benin, West

Figure 14. *Acacia auriculiformis* (Aggarwal 1988).

Africa, emphasize the influence of environmental factors on wood density and structural integrity, which are key considerations for timber use (Tonouéwa et al 2020). The leaf of *A. auriculiformis* contains lignin, hemicellulose, and cellulose. *Acacia auriculiformis* has lignin contents ranging from 19 to 20% (Abdullah et al 2021). These findings underscore the importance of *A. auriculiformis* in forestry and wood industries, highlighting its adaptability and the potential for targeted genetic and environmental management to optimize wood properties for various applications. *Auriculiformis* cultivated in many regions of the world had nearly identical features to that of *A. auriculiformis* planted in social forestry programs in Bangladesh and other nations. This species holds great potential for pulp production in Bangladesh and other Southeast Asian nations (Haque et al 2021).

Dalbergia sissoo

Dalbergia sissoo, a prominent deciduous tree, can ascend to heights of 30 m with a girth of 80 cm, forming a notable presence with a wide, sparse canopy. Its gray bark, etched with longitudinal furrows, tends to peel. The tree develops a central taproot and spreading lateral roots in its youth. Known for its robust growth, *D. sissoo* bark, roots, and young shoots demonstrate its adaptability, with a crown supported by strong limbs, making it a significant species both ecologically and economically (Hossen et al 2023). *Dalbergia sissoo*, a significant tree species, boasts considerable economic value. Its heartwood is characterized by its brown hue and dark streaks, noted for its

Figure 15. *Dalbergia sissoo* (Singh 2015).

hardness, strength, and long-lasting quality. Recognized as one of India's four main timbers—alongside *Tectona grandis* (Teak), *Shorea robusta* (Sal), and *Cedrus deodara* (Cedar)—it is prized for its robustness, flexibility, and endurance, making it a preferred material for construction and various other utilities. *Dalbergia sissoo* is also an ideal species for reforestation projects in challenging environments, such as saline and alkaline terrains, mining areas, and eroded landscapes. Its resilience makes it suitable for restoring degraded woodlands, contributing to environmental conservation efforts (Singh 2015). Research on *D. sissoo* (Indian rosewood) has explored various aspects of its potential in forestry and the pulp and paper industry, focusing on its growth performance, wood properties, and disease susceptibility. Hannan et al (2001) investigated the physical properties of sound and disease-affected *D. sissoo* wood, revealing significant differences in shrinkage and

Table 5. Anatomical properties of indigenous wood property (Anoop et al. 2011).

Species	Fiber length (mm)	Fiber diameter (μm)	Lumen diameter (μm)	CellWall thickness (μm)	Vessel element presence
Albizia lebbeck	0.8-1.5	15-25	5-10	2-5	Moderate
Albizia falcataria	1.0-1.8	20-30	10-15	2-4	Sparse
Gmelina arborea	0.9-1.4	18-28	8-12	1.5-3.5	Moderate to High
Melia dubia	0.6-1.2	10-20	5-10	1-3	Sparse to Moderate
Leucaena leucocephala	0.7-1.3	15-25	7-13	2-4	Moderate
Acacia auriculiformis	0.5-1.0	10-20	4-8	1.5-3	High
Dalbergia sissoo	1.0-1.5	15-25	6-11	2-4.5	Moderate

In a study by Vennila and Parthiban (2021) they studied various properties of Indigenous species for pulp and paper production given in Tables 6 and 7.

Table 6. Physical characteristics of hardwood chips (Vennila and Parthiban 2021).

Sl. No.	Species	Moisture (%) as received	Bulk density (OD basis) (kg/m^3)	Basic density (OD basis) (kg/m^3)	Chips classification: +45 mm	+8 mm (over thick)	+7 mm (accepts)	+3 mm (pin chips)	−3 mm (dust)
1	*Albizia lebbeck*	9.0	266	530	Nil	3.9	81.2	14.2	0.7
2	*Dalbergia sissoo*	9.6	280	580	Nil	4.8	79.8	14.6	0.8
3	*Erythrina indica*	9.9	266	438	Nil	4.8	79.5	15.3	0.4
4	*Grewia tillifolia*	10.3	220	485	Nil	5.1	78.6	15.7	0.6
5	*Melia dubia*	9.1	240	520	Nil	6.2	79.2	14.2	0.4
6	*Melia composita*	9.9	190	505	Nil	6.5	82.6	10.1	0.8
7	*Neolamarckia cadamba*	8.5	160	380	Nil	4.1	79.8	15.6	0.5
8	*Sterculia alata*	10.9	240	510	Nil	6.2	77.8	15.4	0.6

specific gravity that affect its timber quality. This study underscores the importance of managing disease to maintain the wood's value for construction and utility purposes (Hannan et al 2001). These studies collectively highlight the significance of *D. sissoo* in forestry and the pulp and paper industry, its ecological and economic benefits, and the challenges it faces, including disease and the need for accurate species identification to prevent illegal trade.

PROBLEMS AND CONSTRAINTS

Studying the anatomical properties of indigenous tree species for pulp and paper production presents a range of challenges and constraints, both scientific and practical. One of the primary difficulties is the variability in wood properties not only between species but also within a single species due to environmental factors, age, and growth conditions. This variability can significantly impact the reliability of comparative studies, making it challenging to draw definitive conclusions about the suitability of a particular species for pulp and paper production (Downes et al 1997).

Moreover, access to representative samples can be a constraint. Many indigenous tree species are found in remote or protected areas, complicating sample collection efforts. Additionally, there are ethical and legal considerations regarding the use of indigenous species, especially those that may be endangered or hold cultural significance (FAO Report 2011). These factors necessitate careful planning and consultation with local communities and regulatory bodies, which can prolong the research process.

Another significant challenge is the technological and economic feasibility of utilizing new or underutilized species for pulp and paper production. The existing pulp and paper industry infrastructure is optimized for a few well-studied species. Incorporating new species into the production

Table 7. Chemical characteristics of hardwood chips (Vennila and Parthiban 2021).

Sl. No.	Species	Ash content (%)	Acid insoluble lignin (%)	Pentosans (%)	Hollo cellulose (%)	Solubility in (%) – Hot water	1% NaOH	Alcohol benzene
1	*Albizia lebbeck*	0.54	24.1	18.2	71.5**	2.75	12.5	3.2
2	*Dalbergia sissoo*	0.62*	23.9	17.6	70.4	3.05	15.7**	3.8*
3	*Erythrina indica*	0.61	24.3	17.2	69.4	2.80	14.2	4.2*
4	*Grewia tiliifolia*	0.66**	23.7	17.2	68.9	3.75	16.1**	2.7
5	*Melia dubia*	0.64**	22.5	18.7	72.8**	2.75	13.7	3.8*
6	*Melia composita*	0.53	24.5	18.5	69.5	3.65	16.8**	3.4
7	*Neolamarckia cadamba*	0.74**	25.5**	20.4**	70.5	3.12	11.8	3.6
8	*Sterculia alata*	0.54	23.5	16.7	63.5	3.60*	15.9**	2.8

Table 8. Strength characteristics of hardwood chips (Vennila and Parthiban 2021).

Species	Tensile strengh	Tensile index (Nm/g)	Breaking length (M)	Tear strength	Tear index (mNm^2/g)	Tear factor	Bursting strength	Burst index ($kPam^2/g$)	Burst factor
Albizia lebbeck	1270	20.95	2038	180	3.0	30.29	78	1.3	13.12
Dalbergia sissoo	1380	22.81	2257	190	3.1	32.04	74	1.2	12.48
Erythrina indica	1120	18.18	1877	168	2.7	27.81	82	1.3	13.57
Grewia tiliifolia	1150	18.98	1877	184	3.0	30.98	68	1.1	11.45
Melia dubia	1310	22.47	2195	190	3.3	33.24	92	1.6	16.10
Melia composita	1080	18.60	1833	185	3.2	32.49	102	1.8	17.92
Neolamarckia cadamba	1110	17.76	1797	169	2.7	27.58	88	1.4	14.36
Sterculia alata	1210	20.79	2023	175	3.0	30.68	78	1.3	13.67

cycle may require adjustments in processing techniques and equipment, which could be cost-prohibitive (Hendarto 2006). Moreover, the lack of existing knowledge on the best practices for cultivating, harvesting, and processing these species adds another layer of complexity.

Current laws forbid leasing property to private persons, businesses, or joint sector projects. Examples of these laws are the Property Reforms Act of several states, the Forest Conservation Act of 1980; and the National Forest Policy of 1988. Fearing that such land would be permanently taken away, the corporate sector has refrained from actively participating in afforestation (Sharda et al 2000).

Finally, modern technologies and procedures are continually being created in the paper business to increase quality, production, and efficiency. The industry participants may find themselves at a competitive disadvantage if they are unable to keep up with these technical improvements. One of the numerous issues facing the business is the absence of domestic plant and machinery manufacturing capacity.

THE WAY FORWARD

The way forward in leveraging indigenous tree species for pulp and paper production necessitates a multifaceted and sustainable approach. Critical to this endeavor is the advancement of research and development focused on understanding the specific anatomical and chemical properties of these species to optimize their use in paper manufacturing processes. This involves not only detailed scientific studies but also the development of innovative technologies that can efficiently process diverse wood properties while minimizing environmental impact. Collaboration between academia, industry, and government agencies is essential to ensure that the cultivation and harvesting of these species are done sustainably, incorporating best practices for forest management and conservation. Moreover, engaging with local communities and indigenous peoples is crucial to respecting rights and traditions, ensuring equitable benefits, and fostering the sustainable management of forest resources. Developing policies that support the sustainable commercialization of indigenous tree species, coupled with investments in infrastructure that can adapt to a wider range of raw materials, will be key. Ultimately, a holistic approach that balances economic viability with environmental sustainability and social equity will pave the way for the responsible expansion of the pulp and paper industry using indigenous tree species. This path forward promises not only to enhance the sustainability of the industry but also to contribute to biodiversity conservation and the economic development of regions rich in these native species.

CONCLUSION

The comparative review underscores the imperative for a sustainable, multifaceted approach in harnessing indigenous tree species for pulp and paper production. It highlights the necessity of advancing research to uncover the distinct anatomical and

chemical traits of these species, which are pivotal for their optimal use in the paper manufacturing industry. The collaboration across academia, industry, and governmental bodies is emphasized as crucial for ensuring the sustainable cultivation and harvesting of these resources. Furthermore, the study advocates for engagement with local communities and indigenous peoples to ensure that the exploitation of these species is equitable and respects cultural traditions. The development of supportive policies and the investment in adaptable infrastructure emerge as essential components for facilitating the sustainable commercialization of indigenous tree species. This approach not only aims to improve the sustainability of the pulp and paper industry but also contributes to biodiversity conservation and the economic upliftment of areas endowed with these native species, marking a significant step toward environmental stewardship and sustainable development.

REFERENCES

Abdullah M, Majid RA, Zaiton SNA, Mustam MM, Khalid AK, Azman HA (2021) Paper production using *Acacia auriculiformis* leaf. Pages 1-7. *in* Shalygin MG, ed. AIP Conference Proc, Vol. 2339, No. 1, AIP Publishing, 23–24 July 2020, Arau, Malaysia.

Aggarawal (1998) Urban forest. https://uforest.org/Species/A/Acacia_auriculiformis.php (Accessed 21 December 2024).

Akeem Azeez M, Andrew JE, Sithole BB (2016) A preliminary investigation of nigerian *Gmelina arborea* and *Bambusa vulgaris* for pulp and paper production. Maderas, Cienc Tecnol 18(ahead):0-0.

Akhtaruzzaman AFM, Chowdhury AR (1991) Alkaline pulping of *Paraserianthes falcataria* with anthraquinone as an additive. Bangladesh J For Sci 20(1/2):37-43.

Anoop EV, Ajayghosh V, Pillai H, Soman S, Sheena VV, Aruna P (2011) Variation in wood anatomical properties of selected indigenous, multipurpose tree species grown in research trials at LRS Thiruvazhamkunnu, Palakkad, Kerala. J Indian Acad Wood Sci 8(2):100-105.

Bageel A, Honda MD, Carrillo JT, Borthakur D (2020) Giant leucaena (*Leucaena leucocephala* subsp. glabrata): A versatile tree-legume for sustainable agroforestry. Agroforest Syst 94(1):251-268.

Bahuguna V, Unnikrishnan K, Dhaundiyal UC (1989) Studies on the performance of Phillipines and Malaysian provenances of *Albizia falcataria* (L.) Forberg at nursery stage under North Indian moist tropical condition. Indian For 115:209-215.

Balkrishna A, Sakshi, Chauhan M, Dabas A, Arya V (2022) A comprehensive insight into the phytochemical, pharmacological potential, and traditional medicinal uses of Albizia lebbeck (L.) Benth. Evid Based Complementary Altern Med 2022(1):5359669.

Bhola P, Sharma Y (1982) Kraft pulping of *Leucaena leucocephala*. Indian For 108:202-211.

Brockerhoff EG, Barbaro L, Castagneyrol B, Forrester DI, Gardiner B, González-Olabarria JR, Lyver PO, Meurisse N, Oxbrough A, Taki H, Thompson ID, van der Plas F, Jactel H (2017) Forest biodiversity, ecosystem functioning and the provision of ecosystem services. Biodivers Conserv 26(13):3005-3035. https://doi.org/10.1007/s10531-017-1453-2.

CABI Digital library (2017) Albizia lebbeck. https://www.cabidigitallibrary.org/doi/10.1079/cabicompendium.4008 (Accessed 12 February 2024).

Chavan SB, Vishnu R, Kumar N, Kumar D, Sirohi C, Handa AK (2021) *Melia dubia* An indigenous tree species for industrial agroforestry in India. Indian Farming 71(6):7-11.

Chowdhury Q, Ishiguri F, Iizuka K, Hiraiwa T, Matsumoto K, Takashima Y, Yoshizawa N (2009) Wood property variation in *Acacia auriculiformis* growing in Bangladesh. Wood Fiber Sci 41(4):359-365.

Dhaka RK, Gunaga RP, Sinha SK, Thakur NS, Dobriyal MJ (2020) Influence of tree height and diameter on wood basic density, cellulose and fibre characteristics in *Melia dubia* Cav. families. J Indian Acad Wood Sci 17(2):138-144.

Doty SL, Shang TQ, Wilson AM, Moore AL, Newman LA, Strand SE, Gordon MP (2003) Metabolism of the soil and groundwater contaminants, ethylene dibromide and trichloroethylene, by the tropical leguminous tree, *Leuceana leucocephala*. Water Res 37(2):441-449.

Downes GM, Hudson IL, Raymond CA, Dean GH, Michell AJ, Schimleck LR, Muneri A (1997) Sampling plantation eucalypts for wood and fibre properties, CSIRO publishing, Collingwood, Australia.

Elzaki OT, Khider TO, Omer SH, Shomeina SK (2012) Environment friendly alkaline pulping of *Albizia lebbeck* from Sudan. Nat Sci 10(4):76-82.

FAO Report (2011) Commission on genetic resources for food (2014). The State of the World's Forest Genetic Resources, Food & Agriculture Org.

FAO (2023) Forestry production and trade database. http://www.fao.org/faostat/en/#data/FO (7 August 2021).

Gillah PR, Ishengoma RC (1993) Kraft pulping of *Leucaena leucocephala* grown in Morogoro, Tanzania. Holz Als Roh-Und Werkstoff 51(5):353-356.

Goswami M, Bhagta S, Sharma D (2020) *Melia dubia* and its importance: A Review. Int J Eco Plant 7(1):029-033.

Gupta S, Singh CP, Kishan-Kumar VS, Shukla S (2019) Machining properties of *Melia dubia* wood. Maderas, Cienc Tecnol 21(ahead):0-0.

Hai PH, Hannrup B, Harwood C, Jansson G, Van Ban D (2010) Wood stiffness and strength as selection traits

for sawn timber in *Acacia auriculiformis*. Can J For Res 40(2):322-329.

Hannan MO, Hasnin SMM, Islam MS, Islam MA (2001) Study on some physical properties of sound and disease affected sissoo (*Dalbergia sissoo* roxb.) wood. Khulna Univ Stud 3(1):433-435. https://doi.org/10.53808/kus.2001.3.1.0107-l.

Haque MM, Ni Y, Akon AJU, Quaiyyum MA, Jahan MS (2021) A review on *Acacia auriculiformis*: Importance as pulpwood planted in social forestry. Int Wood Prod J 12(3):194-205.

Hendarto KA (2006) Evaluation of non-traditional raw material for pulp and paper industry: Case studies on *Gmelina arborea* and *Acacia mangium*. IPB University, Thailand.

Hossen MF, Nijhu RS, Khatun A (2023) A phytochemical and pharmacological review on *Dalbergia sissoo*: A potential medicinal plant. J Pharmacogn Phytochem 12(1): 52-57.

IBDP (2015) Melia dubia. https://indiabiodiversity.org/species/show/31551 (Accessed 21 January 2024).

Iwuoha SE, Seim W, Onyekwelu J (2021) Mechanical properties of *Gmelina arborea* for engineering design. Constr Build Mater 288:123123, https://doi.org/10.1016/S0921-8009(00)00133-6.

Jozsa LA, Middleton GR (1994) Discussion of wood quality attributes and their practical implications. Special Pub. Canada: N. p., 1994. Web.

Julian TC, Fukuda H, Novianto D (2022) The influence of high-temperature and-pressure treatment on physical properties of *Albizia falcataria* board. Forests 13(2): 239, doi: 10.3390/f13020239.

Kalra K (1990) Delignification of refiner mechanical pulp for *Albizia lebbeck* by soda process. Indian For 116: 819-821.

Kant P, Nautiyal R (2021) India timber supply and demand 2010–2030. Inter Trop Timber Org, Yokohama, 49-60.

Khushi LR, Hossain M, Rubaiot Abdullah SM, Saha S, Siddique MRH (2019) Allometric models for estimation of aboveground biomass of *Gmelina arborea* Roxb. in pulpwood plantations of Bangladesh. South For J For Sci 81(1):45-48.

Kröger M, Nylund J (2012) The conflict over Veracel pulpwood plantations in Brazil application of ethical analysis. For Policy Econ 14(1):74-82. https://doi.org/10.1016/J.FORPOL.2011.07.018.

Kumar D, Bhati HP, Kumar S, Kumari N, Kumar P (2019) Biosorption of malachite green dye by mycomass and phytomass influence by industrial effluent heavy metals. International Conference on Global Research Initiatives for Sustainable Agriculture & Allied Sciences, ICAR-National Acadamy of Agricultural Research Management, Hyderabad, Telangana, India.

Kumar S, Omer S, Patel K, Khan BM (2013) Cinnamate 4-hydroxylase (C4H) genes from *Leucaena leucocephala*: A pulp yielding leguminous tree. Mol Biol Rep 40(2): 1265-1274. https://doi.org/10.1007/s11033-012-2169-8.

Liang J, Crowther TW, Picard N, Wiser S, Zhou M, Alberti G, Schulze E-D, McGuire AD, Bozzato F, Pretzsch H, de-Miguel S, Paquette A, Hérault B, Scherer-Lorenzen M, Barrett CB, Glick HB, Hengeveld GM, Nabuurs G-J, Pfautsch S, Viana H, Vibrans AC, Ammer C, Schall P, Verbyla D, Tchebakova N, Fischer M, Watson JV, Chen HYH, Lei X, Schelhaas M-J, Lu H, Gianelle D, Parfenova EI, Salas C, Lee E, Lee B, Kim HS, Bruelheide H, Coomes DA, Piotto D, Sunderland T, Schmid B, Gourlet-Fleury S, Sonké B, Tavani R, Zhu J, Brandl S, Vayreda J, Kitahara F, Searle EB, Neldner VJ, Ngugi MR, Baraloto C, Frizzera L, Bałazy R, Oleksyn J, Zawiła-Niedźwiecki T, Bouriaud O, Bussotti F, Finér L, Jaroszewicz B, Jucker T, Valladares F, Jagodzinski AM, Peri PL, Gonmadje C, Marthy W, O'Brien T, Martin EH, Marshall AR, Rovero F, Bitariho R, Niklaus PA, Alvarez-Loayza P, Chamuya N, Valencia R, Mortier F, Wortel V, Engone-Obiang NL, Ferreira LV, Odeke DE, Vasquez RM, Lewis SL, Reich PB (2016) Positive biodiversity-productivity relationship predominant in global forests. Science 354(6309):aaf8957. https://doi.org/10.1126/science.aaf8957.

López F, García MM, Yánez R, Tapias R, Fernández M, Díaz MJ (2008) Leucaena species valoration for biomass and paper production in 1 and 2 year harvest. Bioresour Technol 99(11):4846-4853.

MMR (2023) Indian paper & pulp market: Growing packaging industry to boost the market growth, https://www.maximizemarketresearch.com/market-report/indian-paper-pulp-market/29044/ (18 January 2024).

Ogbonnaya CI, Nwalozie MC, Nwaigbo LC (1992) Growth and wood properties of *Gmelina arborea* (Verbenaceae) seedlings grown under five soil moisture regimes. American J Botany 79(2):128-132.

Ogunsanwo OY, Akinlade AS (2011) Effects of age and sampling position on wood property variations in Nigerian grown *Gmelina arborea*. J Agric Soc Res 11(2): 103-112.

Olufunmilayo OD (2013) Determination of pulp and paper making suitability indices of some Nigerian species Leguminosae: Caesalpinoideae. Acad J Interdiscip Stud 13:61-68. https://doi.org/10.5901/ajis.2013.v2n13p61.

Pandey VC, Kumar A (2013) *Leucaena leucocephala*: An underutilized plant for pulp and paper production. Genet Resour Crop Evol 60(3):1165-1171.

Parrotta JA, Roloff A, Weisgerber H, Lang U, Stimm B (2006) Enzyklopädie der Holzgewächse [Encyclopaedia of woody plants]. *Albizia lebbeck* [monograph] [Google Scholar] *in* Roloff A, Weisgerber H, Lang UM, Stimm B, and Schütt P, eds. Enzyklopädie der Holzgewächse: Handbuch und Atlas der Dendrologie, Wiley-VCH Verlag GmbH & Co. KGaA.

Riki JTB, Sotannde OA, Oluwadare AO (2019) Anatomical and chemical properties of wood and their practical

implications in pulp and paper production: A review. J Res For Wildlife Environ 11(3):358-368.

Rojas-Sandoval J (2009) *Falcataria moluccana* (batai wood). Forest. cabidigitallibrary.org Publication: CABI Compendium. https://doi.org/10.1079/cabicompendium.38847.

Saravanan V, Parthiban KT, Kumar P, Marimuthu P (2013) Wood characterization studies on *Melia dubia* cav. for pulp and paper industry at different age gradation. Res J Recent Sci 2277:2502.

Sarwar Jahan M, Sarkar M, Quaiyyum MA (2018) Pulping of gamari roots (*Gmelina arborea*). J Indian Acad Wood Sci 15(1):28-32.

Setyawan YP, Hidayat P, Puliafico KP (2018) Herbivorous insects associated with albizia (*Falcataria moluccana*) saplings in Bogor. *in* IOP Conference Series: Earth and Environmental Science (Vol. 197, No. 1, p. 012018). IOP Publishing, Indonesia.

Shaik N, Arha M, Nookaraju A, Gupta S, Srivastava S, Yadav A, Kulkarni P, Abhilash O, Vishwakarma R, Singh S, Tatkare R, Chinnathambi K, Rawal S, Khan B (2009) Improved method of in vitro regeneration in *Leucaena leucocephala*—A leguminous pulpwood tree species. Physiol Mol Biol Plants 15(4):311-318. https://doi.org/10.1007/s12298-009-0035-5.

Sharda AK, Mukherjee S, Rathor BP (2000) Cellulosic raw materials scenario in future availability, constraints, cost and plantations. IPPTA 12(1):17-24.

Shrivastava S, Saxena AK (2017) Wood is good: But, is India doing enough to meet its present and future needs. Centre for Science and Environment, New Delhi, 13.

Singh A (2015) Disappearing *Dalbergia sissoo* from the Indo-Gangetic Plain of India. https://www.techgape.com/2015/04/dalbergia-sissoo-information.html (21 March 2024).

Singh A, Raghubanshi A, Singh J (2004) Comparative performance and restoration potential of two Albizia species planted on mine spoil in a dry tropical region, India. Ecol Eng 22(2):123-140. https://doi.org/10.1016/J.ecoleng.2004.04.001

Sinha SK, Chaudhari PA, Thakur NS, Jha SK, Patel DP, Dhaka RK (2019) *Melia dubia* Cav. wood properties vary with age and influence the pulp and paper quality. Int Wood Prod J 10(4):139-148. Doi:10.1080/20426445.2019.1688947.

Soosai Raj J, Mayavel A, Mutharaian VN, Nicodemus A (2017) Variations on pulping properties of *Gmelina arborea* Roxb. Grown in different geographical regions of Tamil Nadu, India. Pages 189-197 *in* K Pandey, V Ramakantha, S Chauhan, Arun Kumar A, eds. Wood is good: Current trends and future prospects in wood utilization. Springer, Singapore.

Statista (2024) Global production of pulp and paper https://www.statista.com/statistics/270319/consumption-of-paper-and-cardboard-since-2006/ (24 March 2024).

Sunarti S, Nirsatmanto A (2021). Utilization of interspecific Acacia hybrid for pulp/paper industry and increasing of forest biodiversity. *in* IOP Conference Series: Earth and Environmental Science (Vol. 886, No. 1, p. 012041). IOP Publishing, 4-5 August 2021, Makassar, Indonesia. https://doi.org/10.1088/1755-1315/886/1/012041.

Sunny P (2018) Demand and supply of wood products, https://www.researchgate.net/publication/348295858_DEMAND_AND_SUPPLY_OF_WOOD_PRODUCTS (22 November 2024).

Tonouéwa JFMF, Langbour P, Biaou SSH, Assèdé ES, Guibal D, Kouchade CA, Kounouhéwa BB (2020) Anatomical and physico-mechanical properties of *Acacia auriculiformis* wood in relation to age and soil in Benin, West Africa. Eur J Wood Prod 78(4):745-756.

Trumbore S, Brando P, Hartmann H (2015) Forest health and global change. Science 349(6250):814-818. https://doi.org/10.1126/science.aac6759.

UNECE/FAO (2023) Data Brief 2023 pulp, paper and paperboard, https://unece.org/sites/default/files/2023-11/2023-data-brief-pap-final-web_1.pdf (11 January 2024).

Unnikrishnan B, Gurumurthy DS (2015) Progress on genetic modifications of pulp wood tree species relevance to India—A review. Agric Rev36(4):265-276. https://doi.org/10.18805/AG.V36I4.6663.

Vennila S, Parthiban KT (2021) Screening of indigenous pulpwood for paper production. Int J Chem Stud 9(2):1059-1064.

DEVELOPMENT OF A CONTINUOUS WOOD SURFACE CHARGE DETECTION DEVICE

*Lena Maria Leiter**

Doctoral Candidate
Institute of Wood Technology and Renewable Materials
University of Natural Resources and Life Sciences, Vienna
Vienna, Austria
E-mail: lena.leiter@boku.ac.at

Roman Myna

Doctoral Candidate
Institute of Green Civil Engineering
University of Natural Resources and Life Sciences, Vienna
Vienna, Austria
E-mail: roman.myna@boku.ac.at

Jakub Dömény

Research Associate
Department of Wood Science and Technology, Faculty of Forestry and Wood Technology
Mendel University in Brno
Brno, Czech Republic
E-mail: jakub.domeny@mendelu.cz

Rupert Wimmer

Professor
Institute of Wood Technology and Renewable Materials
University of Natural Resources and Life Sciences, Vienna
Vienna, Austria
E-mail: rupert.wimmer@boku.ac.at

(Received XXX XXXX)

Abstract. Almost all woodworking processes involve mechanical friction and contact electrification, ie triboelectrification, between the wood surface and the woodworking tool. An electric charge is transferred from one solid surface to another when two materials come into contact with each other. Currently, there is no continuous inline-capable electrical surface charge measuring devices. The goal of this work was to create a measurement setup that can be used with a variety of woodworking processes. The proposed continuous surface charge detection (ConSurChaD) device connects an electric fieldmeter to a Faraday cage-style measuring box. Individual elements of the box can be mounted or dismounted to fit various woodworking processes. The application of electrostatic induction principles permitted quantification of the electrostatic surface charge by measuring the accumulated electric field strength generated, expressed in kV/m. The device was compared with a reference method using a commercial discontinuous detection approach. Measurements were made simultaneously using an electrostatic voltmeter, a hand-held instrument that measured the surface charge in volts. The validation confirmed the accuracy of the ConSurChaD device ensuring the applicability for continuous measurement of electrostatic surface charges. This approach allows for a more efficient and targeted application of triboelectrification to wood surfaces, leading to improved surface coatings and other enhancements.

Keywords: Contact electrification, electric fieldmeter, electrical field strength, triboelectrification, woodworking.

* Corresponding author

INTRODUCTION

When materials with solid surfaces come into contact, an electric charge is transferred from one surface to the other, a phenomenon called frictional electricity, contact electrification, or triboelectric charging. The imbalance of the electrostatic charge becomes evident when the materials are again separated. As equal and opposite charges result on the two charging partners, the polarities depend on the effective surface work functions of the two materials (Lowell and Rose-Innes 1980; Greason 2013). The surface work function is the minimum amount of energy required to remove an electron from a solid (Kelly and Spottiswood 1989; Kittel 1996). The consequence of this electron transfer is that the participating materials become oppositely charged. Matsusaka et al (2010) proposed that the amount of net transferred charge, denoted as Δq_C, is determined by the product of the capacitance between the two contacted materials, and the contact potential difference. The net transferred charge Δq_C can be therefore calculated, according to Harper (1951; Eq 1):

$$\Delta q_C = C_0 \frac{-(\text{Ø}_w - \text{Ø}_m)}{e} \quad (1)$$

where Ø_m is the surface work function of the colliding processing tool and Ø_w is the effective work function of the given material. The effective surface work function differences between two surfaces drive the charge transfer, and this charge transfer will cease when the energy levels of the two materials become equal (Matsusaka et al 2010). Although extensive research exists on contact electrification, or triboelectric charging, of metals or polymers, very little is known about the triboelectric surface charging of wood, which is reviewed as follows.

Triboelectric Charging of Wood Surfaces

According to Skaar (1988), wood is semiconductive with the conductivity varying with wood density and MC. When it contacts a machine, wood acts mainly as an insulator. Previous studies showed that contact electrification occurs during wood sawing, cutting, chipping, shredding, or defibrating (Myna et al 2021a, 2021b). We further found electrical surface charges on the wood are generated when the surfaces are brushed (Leiter et al 2022).

The triboelectric series provides insights into the behavior of any material in various applications involving static electricity and charge transfer. A triboelectric series is a list of materials that are ranked by their tendency to gain or lose electrons, and how effectively these charges are exchanged relative to their position within the list (Diaz and Felix-Navarro 2004; Park et al 2008; Burgo et al 2016; Zou et al 2019). The position of a material in the triboelectric series indicates the polarity of the generated charge when two materials are contacted and again separated (Zou et al 2019). A material that donates an electron becomes positively charged and appears on the positive side of the colliding partner. Materials positioned further apart in the series have been found to show higher specific charges (Diaz and Felix-Navarro 2004). Wood is generally positioned near the middle of the triboelectric series, which means it tends to be relatively neutral but can behave as either an electron donor or acceptor, depending on the other materials it comes into contact with (Diaz and Felix-Navarro 2004). For example, Greason (2013) reported that wood becomes charged positively when colliding with a metal.

The underlying triboelectric charging mechanisms, particularly concerning semi insulating materials, including wood, are discussed by Karner and Urbanetz (2013). Myna et al (2021b) discussed triboelectric charging of wood dust particles generated during hand-held circular sawing. Further, Myna et al (2021a) have shown that selected saw blade surface coatings reduce dust formation during wood processing, an idea that was also patented (EP 3 881 958 A1). Leiter et al (2022) modified the measurement setup introduced by Myna et al (2021b), for examining solid wood surfaces instead of wood dust particles, to investigate triboelectric surface charges caused by surface brushing. The following methods can be listed to accurately measure surface electrification: 1) Electrostatic voltmeter measurements: This contactless method measures the electrostatic potential on the material surface

after contact or friction, providing direct insights into the triboelectric charge accumulation (Pandey et al 2009). 2) Faraday cup experiments: An isolated conductor (Faraday cup) captures charges transferred during contact or separation from a material, measuring the total transferred charge directly to quantify triboelectric charging. Using a Faraday cage is a well-established measuring method for triboelectrification (Chen et al 2023). 3) Surface charge density measurements: Techniques such as kelvin probe force microscopy can map the surface potential at the microscale, revealing charge distributions and densities resulting from triboelectric charging (Noras and Pandey 2010). The charge-to-mass ratio works well for the investigating particles or smaller samples however, it is inappropriate for examining a 3D material's surface charge (Zou et al 2019). They suggested a technique that excludes air pockets at the surface-to-surface contact between two solid materials by using liquid mercury. 4) Current and voltage measurements: this method refers to directly measuring the current or voltage generated between two materials during or after contact (Ziegler et al 2009). 5) Electron spectroscopy methods, including X-ray photoelectron spectroscopy, auger electron spectroscopy, or UV photoelectron spectroscopy, which all analyze emitted electrons (Rivière 1990; Michler 2023). Finally, 6) X-ray powder diffraction can visualize charge distributions following triboelectrification (Kato and Tanaka 2016).

Triboelectric charging of wood surfaces holds potential as a process parameter for controlling surface properties such as conductivity and friction, thereby improving adhesion during coating or surface finishing. This approach requires continuous monitoring of the surface charge status to ensure optimal results. Current surface charge detection devices are unsuitable for continuous measurements and cannot be integrated into inline production processes. We introduce continuous surface charge detection (ConSurChaD) device, capable of being used in woodworking processes. The device was designed to be mobile, and capable of continuously recording triboelectric charges near equipment such as saw blades, brushes, or sanding belts. We have developed a universally applicable method, which is described here in detail and compared with a commercially available, discontinuous detection method. We hypothesize that this new continuous detection device can deliver reliable data, ensuring its suitability for use in woodworking processes.

DEVICE DEVELOPMENT

The main element of the ConSurChaD device consists of a 15×20 cm aluminum measuring box, built as a Faraday cage to shield the electrostatic charge. The different elements of the box, as well as the wings and legs, are individually mounted or dismounted with screws. The box has a ground distribution to ensure that all elements are constantly grounded, and an arm through which the connected cables (Bayonet Neill-Concelman (BNC) connector and ground) can be passed to ensure safe operation. The device is equipped with an electric fieldmeter (EFM) 115 electrostatic fieldmeter (Kleinwächter®, Hausen im Wiesental, Germany), for contactless detection of electrical surface charges. This compact and sensitive fieldmeter accumulates voltage readings, based on the field-mill principle (Boldyrev et al 2016). Figure 1 displays the device: (1a) top view, (1b) elevation view, and (1c) side view, as well as a (1d) 3D model and in (1e) the elements of the measuring box. The connector head to attach the EFM via a BNC cable was linked to the metal detection plate. As the Faraday casing was electrically isolated, the detected electrical charges were shielded from potential electrostatic charges of the surroundings. The detection plate has a thickness of 3 mm. Electrostatic induction, which is the displacement of charges (electrons) in the metal plate, occurs when an electrically charged surface including wood emits an electric field (Donnevert 2020). This charge displacement was transmitted by the metal cylinder to the connector head and then to the EFM via the BNC cable. The fieldmeter was attached to a personal computer, which operated the readout software (EFMXX5_ReadOut, Kleinwächter®). The measurement range was set to either 5 kV/m or 25 kV/m, based on pretests, with a zero-calibration that had to be performed before every second

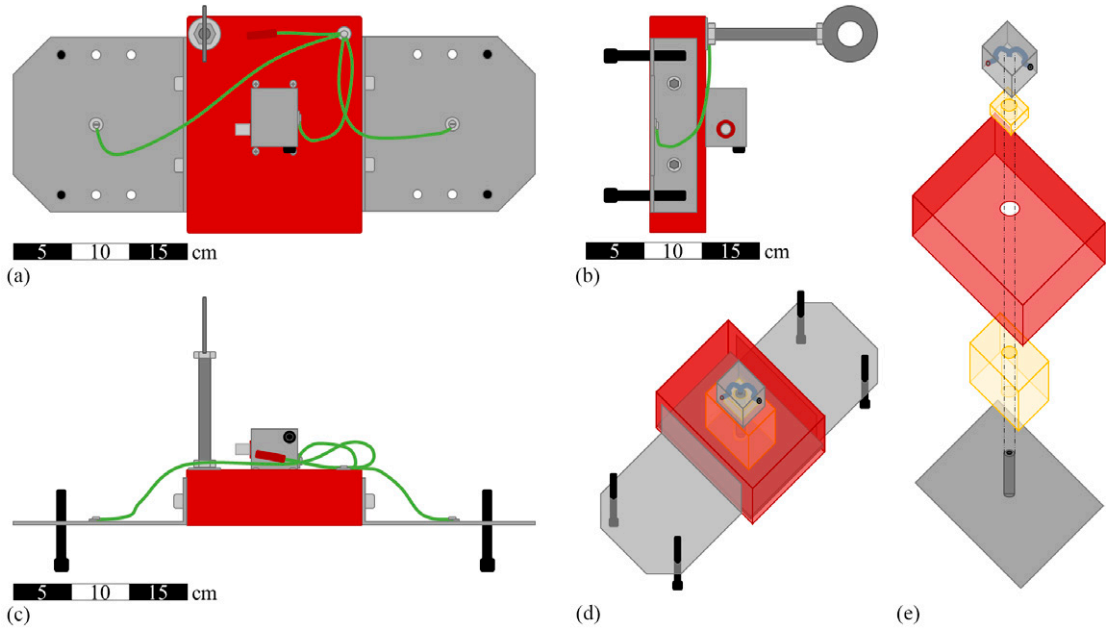

Figure 1. Continuous surface charge detection device (a) top view, (b) elevation view, (c) side view, (d) 3D model, and (e) elements of the measuring box with the dimensions of 15 × 20 cm (top to bottom): connector head to attach the EFM, insulating polytetrafluorethylene cube, Faraday casing, insulating polymer cube, and detection plate – connected to the top box along the dotted lines. EFM, electric fieldmeter.

set of measurements. Grounding was engaged throughout, to ensure that only wood surface charges were recorded, without measuring electric fields from the conveyor belt or the surroundings. Thus, a photo sensor was also installed between the triboelectrification tool (eg brushes) and the ConSurChaD device to deactivate and activate grounding. Surface charges were measured, and the grounding was turned off when the photo sensor detected a moving sample on the conveyor.

The electric circuits of the device are illustrated in Fig 2. The photo-sensitive barrier ensured a continuous flow of protons between the transmitter and the receiver of the photo sensor. The control

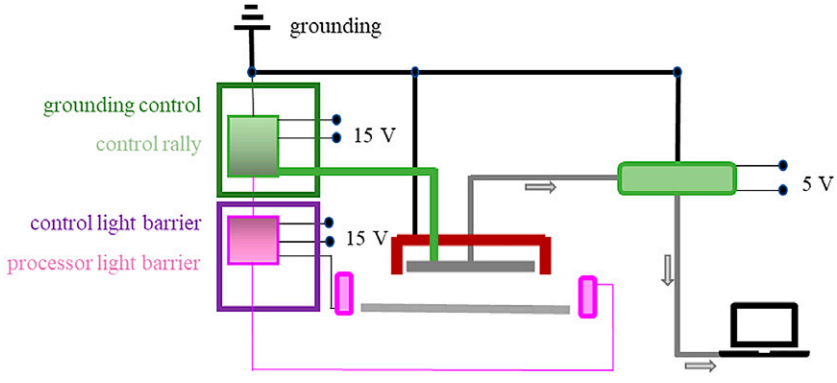

Figure 2. Electrical circuits of the continuous surface charge detection device.

light barrier sent a signal to the grounding control when a wood sample interrupted the proton flow. As a result, the measuring plate's grounding was turned off, allowing triboelectric field strength measurements. The proton beam was built up again when the wood sample left the area of the light barrier, and the control light barrier notified the grounding control to reactivate the measuring plate grounding, and thus stop field strength measurement. The accumulated electrostatic surface charges were measured at a resolution of ±5 V/m as the electric field strength.

The adjustable ConSurChaD device allowed precise positioning above-measured wood surfaces at set distances by mounting suitable wings and legs. Two variables impacted the results: the distance between the detection device and the measured object, and the sample size. First, the detected surface charge weakened when the measuring distance exceeded the initial setting and strengthened when it was shorter. Second, the devices used to measure surface potential assumed the object under measurement had an infinite size. The device delivered repeatable values when the measured objects were noticeably larger than the ConSurChaD device detection area.

VERIFICATION RESULTS

Three Norway spruce (*Picea abies* (L.) Karst) samples 25 mm wide, 600 mm long, and 25 mm thick, were prepared. Samples were conditioned at 20°C and 65% RH. Mechanical friction was applied to triboelectrically charge the solid-wood surfaces using a commercial brushing machine (TWINGO 300 B, Houfek a.s., Czech Republic). Figure 3 shows the installed ConSurChaD device as used in the conducted experiments. The experimental design included five sets of three samples ($n = 15$), which were brushed at four different machine settings, two different brush pressures, and at two different feed rates: 1) high brush pressure and fast feed rate, 2) high brush pressure and slow feed rate, 3) low brush pressure and fast feed rate, and 4) low brush pressure and slow feed rate. The wood samples were sanded and set aside between each of the five sample sets to ensure that the next set started with a fresh,

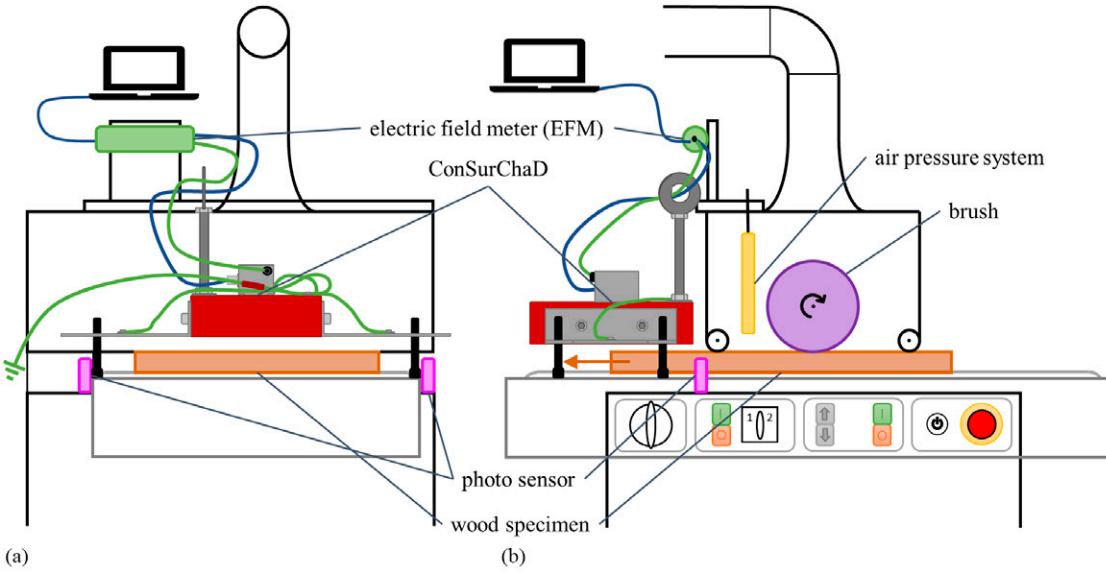

Figure 3. An experimental setup was used to measure the surface charges of wood samples caused by surface brushing: (a) side view and (b) elevational view. ConSurChaD, continuous surface charge detection.

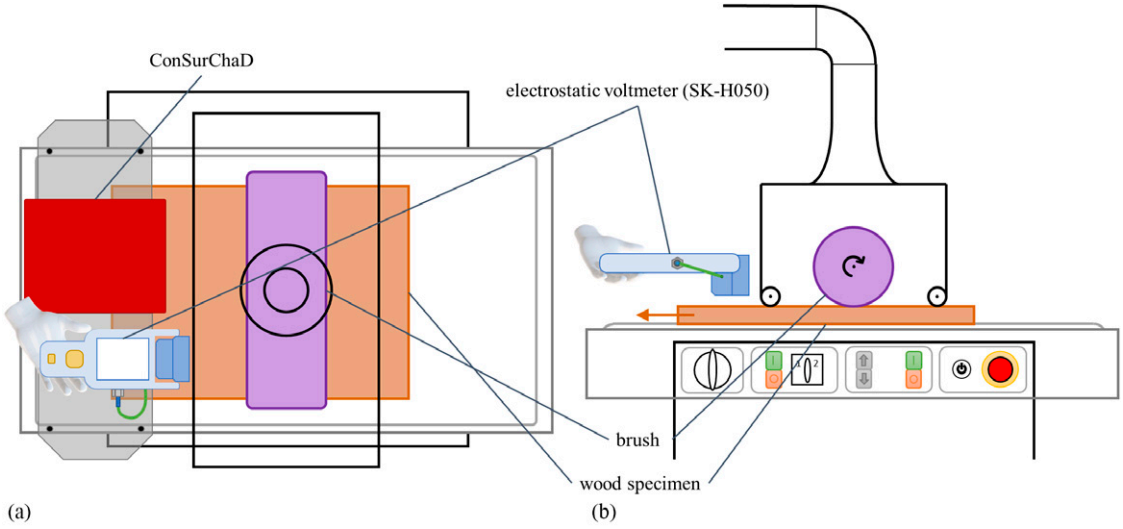

Figure 4. The top view of simultaneous measurement shows the ConSurChaD device and the Keyence SK-H050 reference (a); the elevational view of the brushing machine with the surface-charge measurement, with the installed Keyence device (b). ConSurChaD, continuous surface charge detection.

charge-free surface. As shown in Fig 4, surface charge measurements were simultaneously taken directly after brushing, using the new ConSurChaD device as well as an SK-H050 electrostatic voltmeter (Keyence, Belgium) as the reference method. The SK-H050 made it possible to measure the minimum and maximum surface charge over a period as well as the charge at the end of the measurement period. Unfortunately, the measured values between starting and ending the measurement could not be continuously stored. The SK-H050 measured the surface charge in volts at the set distances of 25 mm for higher accuracy, or 100 mm for a larger detection field, at an accuracy of ± 10 and ± 25 V, respectively, depending on the chosen distance (Keyence Corporation 2010).

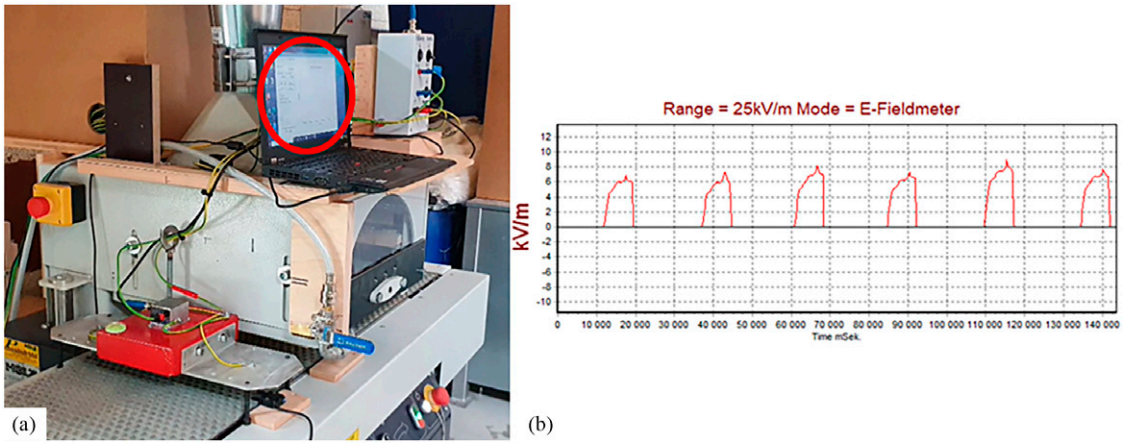

Figure 5. Setup (left) and data plot as produced with the readout software (right) plotting the electric field strength [kV/m] of three samples getting brushed twice.

Table 1. Verification of the self-designed ConSurChaD device with the electrostatic voltmeter SK-H050 (Keyence, Belgium) ($n = 15$).

Measurement method	ConSurChaD				Reference			
Brush pressure	High	High	Low	Low	High	High	Low	Low
Feed rate	Fast	Slow	Fast	Slow	Fast	Slow	Fast	Slow
μ [V]	—	—	—	—	139.5	172	67	136.5
σ [V]	—	—	—	—	31.4	25.8	12.8	19.5
μ [kV/m]	5.81	6.73	2,84	5.31	5.58[a]	6.88[a]	2.68[a]	5.46[a]
σ [kV/m]	1.6	1.36	0.55	0.9	1.67[a]	1.49[a]	0.53[a]	1.11[a]

[a]Converted into kV/m by dividing trough the distance of 25 mm.
ConSurChaD, continuous surface charge detection.

Since higher measurement accuracy was attained, the measuring distance of 25 mm was chosen as the baseline setting for verification.

Figure 5 shows the measurement of the cumulated electric field strength of three samples getting brushed twice. Outcomes from the ConSurChaD and reference methods are displayed in Table 1. The reference data were converted into kV/m for better comparison. It became evident that the two methods did not differ significantly, by a two-way ANOVA using SPSS® Statistics 26 (IBM Deutschland GmbH, Böblingen, Germany) ($p > 0.05$). However, significant differences ($p < 0.05$) were found between the settings (Fig 6). The validation showed that the range of measurement inaccuracies was the only difference between the two results. Overall, it can be concluded that our hypothesis was confirmed. The new continuous detection device delivers reliable data, ensuring its suitability for woodworking processes.

CONCLUSIONS

The correct determination of the electrostatic surface charge on wood was achieved using a self-designed ConSurChaD device. A comparison with readings from a discontinuous reference method showed that the differences were within the range of measurement variations, confirming the accuracy of the ConSurChaD device. This enables applications in continuous woodworking processes, allowing triboelectric charging to be

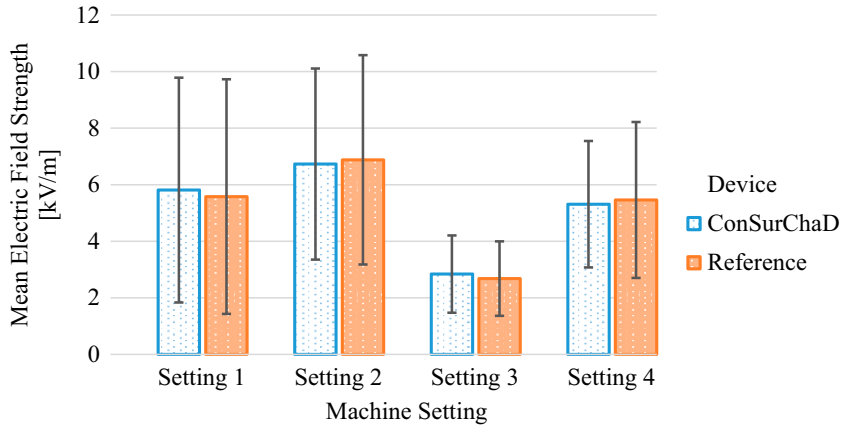

Figure 6. Comparison of electric field strength measurements with the newly developed ConSurChaD device, compared with the Keyence SK-H050 reference. Mean and standard deviations of electric field strength in kV/m are shown, using the machine setting high brush pressure and fast feed rate (1); high brush pressure and slow feed rate (2); low brush pressure and fast feed rate (3); and low brush pressure and slow feed rate (4) ($n = 15$). ConSurChaD, continuous surface charge detection.

applied to wood surfaces to enhance their properties, such as surface conductivity, surface friction, or enhance adhesion for coatings or finishes.

ACKNOWLEDGMENTS

The research leading to these results received funding from the Austrian Academy of Sciences (ÖAW) under a DOC Fellowship. Partial financial support was received from the European Union's Horizon 2020 research and innovation program under Grant Agreement no 952314 (ASFORCLIC).

REFERENCES

Boldyrev AI, Vyazilov AE, Ivanov VN, Kemaev RV, Korovin VY, Melyashinskiy AV, Pamukhin KV, Pamukhina IA, Panov VN, Shvyrev YN (2016) A highly sensitive field mill for registering weak and strong variations of the electric-field intensity of the Earth's atmosphere. Instrum Exp Tech 59(5):740-748.

Burgo TAL, Galembeck F, Pollack GH (2016) Where is water in the triboelectric series? J Electrost 80:30-33.

Chen Q, Cheng B, Wang T, Shang H, Shao T (2023) Method for the measurement of triboelectric charge transfer at solid–liquid interface. Friction 11(8):1544-1556.

Diaz AF, Felix-Navarro RM (2004) A semi-quantitative tribo-electric series for polymeric materials: The influence of chemical structure and properties. J Electrost 62(4):277-290.

Donnevert J (2020) Maxwell's equations: From current density distribution to the radiation field of the Hertzian dipole, 1st edition. Springer Vieweg Wiesbaden, Wiesbaden, Germany.

Greason WD (2013) Triboelectrification of wood with PTFE. J Electrost 71(2):140-144.

Harper WR (1951) The Volta effect as a cause of static electrification. Proc R Soc Lond Ser Math Phys Sci 205:83-103.

Karner S, Urbanetz NA (2013) Triboelectric characteristics of mannitol based formulations for the application in dry powder inhalers. Powder Technol 235:349-358.

Kato K, Tanaka H (2016) Visualizing charge densities and electrostatic potentials in materials by synchrotron X-ray powder diffraction. Adv Phys X 1(1):55-80.

Kelly EG, Spottiswood DJ (1989) The theory of electrostatic separations: A review Part I. Fundamentals. Miner Eng 2(1):33-46.

Keyence Corporation (2010) Electrostatic handbook, Itasca, IL, 59 pp.

Kittel C (1996) Introduction to solid state physics, 8th edition. John Wiley & Sons, New York.

Leiter LM, Myna R, Frömel-Frybort S, Liebner F, Wimmer R (2022) Triboelectric surface field strength of wood after brushing. Wood Sci Technol 56(5):1401-1417.

Lowell J, Rose-Innes AC (1980) Contact electrification. Adv Phys 29(6):947-1023.

Matsusaka S, Maruyama H, Matsuyama T, Ghadiri M (2010) Triboelectric charging of powders: A review. Chem Eng Sci 65(22):5781-5807.

Michler GH (2023). Compact introduction to electron microscopy. Springer, New York.

Myna R, Hellmayr R, Georgiades M, Leiter LM, Frömel-Frybort S, Wimmer R, Liebner F (2021a) Can surface coating of circular saw blades potentially reduce dust formation? Materials 14(18):5123.

Myna R, Wimmer R, Liebner F, Leiter LM, Frömel-Frybort S (2021b) Triboelectric charging of dust particles during hand-held circular sawing of wood and wood-based materials. Wood Mater Sci Eng 16(1):64-73.

Noras MA, Pandey A (2010) Surface charge density measurements. IEEE Ind Appl Mag 16(4):41-47.

Pandey A, Kieres J, Noras MA (2009) Verification of non-contacting surface electric potential measurement model using contacting electrostatic voltmeter. J Electrost 67(2-3):453-456.

Park CH, Park JK, Jeon HS, Chun BC (2008) Triboelectric series and charging properties of plastics using the designed vertical-reciprocation charger. J Electrost 66(11-12):578-583.

Rivière JC (1990) Surface analytical techniques, monographs on the physics and chemistry of materials. Oxford University Press, Oxford, UK.

Skaar C (1988) Wood-water relations (Springer series in Wood Science), 1st edition. Springer-Verlag, Berlin, Heidelberg.

Ziegler S, Woodward RC, Iu HH-C, Borle LJ (2009) Current sensing techniques: A review. IEEE Sensors J 9(4): 354-376.

Zou H, Zhang Y, Guo L, Wang P, He X, Dai G, Zheng H, Chen C, Wang AC, Xu C, Wang ZL (2019) Quantifying the triboelectric series. Nat Commun 10(1):1427.

Errata

Nop, P., Cristini, V., Zlámal, J., Vand, M. H., Šeda, V., and Tippner, J. Dynamic Properties of Wood Obtained by Frequency Resonance Technique and Dynamic Mechanical Analysis. Wood and Fiber Science, 55(2), 2023; pp. 131-142. (https://doi.org/10.22382/wfs-2023-12**):**

Equation 1 contains a typographical error (l^2 instead of l^3). The correct formula used for the $MOED_{FRT}$ calculation is:

$$MOED_{FRT} = \left(\frac{2f}{2.25\pi}\right)^2 \frac{ml^3}{I}$$

***Corresponding author:** Patrik Nop, Department of Wood Science and Technology, Faculty of Forestry and Wood Technology, Mendel University in Brno, Zemědělská 1, 61300 Brno, Czech Republic, E-mail: patrik.nop@mendelu.cz

Valentino Cristini, Jan Zlámal, Mojtaba Hassan Vand, Vít Šeda, Jan Tippner, Department of Wood Science and Technology, Faculty of Forestry and Wood Technology, Mendel University in Brno, Zemědělská 1, 61300 Brno, Czech Republic

Pressley, G.N. and Konkler, M.J. Copper migration from treated wood garden boxes into soil and vegetable biomass. Part I. The first two growing seaosns after installation. Wood and Fiber Science 56(2):91-99. (https://doi.org/10.22382/wfs-2024-09**):**

Abstract. Pressure-treated wood is a commonly used material for constructing garden boxes and concerns about metal leaching into garden soils and garden vegetables persist among the public. This study describes efforts to quantify copper migration from copper azole-treated garden bed frames into garden soil and vegetable biomass. Two garden bed frames were constructed from copper azole 2 × 12-inch nominal Douglas-fir lumber and two were constructed with untreated Douglas-fir lumber before filling with a mixture of native soil and compost. An assortment of common garden vegetables was planted in identical patterns in each of the beds for two growing seasons. During this 2-yr study, we found no difference in copper concentrations between identical vegetables grown in beds constructed with treated or untreated lumber. After 1 and 2 yr, average copper concentrations in soil 0-25 mm from the bed frames were about 23 ppm and 21 ppm higher than soils in the same location in untreated beds, respectively ($p < 0.05$, Tukey's HSD). Elevated copper levels were not detected in beds constructed with treated lumber at **76-102 mm** from the frames or the bed center, indicating that metal migration was limited. This study shows use of treated wood garden beds did not lead to increases in copper concentrations in vegetables grown in those beds. Treated bed materials did lose some copper to garden soil but increases in copper are limited to about 20 ppm immediately next to the treated wood frames and were not detectable at any greater distances from the wood.

Wood, K.C., Konkler, M.J., and Morrell, J.J. Preservative treatment of Tasmanian plantation *Eucalyptus nitens* using supercritical fluids. Wood and Fiber Science, 55(1), 2023; pp. 83-93. https://doi.org/10.22382/wfs-2023-08

Correction in formula converting retention from %m/m to g/m^3:

$$\text{Retention } \left(\text{g/m}^3\right) = \frac{\text{retention } \left(\text{g/m}^3\right) \times \text{oven dry timber density } \left(\text{kg/m}^3\right)}{0.1}$$

Correction in Average g/m^3 by assay zone and total g/m^3 in cross section:

Table 1. Average g/m^3 of propiconazole/tebuconazole in *E. nitens* timbers treated using supercritical carbon dioxide.[a]

Sample thickness (mm)	Assay zone	Average g/m^3 by assay zone[b]	Total g/m^3 in cross section[b]
19	Outer 0-5 mm	277 (68)	191
	Inner 6-14 mm	104 (26)	
25	Outer 0-5 mm	248 (77)	181
	Inner 6-19 mm	113 (28)	
35	Outer 0-5 mm	265 (52)	168
	Middle 6-11 mm	113 (32)	
	Inner 12-24 mm	127 (35)	

[a]Samples were treated to the spruce target retention of 120 g/m^3 of the azole/IPBC mixture.

[b]g/m^3 is a less precise treatment measure as SCF treatments can solubilize wood extractives during the process while simultaneously depositing the biocides, potentially resulting in net weight losses. Values represent analyses of 30 replicates per assay zone for three board thicknesses, and 60 or 90 analyses for the combined cross sections for the 19/25 mm and 35 mm thick samples, respectively. Values in parentheses represent one standard deviation.